

Republic of Iraq
Ministry of Higher Education
and Scientific Research
University of Misan
College of Science
Department of Chemistry



**Study of designation and optimal drug delivery system
in vitro and *in vivo* of Baclofen nano Liposome Vesicles**

A Thesis Submitted to

The College of Science / University of Misan as Partial Fulfillment of the
Requirements for the Master Degree of Science in Chemistry

By

Hasnaa Kadhim Talib

B.Sc. Chemistry University of Misan (2022)

Supervisors

Asst. Prof. Dr. Israa Qusay Falih

2025 A.D

1447 H.D

بِسْمِ اللَّهِ الرَّحْمَنِ الرَّحِيمِ

(وَعَلَّمَكَ مَا لَمْ تَكُن تَعْلَمُ وَكَانَ فَضْلُ اللَّهِ عَلَيْكَ عَظِيمًا)

صدق الله العلي العظيم

سورة النساء آية (١١٣)

Supervisor Certification

I am the supervisor of **Ms. Hasnaa Kadhim Talib**, certify that the thesis (**Study of designation and optimal drug delivery system *in vitro* and *in vivo* of Baclofen nano Liposome Vesicles**) was done and written under my supervision as a partial fulfillment of the requirement for the Master of degree of Science in Chemistry.

Signature:

Asst. Prof. Dr. Israa Qusay Falih

Chemistry department

College of science

University of Misan

Date: / / 2025

Head of Chemistry department Recommendation

According to the recommendation of supervisors, this thesis is forwarded to the examination committee for approval.

Signature:

Dr. Mohammed Abdul Raheem Saeed

Head of Chemistry Department

College of Science

University of Misan

Date: / / 2025

Dedication

***To Allah Glorified and Exalted**, who granted me life, along with the blessings of mind and heart, and to the One in whose hands rests all guidance and from whom comes all support, I dedicate the fruit of my efforts, hoping that He may accept it from me sincerely for His noble sake.*

***To my dear parents**, the source of affection and strength, and to your prayers which have been my nourishment and light along the paths of endeavor, I offer you my love, gratitude, and pride in being a product of you.*

***To my siblings**, who embraced my ambitions and endured my absence, and to those who shared my dream and believed in my abilities, and to every sincere heart that offered me a word, a smile, or a prayer, I dedicate these pages that bear as much of you as they bear of me.*

Hasnaa Al-Wahili

Acknowledgments

All praise is due to Allah, Lord of the worlds, by whose grace good deeds are accomplished. I pray that He grants me success in what is good and beneficial, and makes this work sincerely devoted to His noble countenance. May peace and blessings be upon our Prophet Muhammad, the Seal of the Prophets and Messengers, and upon his pure and righteous family.

I wish to express my sincere gratitude to my esteemed supervisor, **Asst. Prof. Dr. Israa Qusay Falih**, for her meticulous and continuous supervision, and for the valuable guidance she generously provided at every stage of preparing this thesis. Her patience with the challenges of research, her continuous scientific guidance, and her detailed advice have greatly contributed to the development of my academic and personal skills. Her supervision has been a constant source of inspiration and motivation, and her guidance always provided the correct path in scientific research, which played a significant role in the completion of this thesis and the achievement of Its academic objectives.

I also extend my sincere thanks and appreciation to the Head of the Department of Chemistry, **Dr. Mohammed Abdul Raheem Saeed** , for his support and guidance, and for providing the academic environment necessary to accomplish this work.

I further extend my thanks and appreciation to the Honorable Dean of the College of Science, **Asst. Prof. Dr. Tahseen Saddam Fandi**, and to the respected staff of the Dean's Office, for their cooperation and valuable assistance, which helped overcome difficulties during the preparation of this thesis.

I would like to express my sincere gratitude to **Prof. Dr. Ali Qasim**, University of Basrah, for his valuable support and assistance in using the

Electrospinning device, which significantly contributed to the completion of this work. I would also like to thank , **Asst. Prof. Dr. Zaidon Tariq** for facilitating access to an appropriate laboratory environment, which enabled me to carry out my research under suitable conditions, and I express my sincere gratitude for his cooperation and support.

To my beloved **parents**, no words can describe the depth of my gratitude. Their continuous prayers, patience, unconditional love, and encouragement at every moment were a source of strength and determination for me. Without their presence, I could not have completed this journey. To them, I dedicate all possible love, respect, and gratitude.

I would also like to thank my sister, **Nadia kadhim**, for her continuous support throughout the preparation of this thesis. I am also grateful to my dear friends, **Maryam Sabri and Sadiqa Hassan**, for their cooperation and participation during various stages of the research, and for providing support and assistance when needed.

Hasnaa Al-Wahili

Summary

This study aims to develop a transdermal delivery system for baclofen, a muscle relaxant used to treat muscle spasms. Although baclofen offers significant therapeutic benefits, its clinical effectiveness is limited by its short half-life and low bioavailability when administered through conventional routes. This highlights the need for advanced strategies to enhance its absorption and therapeutic efficacy. Nanotechnology-based systems, particularly liposomes, represent one of the most promising approaches for improving drug delivery due to their ability to increase drug stability, penetrate biological barriers, and provide sustained release. Furthermore, incorporating liposomes into hydrogel matrices enhances their stability and performance.

In this research, four formulations of surfactant-modified, baclofen-loaded liposomes were prepared using the thin-film hydration method, followed by extrusion through nylon 6,6 nanofibers to obtain small unilamellar vesicles. Characterization using FT-IR, DLS, zeta potential, and FESEM confirmed successful nanoliposome formation, with particle sizes ranging from 36.67 to 172.6 nm, polydispersity indices of 0.369–0.663, and a zeta potential of –65.6 mV, along with a maximum wavelength λ_{max} of Baclofen at 218 nm.

Among the formulations, BLV₂ was selected as the optimized system based on characterization results. An *in vitro* release study was then conducted after incorporating the selected formulation into Carbopol hydrogel at different concentrations (0.5%, 1%, 1.5%) to evaluate drug release. The results demonstrated that the highest baclofen release rate occurred at a Carbopol concentration of 0.5%, which was therefore selected for subsequent *in vivo* applications.

For the animal study, twenty male rabbits were divided into four groups: a control group, a spasm-induced group administered an intramuscular

injection of lactic acid (30 mM) into the thigh muscle, an untreated spasm group, and a group treated with the baclofen nanoliposome gel (0.5%). Blood samples were collected from the ear vein as follows: from the control group after acclimatization, from the spasm-induced group 12 hours after lactic acid injection, from the untreated group after five days, and from the treated group after five days of daily baclofen nano Liposome hydrogel (0.5%) application. The collected samples were used to analyze blood ions (Ca^{2+} , K^+ , Pi), muscle damage enzymes (CK, LDH), liver enzymes (AST, ALT), and kidney function indicators (Urea, Creatinine).

The optimized formulation showed significant enzyme-inhibitory activity, with IC_{50} values of approximately 72.480 $\mu\text{m}/\text{mL}$ for CK and 86.359 $\mu\text{m}/\text{mL}$ for LDH. Statistically significant improvements ($P < 0.05$) were observed in the treated group compared to the spasm-induced groups, indicating marked reductions in muscle damage biomarkers and improved physiological parameters. These findings demonstrate that baclofen nanoliposome gel provides an effective transdermal delivery platform, ensuring sustained drug release, enhanced therapeutic efficacy, and reduced biomarkers associated with muscle spasm. This study serves as the first scientific evidence supporting the safety and efficacy of topical nanostructured baclofen for spasm management, paving the way for broader future applications in targeted transdermal drug delivery.

Contents

Titles	Page
Summary	I
Contents	III
Figures	IX
Tables	XII
Abbreviations	XIII
Chapter One Introduction	
1.Introduction	1
1.1 Transdermal Drug Delivery System (TDDS)	2
1.2 Challenges in the using of TDDS and innovative solutions	3
1.3 Liposomes	4
1.4 Mechanism of Liposomes penetration and permeation via the skin	6
1.5 Advantages and Disadvantages of Liposome	8
1.6 Classification of Liposomes	9
1.6.1 Based on Size	9
1.6.1.1 ULV- Unilamellar Vesicles	9
1.6.1.1.1 Large Unilamellar Vesicles	10
1.6.1.1.2 Small Unilamellar Vesicles	10
1.6.1.1.3 Giant Unilamellar Vesicles	10
1.6.1.2 Multilamellar Vesicles	10

Chapter One Introduction	
1.6.1.3 Multivesicular Vesicles	11
1.6.1.4 Oligolamellar Vesicles	11
1.6.2 Based on Compositions	11
1.6.2.1 Conventional Liposomes	11
1.6.2.2 Stealth Stable Liposomes	12
1.6.2.3 Actively Targeted liposomes	12
1.6.2.4 Stimuli-Responsive Liposomes	13
1.6.2.5 Bubble liposomes	14
1.7 Liposomes compositions	14
1.7.1 Steroids	15
1.7.2 Natural lipids	16
1.7.3 Synthetic lipids.	17
1.7.4 Surfactants	18
1.7.5 Polysaccharides	19
1.8 Application of Liposomes	19
1.8.1 Cancer Treatment	20
1.8.2 Cosmetic Applications	21
1.8.3 Gene Therapy	21
1.8.4 Treatment of Dermatophyte	21
1.8.5 Ocular Disorders	21
1.9 Baclofen	22

Chapter One Introduction	
1.9.1 Physicochemical properties of Baclofen	23
1.9.2 Baclofen Mechanism of Action	24
1.9.3 Motivations for Converting Baclofen to nano Liposomes-Based Topical Formulation	25
1.10 Carbopol	25
1.10.1 Motivations for Incorporation Baclofen nano Liposomes Vesicles with carbopol gel	26
1.11 Importance of <i>In Vitro</i> Studies in Evaluating Baclofen Delivery System	27
1.12 Study of the Mechanism Muscle Spasm <i>In Vivo</i>	27
1.12.1 Neuronal factors	27
1.12.2 Chemical and Ionic Factors	28
1.12.3 Mechanical Factors	28
1.13 Literature review	30
1.14 Aims of study	33
Chapter Two Materials and Methods	
2. Materials and Methods	34
2.1 Instruments	34
2.2 Materials	35
2.3 Assay kit	36
2.4 Methods	37
2.4.1 Characterization of Baclofen	37

Chapter Two Materials and Methods	
2.4.1.1 Determination of Baclofen melting point	37
2.4.1.2 Determination of λ_{\max} wavelength of Baclofen	37
2.4.1.3 Determination of Calibration Curve of Baclofen	37
2.4.2 Preparation of Baclofen nano-Liposome Vesicles	38
2.4.3 Manufacturing of Nylon 6,6 Nanofibers using Electrospinning	41
2.4.3.1 Sample preparation	41
2.4.3.2 Electrospinning	41
2.4.3.3 Application of Nylon 6,6 nanofibers	43
2.4.4 Characterization of Liposomes	43
2.4.4.1 Fourier Transform Infrared Spectroscopy (FT-IR)	43
2.4.4.2 Field Emission Scanning Electronic Microscope (FESEM)	43
2.4.4.3 Dynamic Light Scattering (DLS) Analysis	44
2.4.4.4 Zeta Potential	44
2.4.5 Preparation of Baclofen nano-Liposomes Vesicles gel	44
2.4.6 Biological Evaluation of Synthesized Baclofen nano-Liposomes Vesicles (BLV ₂) <i>In Vitro</i>	47
2.4.6.1 Determination of the effect of BLV ₂ on inhibition of Lactate Dehydrogenase (LDH) enzyme	47
2.4.6.2 Determination of the effect of BLV ₂ on inhibition of Creatine Kinase (CK) enzyme	48
2.4.6.3 Half-maximal inhibitory concentration IC ₅₀ Calculations	49

Chapter Two Materials and Methods	
2.4.6.4 <i>In vitro</i> release study of BLV ₂ Gel	49
2.4.7 Biological Evaluation of Synthesized BLV ₂ Gel <i>in Vivo</i>	50
2.5.7.1 Experimental Animals	50
2.4.7.2 Division of Experimental Animals	50
2.4.7.3 The method of inducing muscle spasm	51
2.4.7.4 Sample collected	51
2.4.7.5 Biochemical parameters	54
2.4.7.5.1 Creatin Kinase enzyme	54
2.4.7.5.2 Lactate Dehydrogenase enzyme	54
2.4.7.5.3 Aspartate Aminotransferase (AST) enzyme	55
2.4.7.5.4 Alanine Aminotransferase (ALT) enzyme	55
2.4.7.5.5 Calcium	56
2.4.7.5.6 Potassium	56
2.4.7.5.7 Phosphorus	56
2.4.7.5.8 Urea	57
2.4.7.5.9 Creatinine	57
2.4.7.6 Statistical Analysis	58
Chapter Three Results and Discussions	
3. Results and Discussions	59
3.1 Characterization of Baclofen	59

Chapter Three Results and Discussions	
3.1.1. Baclofen melting point	59
3.1.2. Wavelength maximum (λ_{\max}) of Baclofen	59
3.1.3 Baclofen Calibration Curve	60
3.2 Characterization of liposomes	61
3.2.1 Fourier Transform Infrared Spectroscopy (FTIR)	61
3.2.2 Field Emission Scanning Electronic Microscope (FESEM) of Baclofen Liposomes Vesicles	63
3.2.3 Dynamic Light Scattering (DLS) Analysis of Baclofen Liposomes Vesicles	65
3.2.4 Field Emission Scanning Electronic Microscope (FESEM) of BLV ₂ Gel	68
3.2.5 Zeta Potential Analysis	69
3.3 Field Emission Scanning Electronic Microscope (FESEM) of Nylon 6,6 Nanofibers	71
3.4 Applications for Baclofen nano Liposomes Vesicles BLV ₂ <i>In vitro</i>	73
3.4.1 Determination of the effect of BLV ₂ on inhibition of Lactate Dehydrogenase enzyme (LDH)	73
3.4.2 Determination of the effect of BLV ₂ on inhibition of Creatine Kinase enzyme (CK)	76
3.4.3 Half-maximal inhibitory concentration IC ₅₀ Calculations	79
3.4.4 <i>In vitro</i> release of Baclofen from BLV ₂ Gel in PBS for 1-10 h	80
3.5 Applications for BLV ₂ Gel <i>in vivo</i>	81
Chapter Four Conclusions and Recommendations	
Conclusions	88
Recommendations	90
References	91

Figures

Number and Title of the Figure	Page
Figure (1-1): A scheme representing the methods of Transdermal Delivery Systems	4
Figure (1-2) : Structure of liposomes	5
Figure (1-3) : Mechanism of penetration of modified liposomes across the skin layers	7
Figure (1-4): Main advantages and disadvantages of liposomes	8
Figure (1-5): Types of liposomes based on size	9
Figure (1-6):Chemical structure of Steroids (cholesterol, β -sitosterol)	15
Figure (1-7): Chemical structures of natural phospholipids used for liposome preparation	16
Figure (1-8) : Chemical structures of synthetic phospholipids used for liposome preparation	17
Figure (1-9):Structure of surfactants A) Polysorbate 80 B) Sodium deoxycholate	18
Figure (1-10): Schematic representation of the main therapeutic applications of liposomes	20
Figure (1-11): Baclofen Mechanism of Action	24
Figure (1-12): Chemical structure of Carbopol	26
Figure (2-1): Steps for preparing Baclofen nano Liposomes Vesicles	39
Figure (2-2) : Buechner funnel for filtration of liposomes	40
Figure (2-3) :Scheme shows the preparation of nanoliposomes by thin film hydration method	40
Figure (2-4) : Diagram of an electrospinning Device at the laboratory scale	42

Number and Title of the Figure	Page
Figure (2-5) : Image for Deposition of Nylon 66 Electrospun Nanofibers on aluminum foil	42
Figure (2-6): (A) After soaking Carbopol 934 in distilled water (B,C) After adding glycerol, Tween 20 and the optimum liposome formulation (D) After adjusting the pH of the gel using triethanolamine	46
Figure (2-7): Steps for lactic acid injection	52
Figure (2-8): Steps to draw blood from the atrial vein	52
Figure (2-9): Steps to treat muscle spasms by Baclofen gel	52
Figure (2-10): General schematic diagram of experimental group distribution and biochemical parameters	53
Figure (3-1): Absorption Spectrum of Baclofen in PBS	59
Figure (3-2) : Calibration Curve of Baclofen in PBS	60
Figure (3-3) : FT-IR Spectrum of the Baclofen and Liposomes	62
Figure (3-4): Field Emission Scanning Electron Micrographs (FESEM) of Baclofen Liposome Vesicles at Different Magnifications: (A) 100 nm scale; (B) 200 nm scale, (C) 500 nm scale, (D) 10 μ m scale.	64
Figure (3-5): Size Distribution by Intensity of the BLV ₁	66
Figure (3-6): Size Distribution by Intensity of the BLV ₂	67
Figure (3-7): Size Distribution by Intensity of the BLV ₃	67
Figure (3-8): Size Distribution by Intensity of the BLV ₄	67
Figure (3-9): (A) Field Emission Scanning Electron Micrographs of BLV ₂ Gel,(B) Particles Diameters Distribution	69
Figure (3-10) : Zeta Potential of BLV ₂	70
Figure (3-11) : Zeta Potential BLV ₂ gel	70

Number and Title of the Figure	Page
Figure (3-12): FESEM Images of Nylon 6,6 Nanofibers at Different Magnifications (a) 10 μm scale, (b) 1 μm scale, (c) 500 nm scale	72
Figure (3-13): (A) Field Emission Scanning Electron Micrographs of Nylon 6,6 Nanofibers Showing Diameter Measurement, (B) Nanofibers Diameters Distribution	72
Figure (3-14): Michaelis—Menten Equation's curve between the rate of enzymatic reaction V and Substrate concentration [S]	74
Figure (3-15): (Line Weaver Burk Plot) Equation of LDH enzyme without and with inhibitor	75
Figure (3-16): Michaelis—Menten Equation's curve between the rate of enzymatic reaction V and Substrate concentration [S]	77
Figure (3-17): (LineWeaver Burk Plot) Equation of CK enzyme without and with inhibitor	78
Figure (3-18): IC ₅₀ of BLV ₂ as inhibitor to LDH- enzyme	79
Figure (3-19): IC ₅₀ of BLV ₂ as inhibitor to CK-enzyme	79
Figure (3-20) : <i>In vitro</i> release for BFN from BLV ₂ gel With Different concentrations of Carbopol 934 in PBS	81
Figure (3-21): Calcium , Potassium and Phosphorus concentrations in rabbit groups (Control , Spasm-Induce, Untreated Spasm, Treated)	83
Figure (3-22): CK, LDH, ALS and ALT enzyme activities in rabbit groups (Control , Spasm-Induce, Untreated Spasm, Treated)	85
Figure (3-23): Urea and Creatinine concentrations in rabbits groups (Control , Spasm-Induce, Untreated Spasm, Treated)	87

Tables

Number and Title of the Table	Page
Table (1-1): Types of stimuli-responsive liposomes	14
Table (1-2) : Physicochemical properties of Baclofen	23
Table (2-1): Devices used in this study	34
Table (2-2): Materials used in this study	35
Table (2-3): Manual analyses used in this experiment	36
Table (2-4) : Formula for preparation of Baclofen nano Liposome vesicles	39
Table (2-5) : Composition of Baclofen nano Liposome Vesicles Gel Formulations (BLVG1, BLVG2, and BLVG3)	45
Table (3-1): Graph data of Baclofen in (PBS) pH 6.8	60
Table (3-2): All Formulation Hydrodynamic diameters and PDI	66
Table(3-3):Substrate concentrations values and enzymatic reaction rate of LDH Before adding Baclofen nano Liposome vesicles As an inhibitor	74
Table (3-4): The estimated effectiveness of Baclofen nano Liposome vesicles in inhibiting the LDH enzyme was 356 UI/L	74
Table (3-5): Substrate concentrations values and enzymatic reaction rate of LDH after adding Baclofen nano Liposome vesicles as an inhibitor	75
Table (3-6):The kind of inhibition for Baclofen nano Liposome vesicles affecting the LDH enzyme	75
Table (3-7) : Substrate concentrations values and enzymatic reaction rate of CK Before Baclofen nano Liposome vesicles as an inhibitor	77
Table (3-8): The estimated effectiveness of Baclofen nano Liposome vesicles in inhibiting the CK enzyme was 440 UI/L	77

Number and Title of the Table	Page
Table (3-9): Substrate concentrations values and enzymatic reaction rate of CK after adding Baclofen nano Liposome vesicles as an inhibitor	78
Table (3-10):The kind of inhibition for Baclofen nano Liposome vesicles affecting the CK enzyme	78
Table (3-11): Percentage release of BLV ₂ Gel	80
Figure (3-21): Calcium , Potassium and Phosphorus concentrations in rabbit groups (Control , Spasm-Induce, Untreated Spasm, Treated)	83
Figure (3-22):CK, LDH, ALS and ALT enzyme activities in rabbit groups (Control , Spasm-Induce, Untreated Spasm, Treated)	85
Figure (3-23): Urea and Creatinine concentrations in rabbits groups (Control ,Spasm-Induce, Untreated Spasm, Treated)	86

Abbreviations

Abbreviations	Key
ANOVA	Analysis of Variance
AIDS	Acquired Immunodeficiency Syndrome
AST	Aspartate Aminotransferase
ALT	Alanine Aminotransferase
ADP	Adenosine Diphosphate
AMP	Adenosine Monophosphate
ATP	Adenosine Triphosphate
BFN	Baclofen

Abbreviations	Key
BLV	Baclofen nano Liposomes Vesicles
BLVG	Baclofen nano Liposomes Vesicles Gel
CK	Creatin Kinase
Conc	Concentration
CP	Creatine Phosphate
DLS	Dynamic Light Scattering
DMPC	Dimyristoylphosphatidylcholine
DOPC	1,2-dioleoyl-sn-glycero-3-phosphocholine
DOPE	1,2-Dioleoyl-sn-glycero-3-phosphoethanolamine
DOTAP	1,2-Dioleoyl-trimethylammonium-propane(chloride salt)
DTX-LP-G	Docetaxel Liposomes Gel
ΔA	Delta Absorbance
EDTA	Ethylenediaminetetraacetic Acid
EPR	enhanced permeability and retention effect
FAD	Food and Drug Administration
FESEM	Field Emission Scanning Electronic Microscope
FT-IR	Fourier Transform Infrared Spectroscopy
GABA-B	Gama-aminobutyric acid-B
GTCS	Generalized tonic-clonic seizures
GTO	Golgi Tendon Organ

Abbreviations	Key
GUV _s	Giant unilamellar vesicles
G6P	Glucose-6-Phosphate
HK	Hexokinase
HSPC	Hydrogenated soybean phosphatidylcholine
IC ₅₀	Half-maximal inhibitory concentration
IU/L	International units per liter
K _m	Michaelis constant
KV	Kilovolt
LSD	Least Significant Difference
LDH	Lactate dehydrogenase
LUV _s	Larg Unilamellar vesicles
Mm	Millimolar
MLV _s	Multilamellar vesicles
MVV _s	Multivesicular vesicles
μg/mL	Microgram per milliliter
mg/mL	Milligram per milliliter
NAC	N-Acetylcysteine
NADH	Nicotinamide Adenine Dinucleotide
NPs	Nanoparticles
OLV _s	Oligolamellar vesicles

Abbreviations	Key
PA	Phosphatidic acid
PBS	Phosphate buffer saline
PC	Phosphatidylcholine
PE	Phosphatidylethanolamine
PEG	Polyethylene Glycol
PG	Phosphatidylglycerol
PI	Phosphatidylinositol
POPC	1-palmitoyl-2-oleoyl-sn-glycero-3-phosphocholine
ppm	Part Per million
PS	Phosphatidylserine
Rpm	Revolutions Per Minute.
S	Substrate
SC	Stratum Corneum
SD	Standard Deviation
SDC	Sodium deoxycholate
SERCA	Sarcoplasmic/Endoplasmic Reticulum Ca^{2+} -ATPase
SR	Sarcoplasmic Reticulum
Sp80	Span80
SPSS	Statistical Package for the Social Sciences
SUV _s	Small unilamellar vesicles

Abbreviations	Key
TDDS	Transdermal Drug Delivery System
T _m	Phase Transition Temperature
Tw80	Tween 80
ULV _s	Unilamellar vesicles
UV-vis	Ultraviolet-Visible Spectroscopy
V	Rate of enzymatic reaction
V _{max}	Velocity Maximum
λ _{max}	Maximum Wavelength

Chapter One

Introduction

1.Introduction

The constant development of technologies and materials resulting from the collaboration between sectors such as bioengineering, physics, chemistry, materials science, pharmacology, and not least medicine, has allowed the advancement of increasingly efficient drug delivery tools [1] . Researchers and clinicians from all over the world are continuously pursuing the design and implementation of increasingly personalized, safe, and cost-effective therapeutic solutions as new pharmacologically active molecules and nanoparticles. Recently, the application of nanoparticles (NPs) has been established to develop drug delivery efficiency [2], among nano-delivery systems, liposomal drug delivery systems have emerged. These systems have morphological, optical, mechanical, and electrical properties that enhance drug stability and solubility by prolonging circulation time in the bloodstream and improving delivery efficiency. The exploration of liposomal formulations for drug delivery has gained significant traction over the years, reflecting a growing interest in optimizing therapeutic efficacy through advanced delivery systems. This literature review delves into the intricate landscape of liposome-based technologies, highlighting their evolution, design strategies, and applications in both *In vitro* and *In vivo* settings. The foundational studies discusses the safety and efficacy of multivesicular liposomes, particularly in the context of baclofen administration. These investigations sets the stage for understanding how liposomal formulations can enhance drug delivery methods in clinical settings. Likewise, the findings emphasize the potential of optimizing lipid excipients to enhance drug exposure, thereby laying the groundwork for subsequent innovations in liposome drug delivery systems [3]. In this context, transdermal delivery systems have emerged as a modern approach

in the field, offering an innovative solution to overcome the traditional limitations associated with conventional drug delivery methods .

1.1 Transdermal Drug Delivery System (TDDS)

The transdermal drug delivery system (TDDS) is a new pharmaceutical strategy for drug administration, It is highly effective, offering several advantages over conventional administration methods. Conventional drug delivery system formulations require the use of high doses and longer treatment durations to achieve desired therapeutic results, and long-term systems may cause serious side effects, thus causing decreased patient adherence to treatment [4]. Due to its many benefits, the oral route is generally considered the most appropriate, convenient, and optimal method of drug delivery, this method has significant disadvantages, including gastrointestinal enzymatic degradation, gastrointestinal disturbances, limited absorption, and low bioavailability. In the case of injectable drugs, needle phobia is a common psychological condition in children and adults, as well as the risk of infection during drug administration [5]. To overcome these issues, alternative delivery systems have been developed, of which the transdermal drug delivery system (TDDS) is the optimal method for these drugs [6]. The skin is the body's first line of defense as it is the largest organ of the human body and acts as a natural shield, protecting it from direct exposure to toxins, harmful pathogens and environmental viruses, as well as protecting against water loss and maintaining the stability of the internal and external environment [7].

This system has several advantages over oral and parenteral methods, including direct effect on the skin, delivery of active ingredients directly to damaged tissues, bypassing the first-pass effect of the liver, good absorption, maintaining stable drug concentrations in the blood, low incidence of side effects, and the ability to discontinue treatment quickly [8].

1.2 Challenges in the using of TDDS and innovative solutions

Despite the advantages of a transdermal drug delivery system, the biggest barrier to the adoption of TDDS is the presence of an outer layer of skin that is resistant to active substances. The stratum corneum (SC) consists of flat, keratinized cells that act as a primary barrier for active substances in drugs and cosmetics [9]. In addition, the physical and chemical properties of the drug such as molecular weight, polarity, dosage form, and solubility are also a barrier to skin penetration. Therefore, drug formulation is an important factor in developing a dosage form that ultimately reaches the target site effectively [4].

To overcome this barriers or obstacles, different carriers have been developed [10]. Nanomodification of drugs and other active substances improves therapeutic efficacy while minimizing the risk of side effects. Vesicular systems such as liposomes are one way to increase drug permeation. Currently, interest in topical drug delivery *via* liposomes has increased [11]. However, conventional liposomes are unable to penetrate deeply into the skin due to their large particle size [8]. To address this limitation, modified liposomes were prepared by incorporating surfactants to enhance their elasticity and improve transdermal penetration. This modification was based on previous research demonstrating that surfactants can increase the flexibility of liposomes and their efficiency in transdermal drug delivery [12]. In addition to the liposomal system, various other TDDS have been developed, including mechanical, physical, chemical, electrical, and lipid-based carrier methods, as illustrated in figure (1-1) [13] .

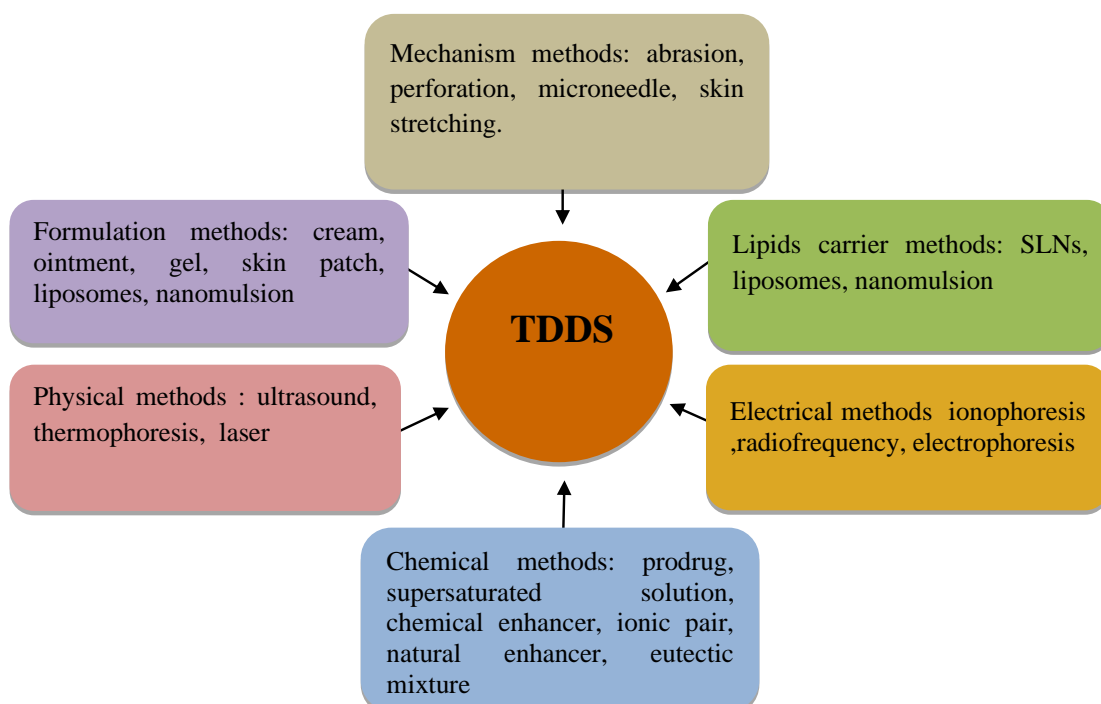


Figure (1-1): A scheme representing the methods of transdermal delivery systems

1.3 Liposomes

Liposomes are spherical structures composed of one or more bilayers of phospholipids containing aqueous compartments at their center, as shown in figure (1-2). Their sizes range from 30 nm to several micrometers, depending on the need for their synthesis [14].

Studies have shown that phospholipids spontaneously form closed structures when hydrated in aqueous media, forming what are known as spherical vesicles. Due to the amphipathic nature of phospholipids in aqueous media, their thermodynamic and self-assembling properties lead to the arrangement of their hydrophobic components within spherical bilayers, known as lamellae [15].

The discovery of liposomes began in the early 1960s by Bangham and colleagues when they observed the formation of lipid vesicles upon the

interaction of egg lecithin smears with water. These vesicles were initially called thick mesophylls and later renamed liposomes. They were initially used as artificial membrane models that mimicked simple biological membranes to study transport functions, mechanisms, and permeability properties, as well as to understand behaviors such as cell adhesion and kinetic membrane fusion [14].

Liposomes were among the first drug delivery systems to be successfully applied in clinical practice. Since their first development in 1965, these systems have undergone significant development in recent years [16] .

They were quickly recognized as a potential drug delivery system. This has led to intensified research into the design of specialized formulations for multiple purposes, particularly in the medical and pharmaceutical fields. The use of liposomes has also expanded to include applications in cosmetics, the food industry, and agriculture. The delivery of therapeutics via liposomes contributes to changing their biodistribution pattern, significantly improving the therapeutic index of various drugs [14]. Various routes of administration for liposomes have been developed, such as intravenous, oral, pulmonary, transdermal, nasal, and ophthalmic routes [17].

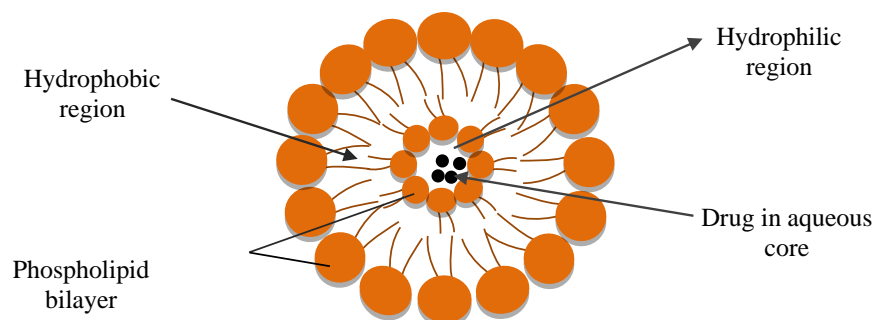


Figure (1-2) : Structure of liposomes.

1.4 Mechanism of Liposomes Penetration and Permeation *via* the Skin

The skin is the primary barrier to topical medication, significantly hindering the absorption of pharmaceutical compounds. Studies have demonstrated the ability of vesicle systems to successfully deliver medication into or through the skin [18].

A series of successive reactions occur with the skin when vesicle systems are applied topically. The concentration of non-volatile active substances on the surface of the skin increases when water evaporates, and when this concentration reaches the degree of saturation, a moisture gradient occurs towards the vesicles, which leads to the difference of water in the outer layers of the skin from the inner layers, for example, the water content in the outer layers of the skin increases from about 10% to 30% compared to the inner layer of the skin, which contains about 75% water, and this water gradient promotes the spread and penetration of vesicles into the skin significantly [19].

These vesicles transfer through the skin toward the inner water-rich layers as a result of the hydration gradient caused by water evaporation from the skin surface, in addition to the high elasticity and hydrophilicity of these vesicles. This gradient acts as a pulling force that drives the vesicles to penetrate the stratum corneum. The movement of intercellular fluid in the skin also contributes to this process. When the hydration gradient is absent, as occurs when the skin is occluded by an impermeable medium, the transport mechanism is completely disrupted, and thus the stratum corneum cannot be penetrated by Vesicles systems [20].

The stratum corneum acts as a barrier to prevent foreign substances from entering the body. This layer contains two hydrophilic pathways: an

inter-cluster pathway, which has lower penetration resistance and constitutes approximately 20% of the pathway area, and an inter-corneal pathway, which resists penetration higher. The latter is more abundant, comprising more than 80% of the pathway area, and has a tortuous shape [21]. Under the stratum corneum is the living epidermis, in addition to the dermis, which is the thickest layer of the skin and contains blood and lymphatic vessels, collagen fibers, nerves, and then subcutaneous adipose tissue, consists of adipocytes to which collagen fibers are attached. In recent years, we have seen increasing interest in exploring new methods to improve the delivery of drugs locally, either within or across the skin. One such approach, vesicle-based systems, has demonstrated significant success compared to conventional systems [18]. Previous research has shown that conventional, unmodified vesicles exhibit limited ability to deliver drugs through the skin, as they tend to accumulate in the upper part of the stratum corneum with little or no penetration into the deeper layers [22]. Therefore, the conventional vesicles were modified by incorporating surfactants. These substances increase the flexibility of the vesicles [23], and in addition change the lipid bilayers of the vesicles, which increases their deformability and thus enables these vesicles to pass through narrow pores [24]. As shown in figure (1-3).

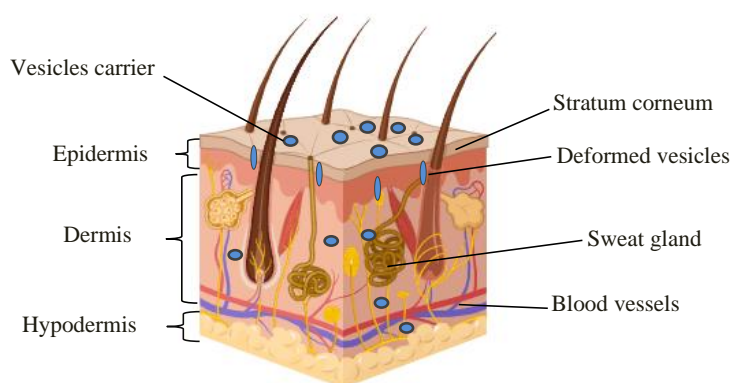


Figure (1-3) : Mechanism of penetration of modified liposomes across the skin layers.

1.5 Advantages and Disadvantages of Liposomes

Liposomes are considered one of the nanocarrier systems used in drug delivery due to their multiple features in enhancing drug efficacy and reducing damage to healthy tissues [25][26]. However, their use may also be associated with some technical and production-related limitations [27]. Figure (1-4) illustrates the major advantages and disadvantages of liposomes.

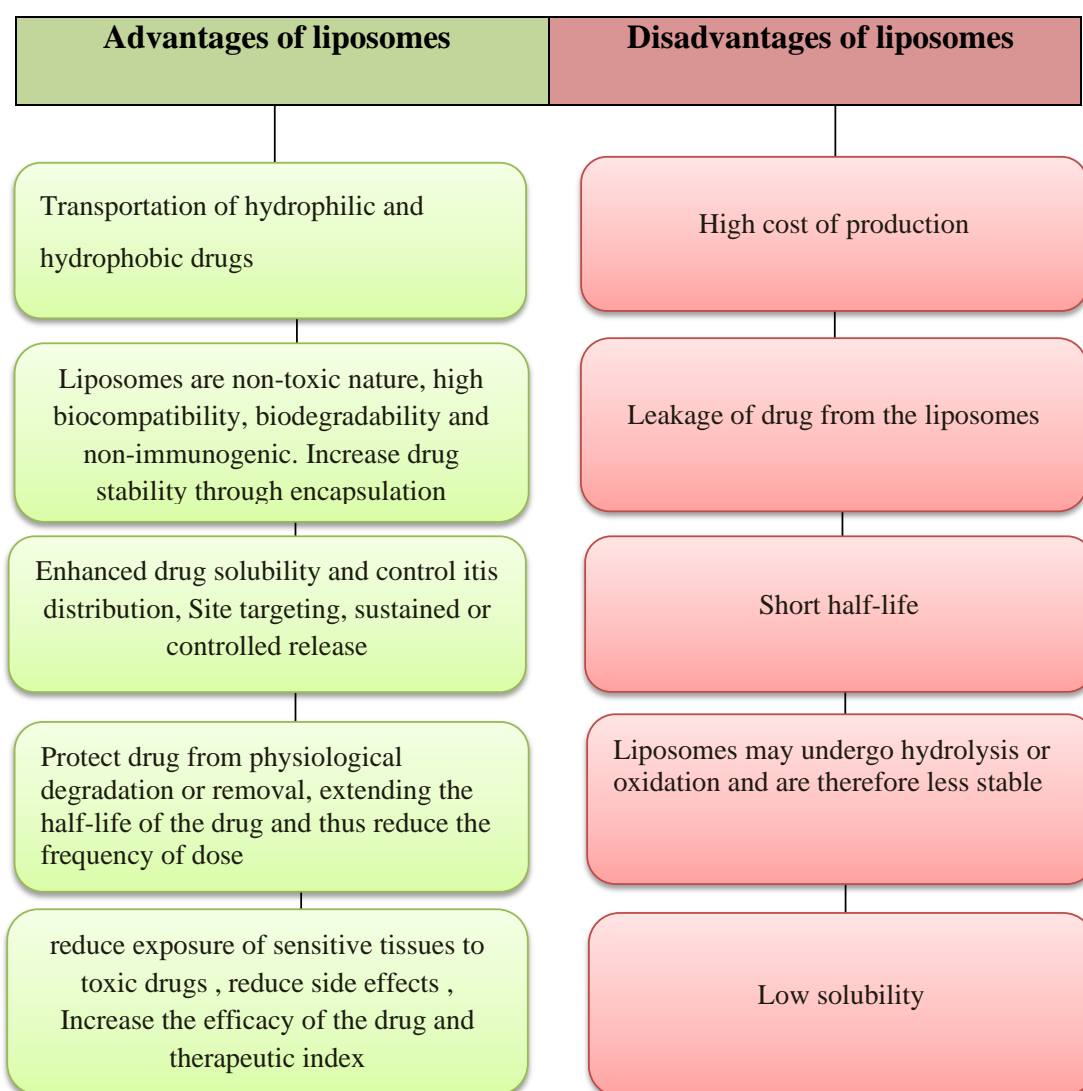


Figure (1-4): Main advantages and disadvantages of liposomes

1.6 Classification of Liposomes

1.6.1 Based on Size

It can be classified into four types [26], as shown in the figure (1-5)

- ULV_S - Unilamellar vesicles
- MLV_S - Multilamellar vesicles
- MVV_S - Multivesicular vesicles
- OLV_S - Oligolamellar vesicles

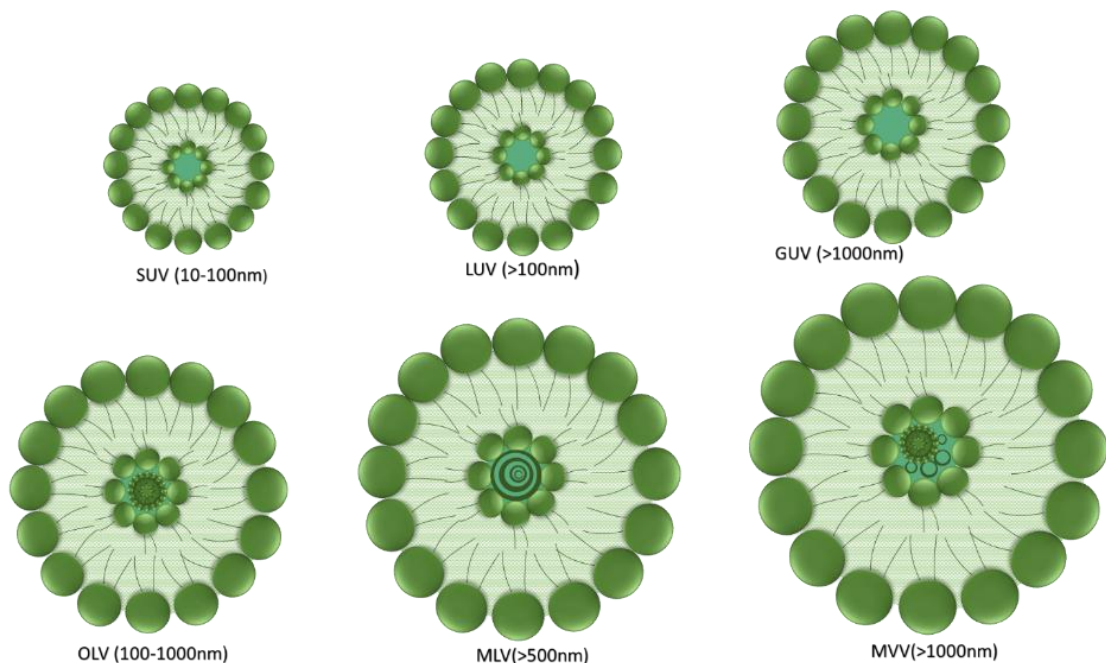


Figure (1-5): Types of liposomes based on size

1.6.1.1 ULV- Unilamellar vesicles

Unilamellar vesicles are the most common type of liposome. They are characterized by a single bilayer of phospholipids surrounding an aqueous solution [28], offering a greater ability to encapsulate hydrophilic compounds [29]. There are several methods for preparing this type of

liposome, including ultrasound, extrusion through filters, and freeze-thaw cycles, their size range from 10-1000 nm [30].

Unilamellar vesicles can be divided into three categories based on their size [31][32].

- LUV_s -Large unilamellar vesicles
- SUV_s -Small unilamellar vesicles
- GUV_s -Giant unilamellar vesicles

1.6.1.1.1 Large unilamellar vesicles

These are vesicles composed of a single bilayer, Its size reaches (>100nm) [33]. They have a high capacity to retain aqueous components, making them suitable for hydrophilic drugs. This type of vesicle can be prepared using reverse-phase evaporation, detergent dialysis, extrusion, ether injection, and ultrasound [34].

1.6.1.1.2 Small unilamellar vesicles

They are small spherical vesicles surrounding an aqueous core, composed of a single bilayer, their size range from 10-100 nm. They are prepared using ultrasound or extrusion technology [35] .

1.6.1.1.3 Giant unilamellar vesicles

They are very large vesicles composed of a single bilayer, exceeding 1000nm in size [29]. This type of liposome can be prepared using electrophoresis, physiological force-regulating solutions, and osmotic shock techniques [30]. This type of vesicle is used in biophysical studies and cell membrane simulation experiments and is also widely used in studies of synthetic cell [36].

1.6.1.2 Multilamellar vesicles

They are vesicles composed of two or more co lipid bilayers concentric ,arranged in an onion-like shape, suitable for encapsulating lipophilic compounds. Their size may reach (>500) [37]. These multilamellar vesicles are prepared spontaneously when dry lipid membranes are moistened with an aqueous solution in the presence of an organic solvent [38].

1.6.1.3 Multivesicular vesicles

It consists of several small, non-concentric vesicles enclosed within a single bilayer. It is ideally suited for encapsulating large volumes of hydrophilic materials [37]. This type of liposome reaches a size of (>1000) [39].

1.6.1.4 Oligolamellar vesicles

They are vesicles composed of several concentric lipid bilayers with relatively larger diameters compared to SUVs. They are intermediate structures between MLVs and SUVs, and provide a compromise between the size homogeneity of SUVs and the stability of MLVs. This type of vesicle is formed through the hydration of lipid membranes [35], and Its size ranges between 100-1000nm [17].

1.6.2 Based on Compositions

Liposomes can be categorized, according to their compositional characteristics, into several types, including conventional liposomes [40], stealth liposomes [41], actively targeted liposomes [42], stimuli-responsive liposomes [43], and bubble liposomes [44].

1.6.2.1 Conventional liposomes

Conventional liposomes are the first generation used in therapeutic applications. These liposomes are manufactured from natural or synthetic phospholipids, with or without cholesterol [16].

Wu et al found that adding cholesterol to liposomes made from hydrolyzed soybean phosphates resulted in a decrease in the rigidity of the liposome membrane. Studies showed that liposomes of medium rigidity were able to penetrate tumors well, enhancing their therapeutic efficacy [45].

Keddah et al studied how the permeability and fluidity of the liposome membrane were affected by cholesterol concentration. The study showed an increase in the average size of liposomes with increasing cholesterol concentration, leading to a change in the shape of the vesicles from irregular to spherical and nanoscale. Furthermore, the fluidity of the bilayer decreased in the presence of cholesterol [46].

1.6.2.2 Stealth Stable Liposomes

Stealth stabilized liposomes are the second generation of liposomes. This type of liposome has shown a longer half-life in the bloodstream compared to conventional liposomes [47].

This type of liposome is characterized by coating the surface of the liposome membrane with hydrophilic synthetic polymers such as poly ethylene glycol (PEG) or chitosan. Coating the liposomes with PEG creates a steric barrier between them and blood components [48], which reduces the uptake of cryptic liposomes by mononuclear macrophages [47]. However, one disadvantages of these liposomes is their random distribution in the body, which means the encapsulated compounds cannot selectively reach the target cells [49]. Stealth stabilized liposomes have also demonstrated efficacy in both chemotherapy and gene therapy [50].

1.6.2.3 Actively Targeted Liposomes

Actively targeted liposomes this type of liposome represents the third generation. This type of liposome enhances the selectivity of liposome interactions with diseased cells. It also stimulates phagocytosis via cell surface receptors and enables the direct delivery of liposome contents to the target site [51]. Through passive targeting, liposomes can accumulate in tumor tissue within a period typically ranging from 24 to 48 hours. This is attributed to the enhanced permeability and retention (EPR) effect exhibited by tumor blood vessels [52]. However, one drawback of passive targeting is that it does not provide cellular targeting alone, meaning it does not distinguish between normal and cancer cells [53]. As a result, liposomes have been shown to actively target cancer cells by binding the liposomes to antibodies, which are specific to the endothelial cells of tumor or cancerous blood vessels [52]. A new type of immunoliposome was designed by Maruyama et al. in 1999. Suspended immunoliposomes by binding antibodies to the immunoliposome at the distal end of the PEG chain. Suspended immunoliposomes showed significantly higher targeting compared to conventional liposomes, both in targeting lung endothelial cells and in accumulating within solid tumors. This is attributed to the presence of free PEG chains not arranged by antibodies, which reduce the uptake of liposomes by ERS, which contributes to prolonging their survival time in the blood and increasing their concentration at the target site [54].

1.6.2.4 Stimuli-responsive Liposomes

Stimuli-responsive liposomes are nano systems that release their drug payload to the target site in response to stimuli they are exposed to [43]. These stimuli may be internal, such as changes in pH, redox reactions, or enzyme activity. Or external stimuli, such as changes in temperature,

magnetic fields, ultrasound, or light [55]. As shown in table (1-1) the most common types of stimuli-responsive liposomes.

Table (1-1): Types of stimuli-responsive liposomes [56].

Stimuli-responsive liposomes	Stimuli
pH-sensitive liposomes	Change in Ph
Enzyme-responsive liposomes	The enzymes amidase, esterase, and protease
Redox-sensitive liposomes	Peroxides, hydroxyl radicals, singlet oxygen, and reactive oxygen species (ROS)
Light-sensitive liposomes	near infrared, or visible light, UV Irradiation
Temperature-sensitive liposomes	Microwave ablation or radiofrequency

1.6.2.5 Bubble Liposomes

Bubble liposomes are thin, spherical, gas-filled particles consisting of a core and a shell. Of shell include silver, proteins, surfactants, lipids, polymers, or sugars. Air and other gases fill the core, and their sizes range from 1-10 μ m [57]. These liposomes are expected to be used in developing innovative gene and drug delivery applications, as their surfaces can be adapted to carry a variety of drugs [58]. Bubble liposomes containing nitric oxide are a promising option for intravenous therapy, as they prevent nitric oxide from reacting with hemoglobin [51]. Oxygen bubble liposomes deliver high concentrations of oxygen to the lungs, making them a promising treatment for hypoxia in tumors [53].

1.7 Liposomes Compositions

Natural or synthetic phospholipids can be used to prepare liposomes. The properties of liposomes such as size, stability, fluidity, charge and hardness are greatly affected by their lipid composition [59], and thus the lipids used in the formation of liposomes are classified :

1.7.1 Steroids

Steroids are hydrophobic lipids compounds consisting of four interconnected carbon rings. Based on this structure, different chemical groups are associated with them to give several types of steroids [60].

The most important steroids used in the preparation of liposomes are cholesterol and β -sitosterol as shown in the figure (1-6). Cholesterol is the most commonly used steroid in the preparation of liposomes, as cholesterol reduces the leakage of the drug from the liposomes, increases their stability and duration of stay in the body and enhances the rigidity of the lipid membrane. and β -sitosterol may be used as a substitute for cholesterol. In a comparison of the effects of beta-sitosterol and cholesterol on liposome membrane properties, they discovered that both steroids produce significant changes in particle size, decrease the phase transition temperature (T_m) and entropy, increase the absolute zeta potential, and decrease the fluidity of the liposome membrane [61].

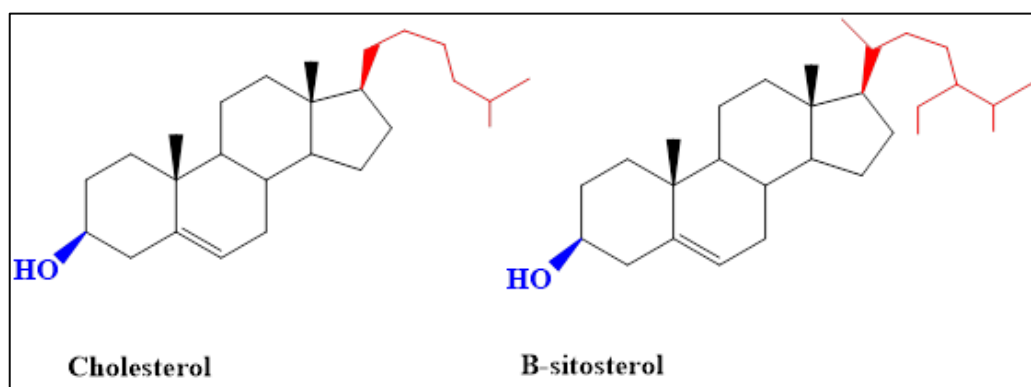


Figure (1-6): Chemical structure of Steroids (cholesterol , β -sitosterol) [62].

1.7.2 Natural lipids

Natural lipids are lipid compounds derived from natural sources such as egg yolks or soybeans. They are primarily composed of glycerophospholipids. These phospholipids consist of a glycerol molecule linked to a phosphate group and two fatty acid chains. The phosphate group can be linked to a small organic molecule such as choline. Phospholipids are classified according to the polar nature of their organic group into several types, including: phosphatidylcholine (PC), phosphatidylserine (PS), phosphatidylethanolamine (PE), phosphatidylglycerol (PG), phosphatidic acid (PA), and phosphatidylinositol (PI) [29]. As shown in figure (1-7).

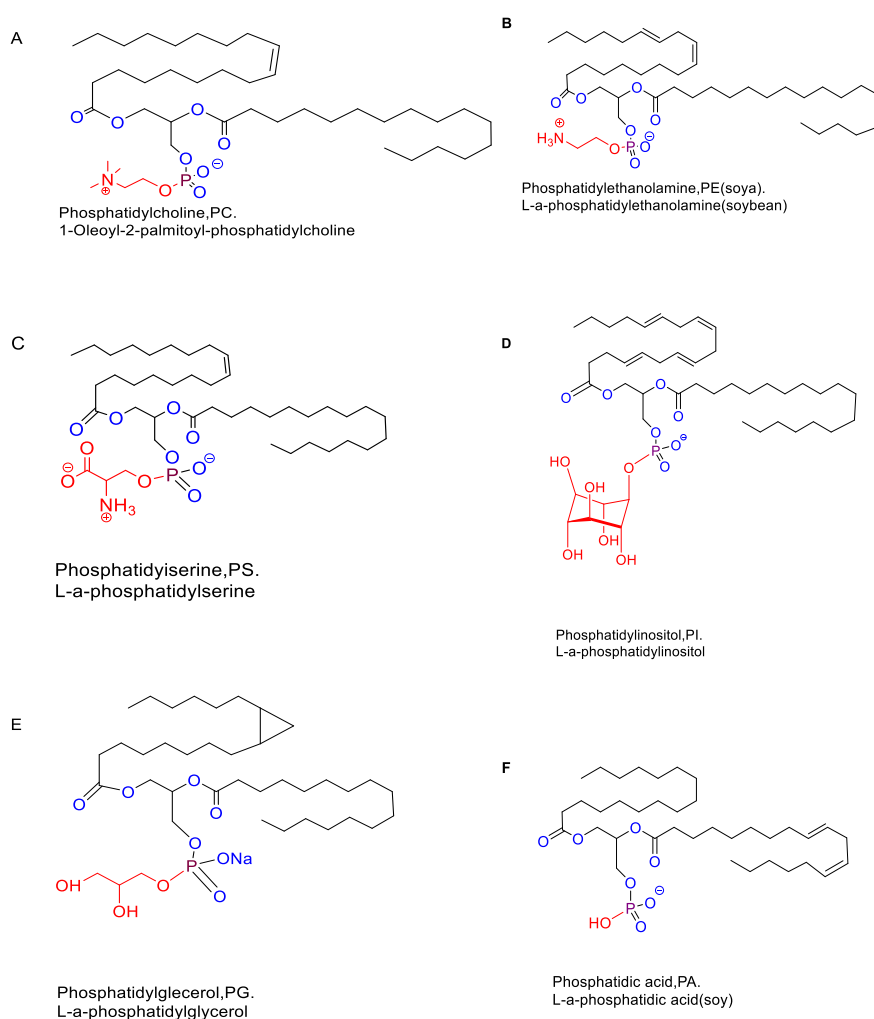


Figure (1-7): Chemical structures of natural phospholipids used for liposome preparation [51].

1.7.3 Synthetic lipids

Synthetic lipids are lipid compounds that do not exist in nature but are manufactured commercially. The polar and nonpolar parts of natural phospholipids are chemically modified to form an unlimited number of synthetic phospholipids. Saturated fatty acids, such as stearic and palmitic, are the majoring components of synthetic phospholipids [51]. Examples of synthetic lipids are 1,2-Dioleoyl-sn-glycero-3-phosphoethanolamine (DOPE), 1,2-Dioleoyl-trimethylammonium-propane(DOTAP), Dimyristoyl phosphatidylcholine (DMPC) Hydrogenated soybean phosphatidylcholine (HSPC), 1-palmitoyl-2-oleoyl-sn-glycero-3-phosphocholine(POPC), 1,2-dioleoyl-sn-glyceron phosphocholine (DOPC) [60]. AS shown in figure (1-8).

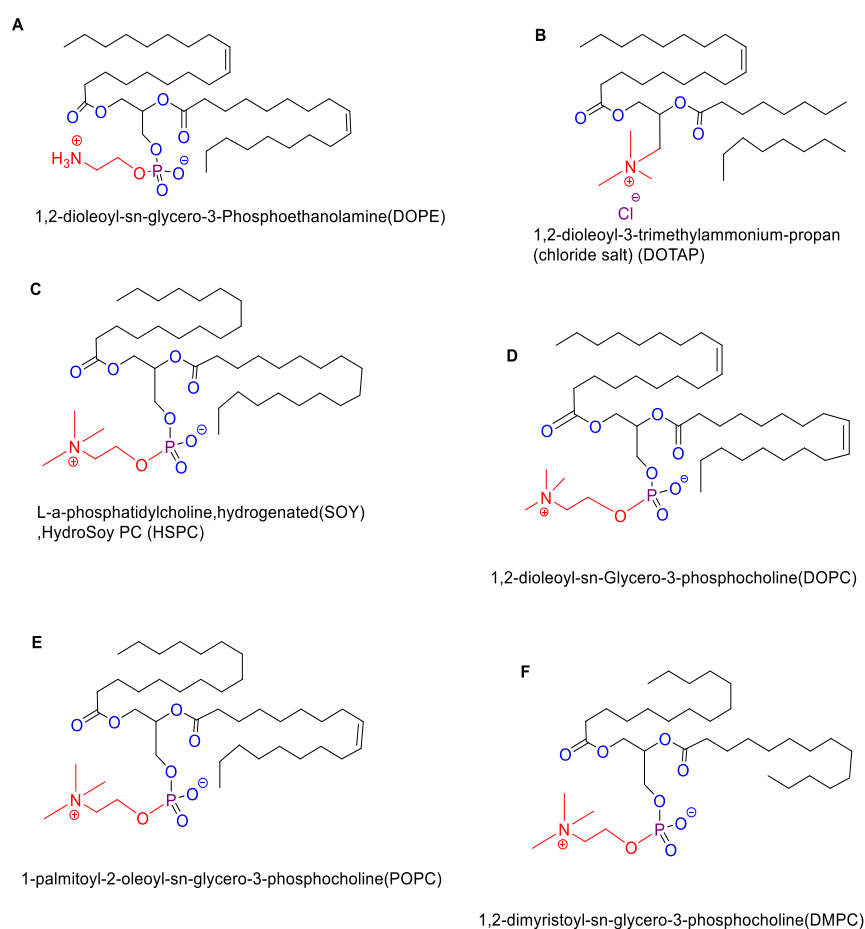


Figure (1-8) : Chemical structures of synthetic phospholipids used for liposome preparation [51].

1.7.4 Surfactants

They are amphipathic molecules meaning they contain a hydrophilic part and a hydrophobic part, and have a single acyl chain [63]. Surfactants modify the encapsulation and release properties of liposomes by reducing the surface tension between immiscible phases [64]. They also make liposomes more elasticity and less rigid, increasing their deformability, enabling them to pass through skin barriers more easily. They also help produce smaller vesicles [65]. AS shown in figure (1-9).

The most commonly used surfactants [66] :

- Polysorbate 80 (Span 80, Tween 80)
- Tween 20 , Span 60
- Sodium deoxycholate

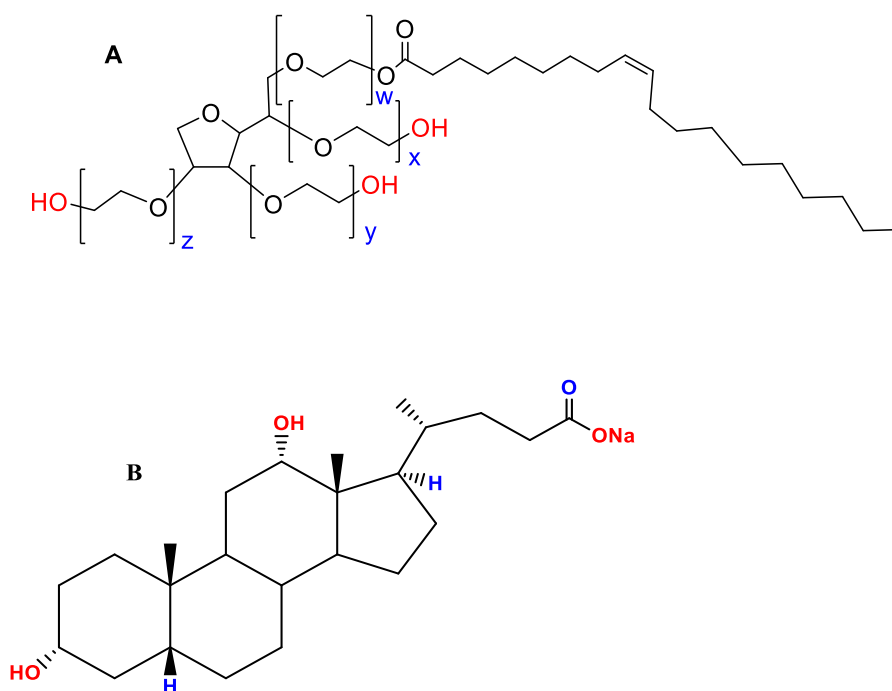


Figure (1-9): Structure of surfactants A) Polysorbate 80 [67], B) Sodium Deoxycholate [68].

1.7.5 Polysaccharides

Polysaccharides are long-chain polymeric carbohydrates, consisting of repeating monosaccharide units linked by glycosidic bonds. Polysaccharides serve an important function in cell communication, helping to recognize tissues and cells and assisting in various transport systems [69]. Studies have shown that coating liposomes with oligosaccharides or polysaccharides can enhance the targeting of liposomes to specific cell receptors [70]. Polysaccharides have unique properties, such as biocompatibility and antibacterial, antiviral, and antitumor properties, making them a promising choice for drug delivery systems [71]. The most important polysaccharides are hyaluronan [72] and chitosan [73].

1.8 Application of Liposomes

Liposome-based drug delivery systems have shown promising results for several types of clinical treatments. Extensive research into the use of liposomes in medical fields has led to the improvement and development of various liposomal structures aimed at treating a wide range of diseases. These liposomes can encapsulate hydrophilic or hydrophobic drugs, and this encapsulation improves the therapeutic effect of the drugs through changes in pharmacokinetics and pharmacodynamics. Although the clinical applications of liposomes primarily focus on the treatment and diagnosis of cancer, these systems represent a versatile therapeutic platform in medical and research fields [37], as shown in figure (1-10) .

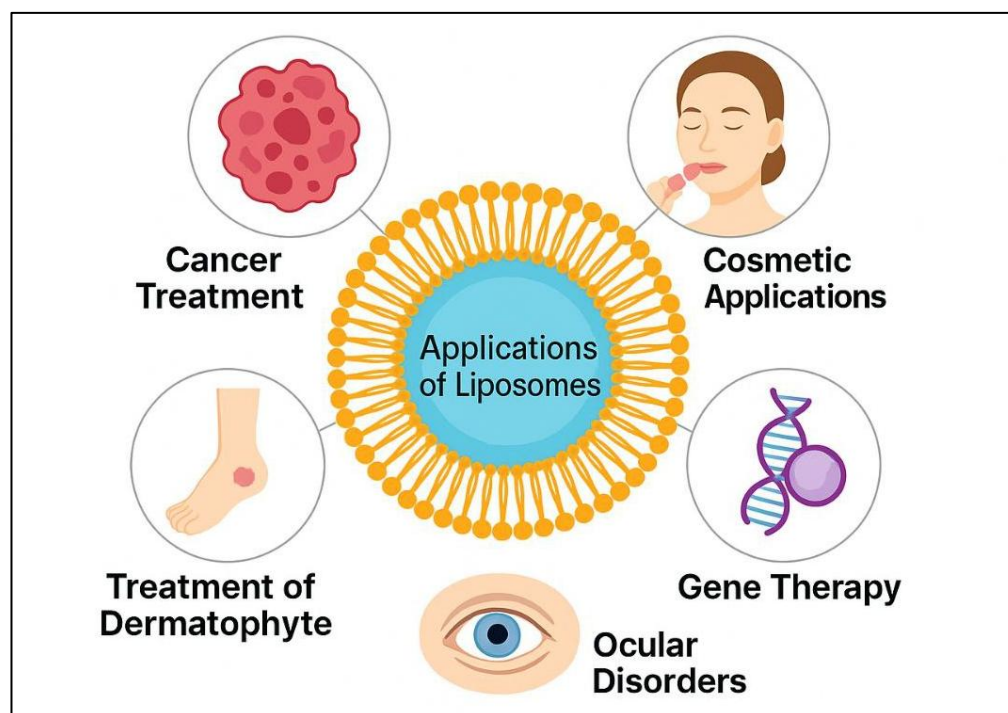


Figure (1-10): Schematic representation of the main therapeutic applications of liposomes [74].

1.8.1 Cancer Treatment

Cancer is one of the most common causes of death. Global cancer data for 2020 showed approximately 10 million cancer deaths and 19.3 million new cancer cases [75]. Currently, existing treatments may face limitations in terms of efficacy and side effects. Therefore, scientists have focused on developing safer alternatives using nanotechnology in cancer treatment, producing nanoparticles that specifically target malignant tumors. These nanomaterials include liposomes [76]. Liposomes have been widely used and studied in tumors due to their unique properties, making them suitable drug delivery vehicles in oncology. Several liposome-based drugs have successfully transitioned to clinical applications in recent years due to rapid advances in liposome technology, and several liposome-based drugs are currently under study [16]. Doxil, the first liposome-based drug, was launched in the United States in 1995 to treat patients with ovarian cancer and AIDS-related Kaposi's sarcoma [17].

1.8.2 Cosmetic Applications

Cosmetics are beauty products containing active ingredients. When some of these products reach their target sites in the deeper layers of the skin, they are effective. However, the nature of the skin makes it difficult for these substances to pass through it. Therefore, scientists have developed liposomal formulations as a system for delivering cosmetics through the skin with high efficiency [11].

1.8.3 Gene Therapy

Gene therapy, a modern approach to treating genetic diseases, aims to introduce a healthy or modified gene into an affected cell to correct genetic defects or a cellular process. Viruses, nucleic acids, or microorganisms are used as vectors to deliver genetic material to cells [77]. Despite advances in this technology, the immune response remains a major obstacle to the clinical development of viral gene therapy [78]. In this case, liposomes emerge as non-viral vectors for gene delivery due to their unique properties, most notably low immune response, high biocompatibility, and ability to encapsulate genetic material and protect it from degradation [77].

1.8.4 Treatment of Dermatophyte

The long-term use of antifungal drugs to treat fungal skin diseases is associated with numerous undesirable side effects. Therefore, there is an urgent need for new treatments with better absorption and fewer side effects. In this context, liposomes have been used as a transdermal drug delivery system. Liposome-encapsulated antifungal drugs have demonstrated effective drug delivery to the target, improved skin penetration, and reduced side effects [79].

1.8.5 Ocular Disorders

Controlling the entry of foreign materials is one of the key functions of the eye. Due to this property, drugs used in treatment are difficult to access into the eye chamber. Furthermore, tear drainage forms a barrier, reducing drug resistance and reducing the effectiveness of treatment on the ocular surface. Therefore, the emergence of drug delivery systems (liposomes) represents an important step in solving these problems. These liposomes can penetrate the ocular barrier, increasing drug resistance on the ocular surface and thus enhancing drug efficacy [80].

1.9 Baclofen

It is a chemical derivative of the neurotransmitter γ -aminobutyric acid (GABA), which acts as an agonist of GABA_B receptors and a depressant of the central nervous system [81]. It is drug a skeletal muscle relaxant and anti-inflammatory [82]. It is commonly used to relieve spastic movement disorder or to treat spinal cord injuries, multiple sclerosis, or motor neuron disease [81]. It has also been increasingly used to treat gastroesophageal reflux disease and musculoskeletal pain [83].

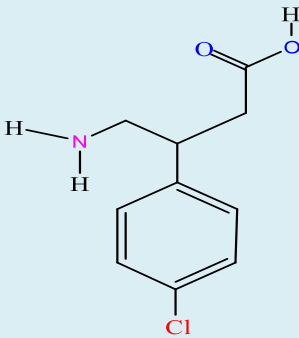
Oral baclofen was initially designed by Heinrich Keberle to treat epilepsy. Despite its limited efficacy in treating epilepsy, baclofen has been found to be effective in relieving spasms. A decrease in muscle strength was observed in patients who took this drug [84] .

In 1971, baclofen was reintroduced to treat muscle spasms resulting from multiple sclerosis and spinal cord injuries, as well as to relieve of flexor spasms and the accompanying pain, in addition to relieving spasms resulting from skeletal muscle damage. It was approved by the US Food and Drug Administration (FDA) in 1977 [85].

1.9.1 Physicochemical properties of Baclofen

Baclofen has physical and chemical properties that make it suitable for pharmaceutical use. It is a white, odorless crystalline compound with good water solubility and chemical stability under normal conditions. Its molecular formula indicates that it contains chlorine and amine atoms, which influence its acidic and basic properties and enable it to interact in various biological environments AS shown in table (1-2).

Table (1-2) : Physicochemical properties of baclofen [86]

Chemical name	4-amino-3-(4-chlorophenyl)butanoic acid
Molecular formula	$C_{10}H_{12}ClNO_2$
Molecular weight	213.66 g/mol
Chemical structure	
Melting point	206-208°C
The appearance	White crystalline powder
Solubility	It is soluble aqueous solution and weak soluble in organic solvent

1.9.2 Baclofen Mechanism of Action

Baclofen activates GABA_B receptors located in presynaptic type Ia neurons and postsynaptic motor cells in both the central and peripheral nervous systems. Thus, its effect leads to inhibition of nerve signal transmission, especially both monosynaptic and polysynaptic reflexes in the spinal cord, which leads to the relief of spasticity and muscle tension. The activation of GABA_B receptors leads to the efflux of potassium (K⁺) from neurons, causing hyperpolarization of the neuron's membrane. In addition, the influx of calcium ions (Ca⁺²) to presynaptic nerve endings is reduced, leading to a reduction in the induced release of neurotransmitters such as glutamate. As a result of these changes, the rate at which presynaptic Ia neurons reach a threshold that allows the initiation of an action potential is reduced, and the amplitude of the excitatory postsynaptic potential within the gamma motor neurons that innervate the fibers within the nerve spindle is reduced. This mechanism illustrates the role of baclofen in reducing muscle spasms through its therapeutic effect, as shown in figure (1-11) [83].

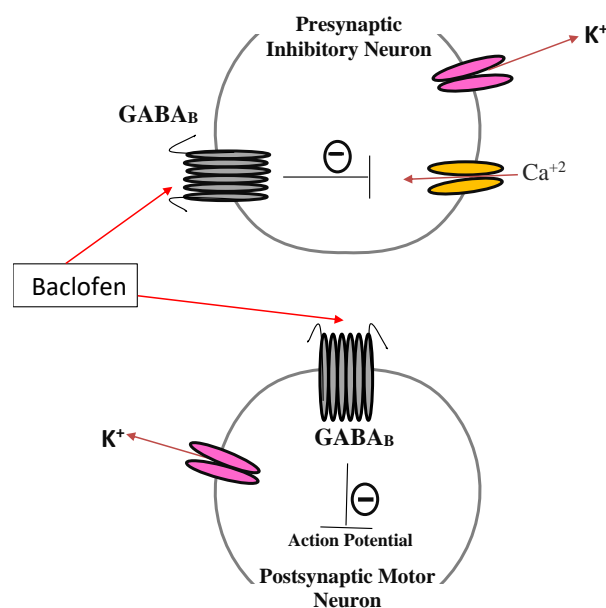


Figure (1-11) : Baclofen Mechanism of Action.

1.9.3 Motivations for Converting Baclofen to nano Liposomes Based Topical Formulation

Oral baclofen is effective in treating muscle spasms, but it causes several undesirable systemic side effects [87], including nausea, dizziness, bradycardia, delirium, drowsiness, psychotic disturbances, sedation, and excessive weakness [88][89]. In addition, oral baclofen has a narrow therapeutic index and a short half-life of 2-4 hours [87], which necessitates frequent dosing to maintain therapeutic levels. This repeated administration increases the risk of severe complications, such as generalized tonic–clonic seizures (GTCS) and non-convulsive status epilepticus [81].

These limitations have encouraged the development of an alternative pharmaceutical form. Therefore, in this study, a topical baclofen formulation based on nano-liposomes was designed to enhance its bioavailability and prolong its half-life in systemic circulation. This approach aims to reduce dosing frequency, deliver the drug directly to the target site, and protect it from premature degradation—thereby improving therapeutic efficacy and minimizing the adverse effects associated with oral administration [87].

1.10 Carbopol

It is a synthetic high-molecular-weight polymer, derived from acrylic acid cross-linked with polyalkenyl ethers or diphenyl glycerol. In recent years, interest has increased in the using of carbopol as an auxiliary material of pharmaceutical applications, as it can be an ideal gel for topical application. as carbopol is an effective material in modifying rheological behavior, offering excellent properties in improving stability, suspending molecules and thickening, and is biocompatible and non-toxic. Carbopol is classified into several types including Carbopol 934, Carbopol 940, Carbopol 974, and Carbopol 981 [90]. AS shown in figure (1-12).

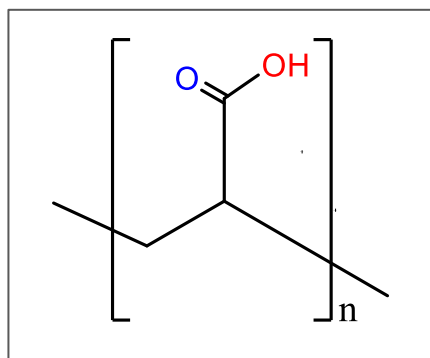


Figure (1-12): Chemical Structure of Carbopol [91].

1.10.1 Motivations for Incorporation Baclofen nano Liposomes Vesicles with Carbopol gel

Despite the development of hydrogel and liposome technologies. However, the capability of these techniques to deliver drugs is limited by several obstacles, such as the potential for rapid degradation and instability. To overcome these issues, liposomes can be combined with hydrogels such as carbopol gels to reduce the speed of drug release and enhance its efficacy, especially in special areas such as prolonged drug delivery, both liposomes and hydrogels may improve each other structurally, for example, carbopol gels can maintain the integrity of liposome membranes and support mechanical stability, and in addition, it provides bio adhesive properties to extend the contact time with the skin surface. The interaction of liposomes with hydrogels may improve their physical and chemical properties, which in turn may change the drug release patterns in the hybrid system. As a result, the combination of liposomes and gels improves drug formulations and administration methods [92].

1.11 Importance of *In Vitro* Studies in Evaluating Baclofen Delivery System

In vitro studies represent a necessary step to evaluate the efficacy of a drug delivery system, providing preliminary results on drug release characteristics a step before in vivo studies [93]. Among these systems, the incorporation of baclofen liposome vesicles into Carbopol gel is a promising approach aimed at achieving controlled and sustained drug release [94]. Performing in vitro studies on such a system provides the possibility of understanding drug release behavior in a physiologically simulated environment and assessing the stability of the vesicles after their incorporation into the gel [95]. This study also enables comparison of the release rate between baclofen liposomes vesicles and those incorporated into the gel, providing practical evidence of the importance of incorporation in enhancing baclofen is half-life and therapeutic efficacy. In vitro testing is therefore an essential tool for clarifying the relationship between gel-vesicle properties and drug release rate, paving the way for designing more efficient and therapeutically effective drug formulations [94] .

1.12 A Study of the Mechanism of Muscle Spasm *in Vivo*

Muscle Spasms are a common clinical and physiological phenomenon associated with a wide range of conditions, from simple muscle fatigue to neurological or systemic disorders. Despite their prevalence, the underlying mechanisms of muscle spasms in vivo remain incompletely understood, as they involve a complex interplay of neuronal, chemical, ionic and mechanical factors [96].

1.12.1 Neuronal factors

One of the primary contributors to spasms is neuromuscular hyperexcitability. Normally, muscle spindles provide excitatory input, while

Golgi tendon organs (GTO) provide inhibitory feedback to motor neurons. An imbalance in these signals may lead to excessive excitatory drive and repetitive, uncontrolled firing of the α -motor neuron, producing sustained involuntary contractions [97] [98].

1.12.2 Chemical and Ionic Factors

Metabolic changes within the muscle also influence cramp development. Accumulation of lactate and hydrogen ions during intense activity lowers intracellular pH, which can impair sarcoplasmic reticulum (SR) calcium handling and slow relaxation [99]. Electrolyte imbalances play a more direct role. Altered concentrations of calcium (Ca^{2+}), potassium (K^{+}), and sodium (Na^{+}) affect the excitability of muscle fibers and motor neurons, thereby increasing the likelihood of abnormal, repetitive firing.

1.12.3 Mechanical Factors

Spasms are often precipitated when muscles are shortened or remain under tension (e.g., during exercise, weightlifting, or prolonged sitting). In such conditions, muscle fibers are insufficiently stretched and the force generated does not adequately activate the GTO. This reduces inhibitory signaling to the spinal cord and favors persistent activation of the α -motor neuron. The GTO reflex normally serves to protect muscle fibers and tendons from excessive strain by inducing relaxation in response to tension. When its feedback is diminished, the risk of spasms increases. Ionic and Metabolic Changes During spasms [100].

During normal contraction, Ca^{2+} is released from the SR and binds to troponin, initiating cross-bridge cycling. Relaxation occurs when Ca^{2+} is actively resequenced back into the SR by ATP-dependent SERCA pumps [101]. In spasms, excessive or repetitive Ca^{2+} release, together with impaired reuptake due to ATP depletion, keeps cytosolic Ca^{2+} levels elevated. This

sustained elevation maintains cross-bridge binding and prolongs contraction, This keeps the muscle in a state of sustained contraction. It can also lead to a large influx of calcium into the muscle fibers, which may result in a potential decrease in blood calcium levels [102].

Potassium flux is also altered. Under normal conditions, depolarization occurs via Na^+ influx, followed by repolarization through K^+ efflux, with ion balance restored by the Na^+/K^+ ATPase pump [103]. During spasms, rapid repetitive discharges lead to accumulation of K^+ in the extracellular space and Na^+ inside the cell [104]. The Na^+/K^+ pump works at near-maximal capacity but requires large amounts of ATP. As ATP availability decreases, the pump cannot maintain ionic gradients, further predisposing the fiber to hyperexcitability and sustained contraction [105].

Inorganic phosphate (Pi), a byproduct of ATP hydrolysis and creatine phosphate breakdown, accumulates inside the muscle during sustained activity [106]. High intracellular Pi contributes to fatigue and impaired cross-bridge function. However, significant increases in plasma phosphate occur mainly in severe muscle injury (e.g., rhabdomyolysis).

Enzymatic changes during muscle spasm, In addition to ionic and metabolic disturbances, muscle spasm are also accompanied by changes in the levels of certain muscle enzymes in the blood. Creatine Kinase (CK) is one of the most important biochemical parameter of muscle fiber membrane damage. Normally, it remains within the cell, but during prolonged or repeated spasm, the muscle membrane may be exposed to mechanical or chemical stress or an imbalance in the ionic balance, leading to increased permeability. CK leaks into the blood [107]. Elevated CK is used as an indicator of muscle damage or rhabdomyolysis [108]. Lactate dehydrogenase (LDH) elevated activity reflects increased reliance on anaerobic metabolism and may rise in blood when muscle fibers are

injured [109]. Aspartate aminotransferase (AST) and alanine aminotransferase (ALT) although typically used as liver function markers, they are also present in muscle tissue. Elevated levels may arise from muscle injury, potentially mimicking hepatocellular damage[110].

In addition to ionic and enzymatic changes within muscle fibers, repeated or severe spasms may affect vital organs such as the kidneys and liver.

In cases of severe muscle spasms associated with rhabdomyolysis, intracellular proteins, enzymes, and electrolytes—including myoglobin, potassium, and phosphate—are released into the bloodstream. Myoglobin can precipitate within renal tubules, promote oxidative stress, and lead to acute kidney injury, clinically reflected by elevated serum creatinine and urea [111]. The liver itself is not directly damaged by cramps, but elevations of AST and ALT may misleadingly suggest hepatic injury when the true source is muscle. Differentiating between muscular and hepatic origins requires careful clinical and laboratory assessment [112].

1.13 Literature review

- The study (Raveendhra et al., 2018) focused on the development of a topical gel for controlled release of baclofen at a concentration of 0.5% using a range of hydrophilic polymers such as Carbopol, Carrageenan, Xanthum and others. The results showed that the gel systems had good physical properties, no interaction between the drug and the polymers was observed, and no skin irritation was observed during topical application. The prepared formulations showed a high in vitro drug release rate of 98% within (22-24) hours. In transdermal permeation experiments in rats ex vivo, the formulations showed high permeability to baclofen [113].
- In a study by (Keservani et al. 2020), baclofen-loaded liposomes were prepared by the ethanol injection method, where different ratios of

cholesterol, lecithin, and ethanol were used with stabilized drug and stearic acid ratios. The physical and chemical properties of the liposomes were studied. The results showed that the average size of the liposomes ranged between (3.98 ± 0.45 - 4.24 ± 0.65 μm) with the observation that the vesicles are small, single membrane spherical, with a gradual release of ($67.66 \pm 5.32\%$) within 10 hours. In addition to in vitro studies, the efficacy of the formulation was evaluated in vivo using Swiss Benoit mice, where it showed muscle relaxant activity by increasing the number of falls in the Rota-Rod test compared to the control group. The researchers concluded that baclofen-loaded liposomes show high efficiency in improving the pharmacological effect of baclofen when used topically [114]

- In this study (Mahesh et al. 2021), liposomes were prepared using thin lipid film hydration method. The liposomes were evaluated using zeta sizer, encapsulation efficiency and drug release in vitro. The drug used in the liposomes formulation was diclofenac sodium, which has anti-inflammatory and antipyretic properties. The bioavailability of diclofenac sodium is 50% , when this drug is encapsulation in liposomes its bioavailability increases. The results indicate that the liposome formulation of diclofenac demonstrated a more substation drug release into the systemic circulation, along with anti-inflammatory effects and reduced side effects [115].
- A study conducted by (Tayal et al. 2024) addressed the design of a topical delivery system for the treatment of arthritis. Diclofenac sodium is encapsulated by liposomes and then carried in a hydrogel. The results of this study showed that the average vesicle size ranged from 100 to 200 and that drug release exceeded 96% in all liposomal gel formulations. These results indicate that liposomes gels have proven to be an effective vehicle for transdermal delivery of

diclofenac sodium and the treatment of inflammatory conditions [116].

- (Jia et al., 2025) developed a topical delivery system for docetaxel for the treatment of psoriasis using gel-loaded liposomes. This system was developed to overcome problems with the drug, such as its low bioavailability and insolubility. The results showed that the DTX-LP-G formulation released the drug cumulatively, releasing larger amounts of the drug into the skin compared to liposome-loaded and gel-loaded docetaxel. The DTX-LP-G formulation also demonstrated high efficacy in removal hydrogen peroxide free radicals *in vitro*. This study was conducted *in vivo* (mouse), and the formulation was a therapeutic agent for psoriasis in terms of improving the skin's external appearance, reducing splenomegaly, and inhibiting MDA in skin tissue [117].

A review of previous studies has shown that most research on topical drug delivery has focused on the use of liposomes as carriers, exploring various active ingredients, preparation methods, and applications, including *in vitro* studies and animal models. Studies have successfully demonstrated the advantages of liposomes in enhancing drug stability, controlling release rates, and improving therapeutic effects. Similarly, baclofen has been formulated in topical gels and other delivery systems, showing promising results in terms of drug release and skin permeation. However, none of the previous studies have combined baclofen with liposomes incorporated into a gel formulation and further evaluated it both *in vitro* and *in vivo* in a rabbit model.

Therefore, the novelty of this work lies in the development of a baclofen nano liposome gel and its comprehensive evaluation, including drug release, permeation behavior, and *in vivo* efficacy. This study addresses a clear gap

in the scientific literature, offering a new approach for topical baclofen administration that has the potential to improve therapeutic outcomes, reduce systemic side effects associated with oral administration, and provide a more effective treatment option for localized conditions.

1.13 Aims of Study

1-To design and formulate a gel-based nanoliposome Baclofen vesicles composition, and to characterize its physicochemical properties, including particle size, distribution, stability, and drug entrapment efficiency.

2- To fabricate polyamide (Nylon 6,6) fibers and use them as a filtration medium for the prepared liposomal vesicles, aiming to obtain small unilamellar liposomes.

3-To induce a direct muscle spasm model by injecting specific concentrations of lactic acid into the muscles of laboratory animals, simulating acute muscle spasticity conditions.

4- To monitor selected clinical and physiological parameters relevant to muscle spasm, such as spasm severity, mobility range, and inflammatory markers, for therapeutic assessment.

5-To evaluate the therapeutic efficacy of the optimized nanoliposome Baclofen gel formulation in treating induced muscle spasms, in comparison to conventional treatment approaches.

Chapter Two

Materials and Methods

2. Materials and Methods

2.1 Instruments

All devices used in this study were listed in table (2-1) with the companies and origin mentioned.

Table (2-1): Devices used in this study

Ser	Devise	Company	Origin
1	Bath sonicator	Daihan Scientific	China
2	Buechner funnel	Chemlab	UK
3	Centrifuge	Hettich-D-78532	Germany
4	Dynamic light scattering (DLS) Analysis	Malvern	UK
5	Electrospinning device ,16kv	Homework	Basra
6	Field Emission Scanning Electronic Microscope (FESEM) , 15kv	TESCAN	USE
7	FT-IR Spectrophotometer, FT-IR-8400s	Shimadzu	Jaban
8	Hotplate magnetic stirrer	Medilab	Korea
9	Micropipette	Dragonmed	China
10	Overhead stirre	Joanlab	China
11	pH meter	Inolab	Germany
12	Rotary evaporator	Heidolph	USA
13	Stuart Melting Point Apparatus-SMP30	Bibby Scientific Limited	UK
14	UV-Vis spectrophotometer UV-1800	Shimadzu	Jaban
15	Vortex mixer	Joanlab	China
17	Vacuum filtration	Value	China
18	Zeta potential analysis	Horiba Scientific	Jaban

2.2 Materials

All materials used in this study were listed with their companies, origin and chemical formulas in table (2-2).

Table (2-2): Materials used in this study

Ser	Materials	Molecule Formula	M.wt	Purity	Company	Origin
1	Baclofen	$C_{10}H_{12}ClNO_2$	213.66 g.mol ⁻¹	99%	Baoji Guokang	China
2	Carbopol 934	$(C_3H_4O_2)_n$	$(72.1)_n$ g.mol ⁻¹	99%	Himedia	India
3	Cholesterol	$C_{27}H_{46}O$	386.66 g.mol ⁻¹	99.8%	Avonchem	UK
4	Chloroform	$CHCl_3$	119.38 g.mol ⁻¹	99%	Chemlab	UK
5	Distilled water	H_2O	18 g.mol ⁻¹	98%	Chemlab	UK
6	Ethanol	C_2H_5OH	46 g.mol ⁻¹	99.8%	Chemlab	UK
7	Formic acid	$HCOOH$	46 g.mol ⁻¹	90%	Chemlab	UK
8	Glycerol	$C_3H_8O_3$	92 g.mol ⁻¹	99%	Thomas Baker	India
9	Lactic acid	$C_3H_6O_3$	90 g.mol ⁻¹	98%	Lobachemie	India
10	Nylon 6,6	$(C_{12}H_{22}N_2O_2)_n$	$(226.32)_n$ g.mol ⁻¹	99%	Mackin	China
11	Phosphate buffer saline (Ph 6.8)	NaCl KCl Na_2HPO_4 , KH_2PO_4	58.44 g.mol ⁻¹ 74.55 g.mol ⁻¹ 89.98 g.mol ⁻¹ 136.1 g.mol ⁻¹	99%	Himedia	India
12	Sodium deoxycholate	$C_{24}H_{39}NaO_4$	414.6 g.mol ⁻¹	97%	Lobachemie	India
13	Soya lecithin	$C_{44}H_{87}NO_8P$	789.2 g.mol ⁻¹	89%	Himedia	India
14	Span 80	$C_{24}H_{44}O_6$	428.6 g.mol ⁻¹	99%	Lobachemie	India
15	Triethanolamine	$C_6H_{15}NO_3$	147.2 g.mol ⁻¹	85%	Lobachemie	India
16	Tween 20,80	$C_{58}H_{114}O_{26}$, $C_{64}H_{124}O_{26}$	1227 g.mol ⁻¹ 1309 g.mol ⁻¹	97%	Lobachemie	India

2.3 Assay kit

Table (2-3) shows a set of manual analyses used in this experiment.

Table (2-3): Manual analyses used in this experiment

No	Kits	Company	Origin
1	Alanine Aminotransferase enzyme	Human	Germany
2	Aspartate Aminotransferase enzyme	Human	Germany
3	Calcium	Biosam	UAE
4	Creatin kinase enzyme	Medichem Middle East	Syria
5	Creatinine	Spinreact	Spain
6	Lactate dehydrogenase enzyme	Biolabo	France
7	Phosphorus	Spinreact	Spain
8	Potassium	Biosam	UAE
9	Urea	Randox	UK

2.4 Methods

2.4.1 Characterization of Baclofen

2.4.1.1 Determination of Baclofen melting point

The melting point of baclofen was measured using the capillary tube method and recorded using a Stuart melting point apparatus (SMP30) (UK).

2.4.1.2 Determination of λ_{\max} Wavelength of Baclofen

Baclofen 50mg was dissolved in 100 ml of phosphate-buffered saline (PBS) (pH 6.8) to prepare a stock solution 500 $\mu\text{g/mL}$. The maximum wavelength (λ_{\max}) of baclofen was determined by preparing a dilute solution of 25 $\mu\text{g/mL}$ of the stock solution and spectral scanning was measured at wavelength range (200-400 nm) using a UV-vis spectrophotometer [118][119].

2.4.1.3 Determination of Calibration Curve of Baclofen

To determine the calibration curve, a series of diluted solutions with different concentrations (5,10,15,20 and 25 $\mu\text{g/mL}$) were prepared from the previously prepared stock solution 500 $\mu\text{g/mL}$. The absorbance of each diluted solution was measured at the maximum wavelength (λ_{\max}) of baclofen using an UV-visible spectrophotometer. The absorbance of each diluted solution was then plotted against its concentration [119]. Sample types, experimental repeats, and statistical analyses of the data were presented as mean \pm S.D. (n = 3).

2.4.2 Preparation of Baclofen nano-Liposome Vesicles

1. Liposomes were prepared using the thin film hydration method, as reported in the study conducted by Alec Bangham in 1964 [120], with some modifications.
2. These modifications included the addition of surfactants to improve liposome permeability by increasing the flexibility of the lipid membrane, which facilitates penetration of biological barriers. The addition of surfactants also increased the membrane's hydrophilicity, which improved drug release and distribution [121].
3. In this method, lecithin, cholesterol, and surfactants were dissolved in an organic solvent (chloroform) in a round-bottomed flask under continuous stirring using a magnetic stirrer.
4. The organic solvent was subsequently evaporated using a rotary evaporator, resulting in the formation of a thin film lipid.
5. This film was placed in a vacuum to remove any residual solvent. The lipid film was hydrated using 10ml of PBS (pH 6.8) containing the baclofen to be loaded into the liposomes.
6. The mixture was heated at 58 ± 1 °C for 10 minutes to ensure the lipid film was combined with PBS solution. This resulted in the formation of multilamellar vesicles. This mixture was stirred using a Vortex for 10 minutes to accelerate vesicle formation as shown in the figure (2-1) [122].
7. These vesicles were subjected to ultrasonication using a sonication bath for 30 minutes at 400 watts to produce unilamellar vesicles. However, sonication produces heterogeneous liposomes, so these vesicles were filtered by passing them through Nylon 6,6 nanofibers to improve homogeneity and allow small unilamellar vesicles to pass through [86], The preparation of liposomes by the thin film hydration

method, encompassing the formation of multilamellar and unilamellar vesicles, is schematically detailed in Figure (2-3).

8. This filtration process was performed using a Buechner funnel technique, as shown in the figure (2-2).
9. After preparing the liposomes loaded with the active ingredient (BFN), they were stored in a cool, dry place to ensure their stability [123].
10. The BLV₂ formulation, which demonstrated the optimum vesicle size, was identified for further studies.
11. This method uses different ratios of lecithin and surfactants, while maintaining a constant ratio for baclofen and cholesterol, as shown in the table (2-4) [118] .

Table (2-4) : Formula for preparation of Baclofen liposome vesicles

Formulation	Baclofen	Soya Lecithin	Cholesterol	Surfactants
BLV1	50mg	80mg	10mg	Tween80 (10mg) Span80 (10mg)
BLV2	50mg	85mg	10mg	Tween80 (15mg)
BVL3	50mg	80mg	10mg	Span80 (20mg)
BVL4	50mg	85mg	10mg	Sodium deoxycholate(15mg)

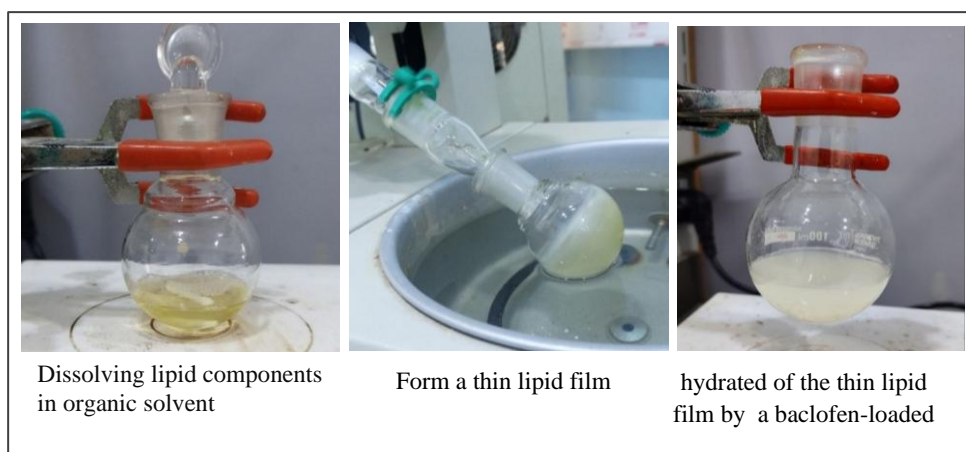


Figure (2-1): Steps for preparing Baclofen nano-Liposomes Vesicles

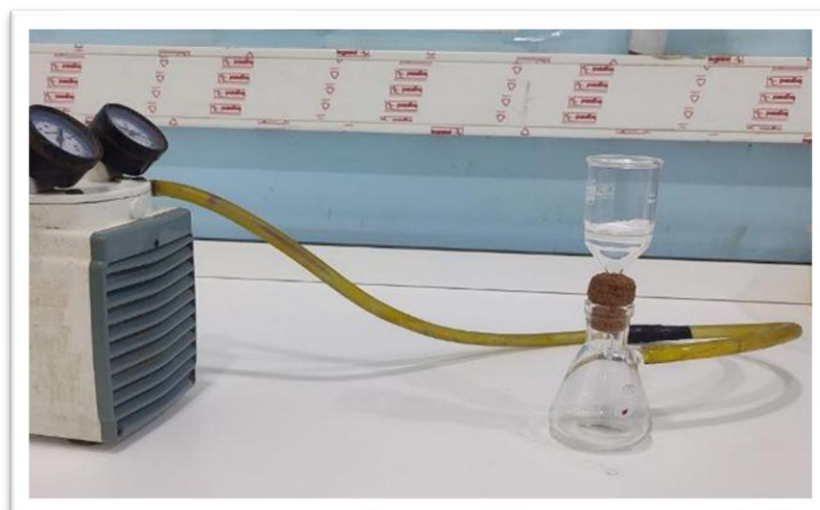


Figure (2-2) : Buechner funnel for filtration of liposomes

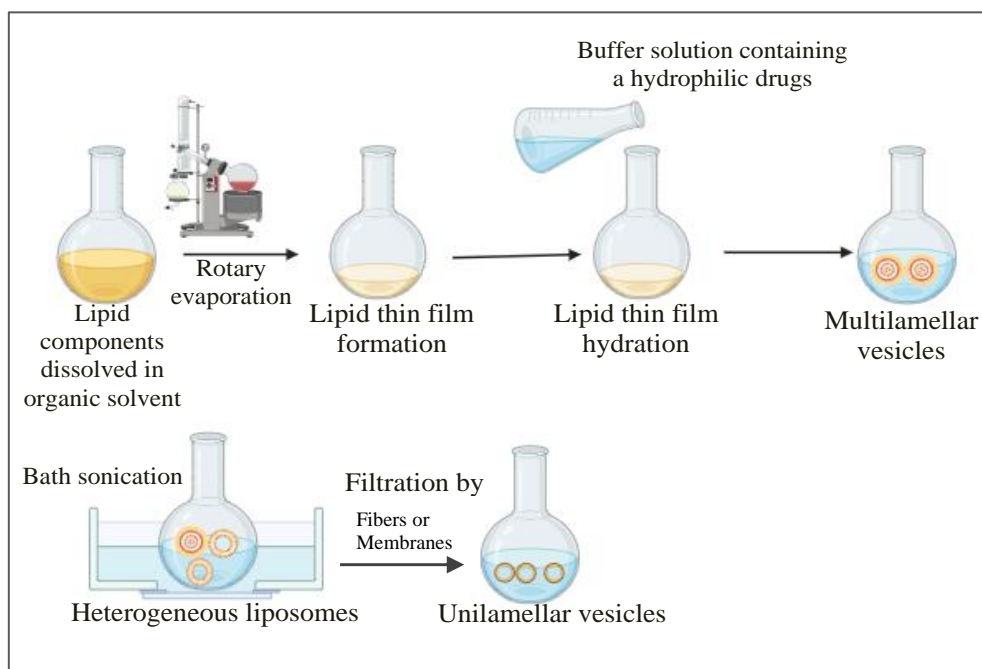


Figure (2-3): Scheme shows the preparation of nano-Liposomes by thin film hydration method

2.4.3 Manufacturing of Nylon 6,6 Nanofibers using Electrospinning

2.4.3.1 Sample preparation

In this study, the materials used were Nylon 6,6 and formic acid to prepared nylon 6,6 solution at room temperature. 25 ml of formic acid was used to dissolve 3.6 g of nylon 6,6 granules. The solution was continuously stirred with a magnetic stirrer for 90 minutes for homogeneous solution. Afterwards the solution was kept idle in the refrigerator for 15 minutes before electrospinning [124] .

2.4.3.2 Electrospinning

The electrospinning device consists of a syringe (5 ml) and a flat collector. The electric voltage was (16 kV) and the flow rate was 0.5 ml/hour. The distance between the needle tip and the flat collector was maintained at 15 cm [124], as shown in Figure (2-4) . To form nanofibers made of Nylon 6,6, the previously prepared solution was poured into a 5 ml syringe. subsequently, aluminum foil was fixed on the flat collector and the nanofibers were deposited on the aluminum foil using electrospinning technique for 10-20 hours as show in the figure (2-5). After the deposition process, the nanofibers were heat treated at 50°C to remove the remaining solvent and to separate the fibers from the aluminum foil. The fibers were stored in suitable conditions away from contamination [125].

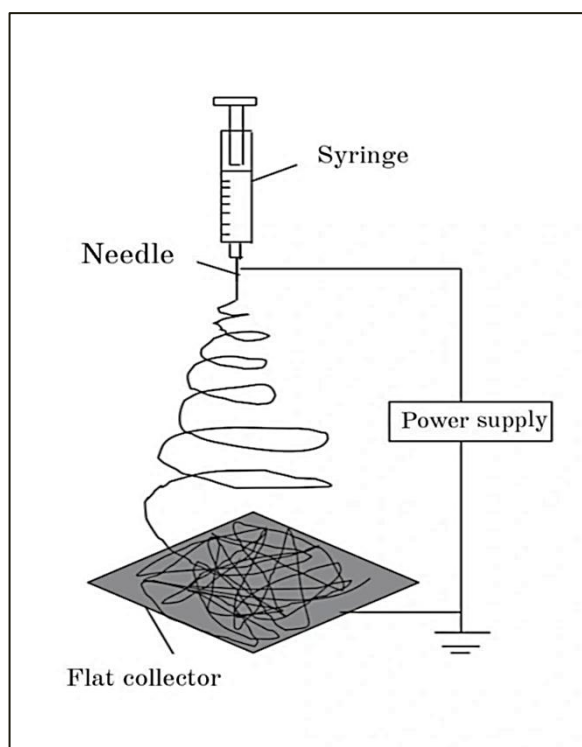


Figure (2-4) : Diagram of an electrospinning Device at the laboratory scale:[126]



Figure (2-5) : Image for Deposition of Nylon 6,6 Electrospun Nanofibers on aluminum foil

2.4.3.3 Application of Nylon 6,6 nanofibers in Liposome Filtration

In this study, Electrospun nylon-6,6 nanofibers were employed as a filtration medium for a liposomes suspension to obtain small unilamellar vesicles (SUVs) [86]. The nanofibers were prepared and cut to match the diameter of a Buchner funnel, after which they were placed directly onto the funnel plate. The liposomes suspension was carefully applied onto the surface of the nanofibers, and vacuum filtration was subsequently performed to facilitate the passage of the suspension through the fibers. Due to the nanostructure and small pore size of the fibers, larger unilamellar vesicles and heterogeneous were retained on the fiber surface, whereas smaller vesicles successfully permeated through the fibers and were collected in the receiving flask. This approach enabled the production of liposome vesicles with reduced size and enhanced size homogeneity.

2.4.4 Characterization of Liposomes

2.4.4.1 Fourier Transform Infrared Spectroscopy (FT-IR)

An FTIR spectrophotometer was used to get the FTIR spectra of Baclofen and the Baclofen-loaded liposome vesicles to anticipate and explore any physicochemical intuitive between different components in a detailing.were analyzed of the samples at wave numbers ($400\text{-}4000\text{ cm}^{-1}$) [118].

2.4.4.2 Field Emission Scanning Electronic Microscope (FESEM)

The sample was examined using a scanning electron microscope to determine the size and shape of the particles in the sample at an accelerating voltage of 15 kV and under a high vacuum. Baclofen liposomes vesicles

were frozen using liquid nitrogen, the sample was mechanically crushed. After crushing, the surface of the sample was coated with a thin layer of carbon, which allows the surface structure of the liposomes to be clearly seen when examined by a scanning electron microscope [127].

2.4.4.3 Dynamic Light Scattering (DLS) Analysis

Using dynamic light scattering analyzer, the average particle size and the polydispersity index were determined. When measuring liposomes using DLS, they were diluted with PBS to increase the accuracy of the measurement and the temperature was fixed at 25°C because it affects the movement of the particles.

2.4.4.4 Zeta Potential

A ζ -potential (zeta potential) analysis was performed to evaluate the surface charge of the liposomal formulations and to assess their colloidal stability. Measurements were taken using a ζ -potential analyzer after diluting the samples in PBS in order to avoid particle aggregation. The resulting values provided an indicator of the magnitude of electrostatic repulsion between the vesicles; higher $|\zeta\text{-potential}|$ values (either positive or negative) correspond to greater stability and lower likelihood of aggregation. This analysis was essential to confirm the physical stability of the liposomes during preparation and storage.

2.4.5 Preparation of Baclofen nano-Liposome Vesicles Gel

To prepare the Carbopol gel, 0.5 g (0.5% w/v) of Carbopol polymer was weighed and added to distilled water under continuous stirring with a mechanical mixer a 2000rpm and for 60 minute, take care to avoid aggregation [118]. The mixture was left for two hours to fully hydrate and expand.

Subsequently , glycerol was added (2% v/v) to hydrate and improve the gel consistency and Tween 20, which helps reduce the surface tension between the liposomes and the aqueous medium of the carbopol gel, which improves the stability and homogeneity of the distribution of liposomes within the gel .

The previously prepared optimum liposome formulation was gradually added to the gel base containing glycerol and tween 20 under continuous stirring to obtain a homogeneous gel. The pH of the gel was adjusted using triethanolamine in the range of (5-7), It was considered suitable for the stability of the Carbopol gel [128].

The drug-loaded gel was stored in sealed containers away from light and at various temperatures [3]. The same steps were followed for the remaining concentrations found in the table (2-5).The practical steps for the preparation of the BLVG were illustrated in figure (2-6).

Table (2-5) :Composition of Baclofen nanoliposome Vesicles Gel Formulations (BLVG1, BLVG2, and BLVG3)

INGREDIENTS	BLVG ₁	BLVG ₂	BLVG ₃	%
Baclofen liposomes	5%	5%	5%	v/v
Carbopol 934	0.5%	1%	1.5%	w/v
Glycerol	2%	2%	2%	v/v
Tween 20	5%	5%	5%	v/v
Triethanolamine	Q.s	Q.s	Q.s	v/v
Distilled water	Q.s	Q.s	Q.s	v/v

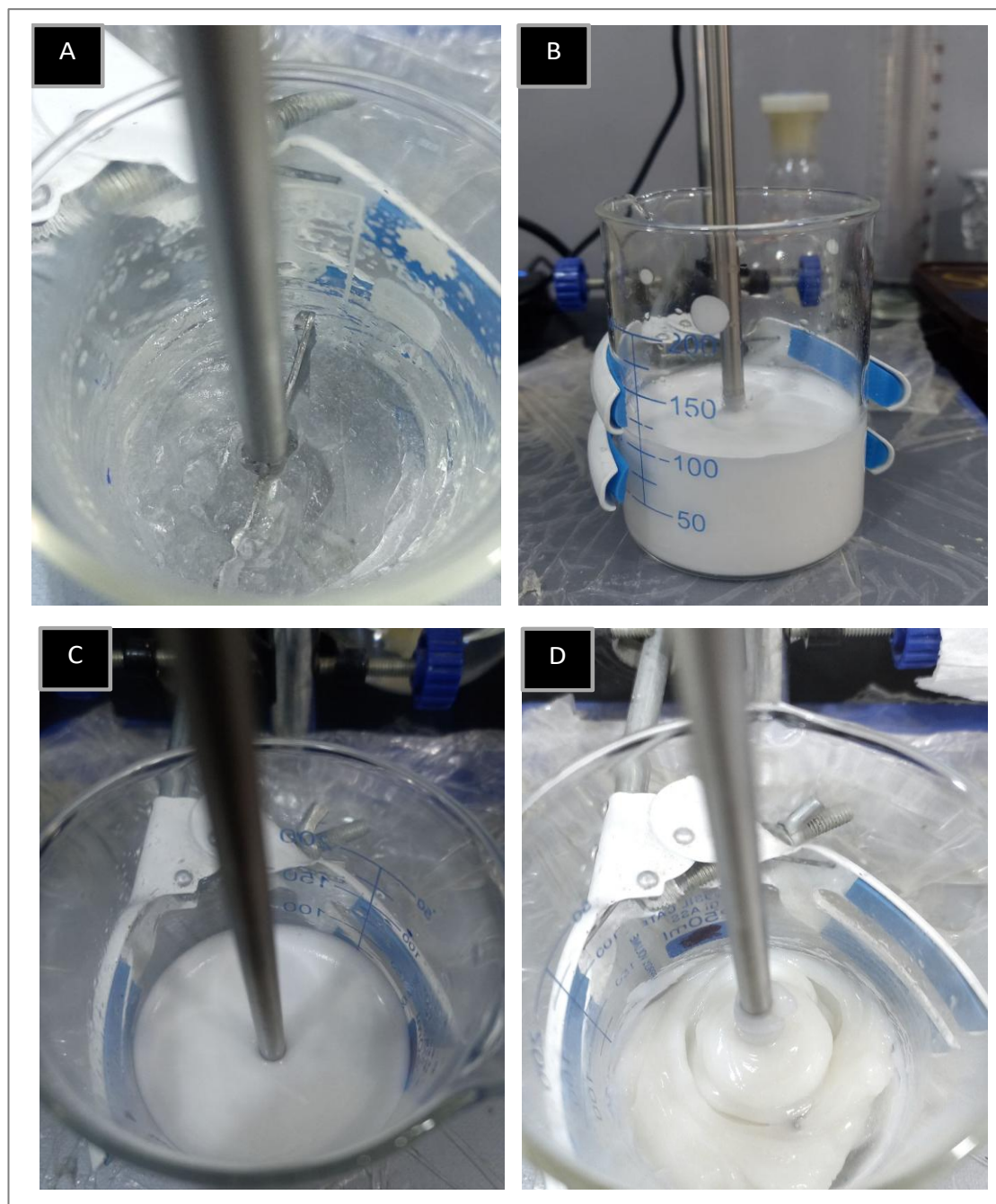


Figure (2-6): (A) After soaking Carbopol 934 in distilled water (B,C) After adding glycerol, Tween 20 and the optimum liposome formulation (D) After adjusting the pH of the gel using triethanolamine

2.4.6 Biological Evaluation of Synthesized Baclofen nano Liposome Vesicles (BLV₂) *In Vitro*

2.4.6.1 Determination of the effect of BLV₂ on inhibition of Lactate Dehydrogenase enzyme (LDH)

According to the manufacturer's instructions (BIOLABO SAS, France), the estimation of LDH enzyme activity was assessed using tris pH 7.2 (80 mmol/L) as a buffer, pyruvate (1.6 mmol/L) as a substrate, and NADH (0.2 mmol/L) as a coenzyme.



To stimulate the inhibition of LDH enzyme activity, several diluted concentrations of baclofen nanoliposome vesicles (15, 30, 45, 60, 75, and 100 ppm) were prepared as enzyme inhibitors. Accordingly, 1 mL of the LDH working reagent was placed in a water bath for 5 minutes at 37°C, followed by the addition of 20 µL of each inhibitor solution and a serum sample (from patients with muscle spasms). The enzyme activity absorbance was measured at 340 nm before and after adding the inhibitor using a UV-Vis spectrophotometer after 30 seconds, 1 minute, and 2 minutes. The enzyme activity rate was calculated using Equation (1) [129].

$$\text{IU/L} = (\Delta\text{Abs/min}) \times 8095 \dots\dots\dots(1)$$

While equation (2) was used to measure the percentage inhibition.

$$\% \text{ Inhibition} = 100 - \left(\frac{\text{Activity (IU/L) with inhibitors}}{\text{Activity (IU/L) without inhibitors}} \right) \times 100 \dots\dots\dots(2) \text{ [130]}$$

2.4.6.2 Determination of the effect of BLV₂ on inhibition of Creatine Kinase enzyme

According to the manufacturer's instructions (Medichem Middle East, Syria), the estimation of CK enzyme activity was assessed using Buffer/Glucose/NAC. Imidazol buffer(100 mmol/L) pH 6.7, glucose(40 mmol/L), NAC (30 mmol/L), magnesium acetate (15.3 mmol/L), NADP (2.5 mmol/L), HK \geq 4000U/L, EDTA (2.6 mmol/L). Substrate/Coenzymes CP (150mmol/L), AMP (5mmol/L), ADP (5.88mmol/L), di(adenosine-5) pentaphosphate (10 μ mol/L), G6P- DH \geq 2800 U/L.



To inhibit the CK enzyme, several diluted concentrations of baclofen nanoliposomes vesicles (15, 30, 45, 60, 75, 100, ppm) were prepared. Thus, 1ml of the CK enzyme the working reagent put in a water bath for 5 min at 37°C ,then 20 μ L of each of the inhibitor and serum (from people suffering from severe muscle spasms) were added. The absorbance of the enzyme activity was measured after and before adding the inhibitor at 1, 2 and 3 minutes using UV-Vis Spectrophotometer at a maximum wavelength of 340 nm . The enzyme activity rate was estimated using the equation (1).

$$\text{IU}\backslash\text{L} = (\Delta\text{Abs}/\text{min}) \times 8095 \dots\dots\dots(1)$$

The inhibition percentage was measured using Equation (2).

$$\% \text{ Inhibition} = 100 - \left(\frac{\text{Activity (IU}\backslash\text{L) with inhibitors}}{\text{Activity (IU}\backslash\text{L) whiout inhibitors}} \right) \times 100 \dots\dots\dots(2) \text{ [130]}$$

2.4.6.3 Half-maximal inhibitory concentration IC₅₀

Calculations

The IC₅₀ values were calculated by plotting the relationship between the percentage of inhibition (%) and the concentration of the inhibitor BLV2 for both LDH and CK enzymes. The half-maximal inhibitory concentration IC₅₀ is the concentration that results in 50% inhibition of the enzymatic activity, and it is an important indicator for measuring the strength and effectiveness of the inhibitor. To obtain these values, experiments were performed at different levels of BLV2, and the enzymatic activity was measured at each concentration, followed by calculation of the percentage of inhibition in comparison with the enzymatic activity in the absence of the inhibitor. Subsequently, a plot of the percentage of inhibition versus BLV2 concentration was drawn, from which the concentration that produced 50% inhibition of the enzymatic activity was determined. This method is standard for evaluating the effectiveness of chemical inhibitors.

2.4.6.4 *In Vitro* release study of BLV₂ Gel

In this study, the release rate of Baclofen was measured at different formulations of baclofen Nano-Liposome vesicles gel. The gel was immersed in 100 ml of phosphate-buffered saline PBS (pH 6.8). UV-Vis spectrophotometer at 218 nm was used to measure the absorbance of the drug released from the gel at times 1, 2, 3, 4, 5, 6, 7, 8, 9, and 10 h. The standard calibration curve was used to calculate the baclofen concentration and the amount of drug released according to Equation (1), and the percentage of baclofen released from the gel was calculated using Equation (2) [127].

$$\text{Amount of drug released} = \frac{\text{Concentration} \times \text{Dissolution bath volume} \times \text{dilution factor}}{1000} \dots\dots\dots$$

(1)

$$\text{Percentage of drug release} = \frac{\text{Amount of drug released}}{\text{weight of BLV gel}} \times 100 \dots\dots\dots (2)$$

2.4.7 Biological Evaluation of Synthesized BLV₂ Gel *in Vivo*

2.4.7.1 Experimental Animals

In this experiment, twenty male rabbits of the species domesticus, with a weight ranging between 1900-2200 g and an age of 6-7 months, were used. They were obtained from some rabbit breeders in Basra governorate.

The rabbits were placed in large plastic cages and raised under temperature conditions of 25-20°C, with a 12-hour light /12-hour dark cycle, during the two-week experimental period. The animals' nutrition and health were monitored daily with appropriate feed and water provided throughout the study duration.

2.4.7.2 Division of Experimental Animals

Rabbits were divided into four groups, with five animals in each group, as follows:

Control Group: This group received no treatment or spasm induction. Blood samples were collected directly and used as a reference for normal physiological conditions.

Spasm-Induced Group: Muscle spasms were induced using lactic acid at a concentration of 30mM. Blood samples were collected 12 hours after spasm induction.

Untreated Spasm Group: Rabbits in this group also underwent muscle spasm induction as described above, but received no treatment. Blood samples were collected after 5 days.

Treated Group: Muscle spasms were induced in the same manner as in the previous groups. The affected area was treated topically with baclofen gel twice daily (every 12 hours) for 5 days. Blood samples were collected at the end of the treatment period.

2.4.7.3 The method of inducing muscle spasm

The rabbit was placed in a 3-meter-long enclosed corridor and visual stimuli such as a hand were used to guide the rabbit to run intermittently for 15 minutes

Ten minutes after the end of the exercise, 30mM lactic acid was injected into the rabbit's thigh muscle at a dose 1ml, according to the weight of the rabbit using a 1ml syringe.

Lactic acid injections with strenuous exercise leads to an accumulation of acids in the muscles, which increases the concentration of hydrogen ions [H^+] within muscle cells. This leads to a decrease in pH, making the muscle environment more acidic. This directly impacts the efficiency of enzymes involved in energy generation, thus reducing the muscle's ability to produce ATP effectively [131]. Additionally, the balance of ions inside and outside the cell, particularly potassium, is affected, increasing the likelihood of muscle spasm [132]. The motor behavior of the rabbits was relied upon, a biomarker for muscle spasm Along with performing some biochemical analyses .

2.4.7.4 Sample collected

Blood samples were drawn from all groups at the specified times from the rabbit's auricular vein using a 3 ml syringe .After that, the blood samples were placed in gel tubes and left to coagulate at room temperature for 10 minutes and then transferred to a centrifuge at 5000 rpm for 10 minutes to separate blood components and obtain serum. After that, the serum was separated by micropipettes and placed in Eppendorf tubes and stored at 4°C for several hours, until biochemical Analyses are performed on it.

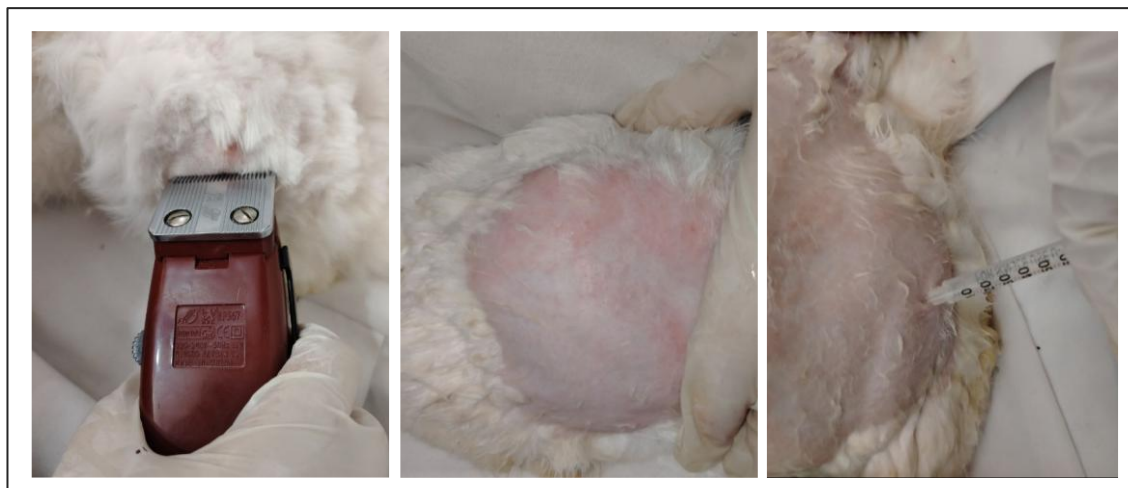


Figure (2-7): Steps for lactic acid injection



Figure (2-8): Steps to draw blood from the atrial vein



Figure (2-9): Steps to treat muscle spasms by BLV₂ gel

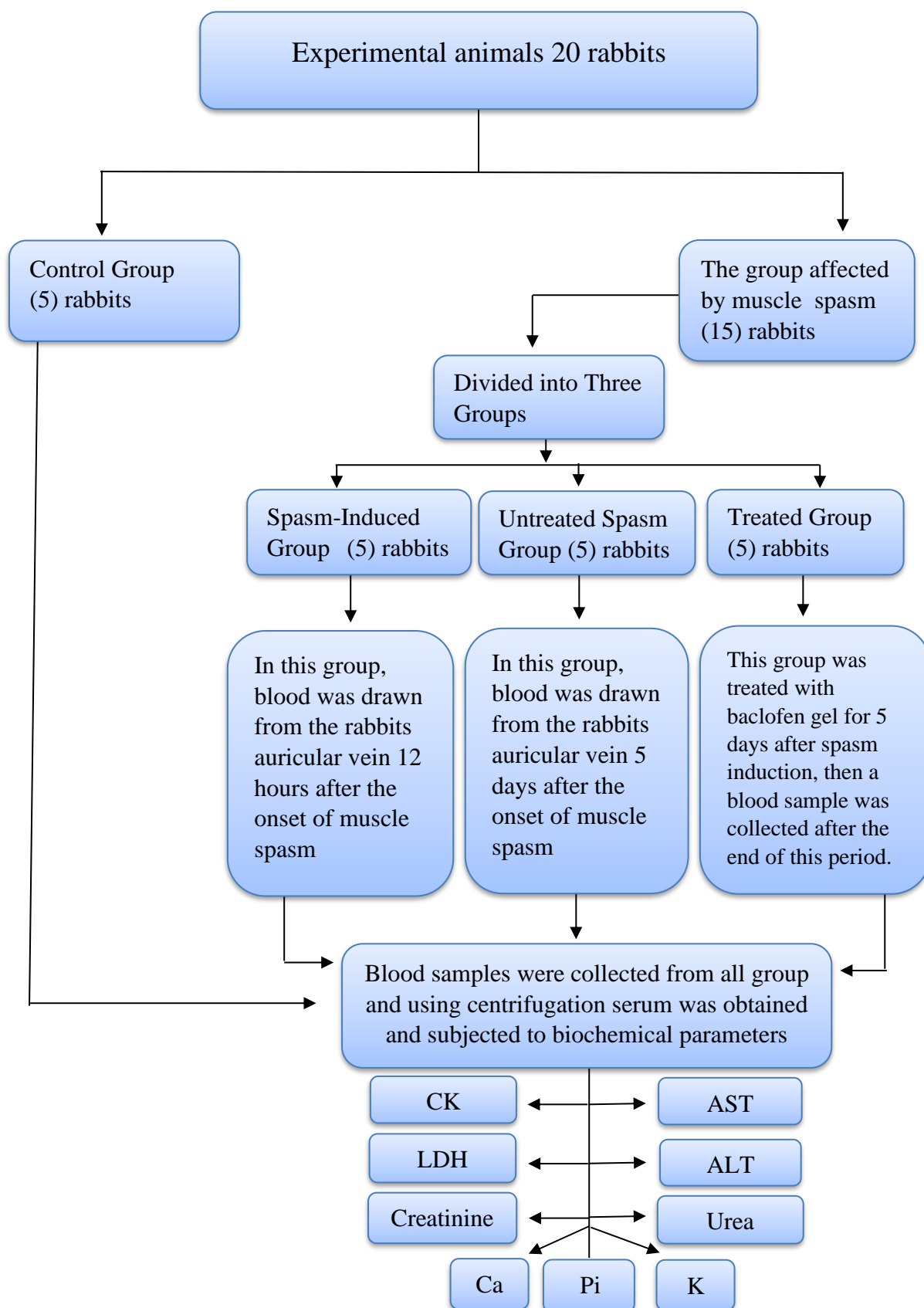


Figure (2-10): General schematic diagram of experimental group distribution and biochemical parameters

2.4.7.5 Biochemical parameters

2.4.7.5.1 Creatin kinase enzyme

CK activity was measured manually in serum samples using the kinetic enzymatic method. This method uses reagents from Medichem Middle East, Syria. The measurement is based on the following reaction:



In this method, changes in absorbance at a wavelength of 340 nm were recorded using a UV-Vis spectrophotometer. Enzyme activity was calculated in U/L according to the following equation:

$$\text{U/L} = (\Delta\text{Abs/min}) \times 8095$$

2.4.7.5.2 Lactate Dehydrogenase enzyme

LDH activity is measured manually in serum samples using the Modified Method (SFBC) based on reagents from Biolabo ,France. The measurement is based on the following reaction:

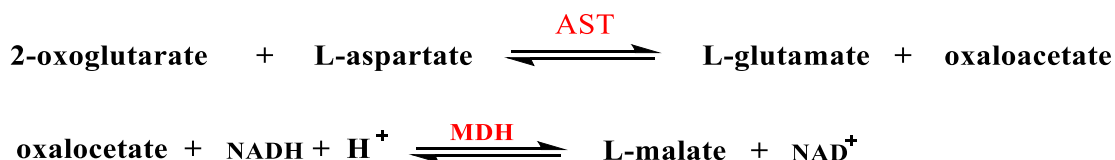


In this method absorbance changes were tracked at a wavelength of 340 nm using UV-Vis spectrophotometer. Enzyme activity was calculated in U/L according to the following equation:

$$\text{U/L} = (\Delta\text{Abs/min}) \times 8095$$

2.4.7.5.3 Aspartate Aminotransferase (AST) enzyme

The concentration of AST enzyme in serum samples was measured manual using the kinetic enzymatic method without pyridoxal phosphate activation. This method relies on the following reactions:



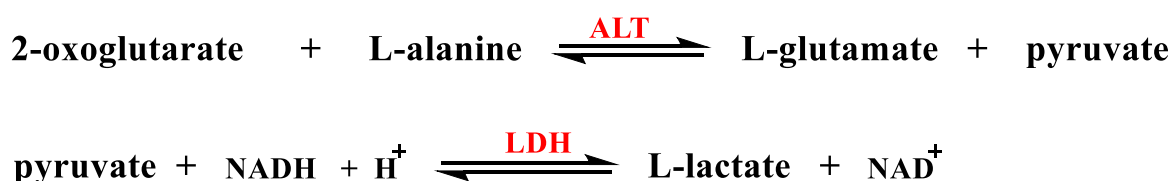
Absorbances were read at a wavelength of 340 nm using UV-Vis spectrophotometer. Enzyme activity U/L was calculated based on the following equation:

$$\text{U/L} = \frac{(A_2 - A_0)}{2} \times 1745$$

The reagents were used in this method from Human ,Germany.

2.4.7.5.4 Alanine Aminotransferase (ALT) enzyme

The concentration of AST enzyme in serum samples was measured manual using the kinetic enzymatic method without pyridoxal phosphate activation. This method relies on the following reactions:



Absorbances were read at a wavelength of 340 nm using UV-Vis spectrophotometer. Enzyme activity U/L was calculated based on the following equation:

$$\text{U/L} = \frac{(A_2 - A_0)}{2} \times 1745$$

The reagents were used in this method from Human ,Germany.

2.4.7.5.5 Calcium

Calcium concentration in blood serum samples is determined manually using Calcium (Arsenazo III) reagents from Biosam, Dubai UAE. This method was based on the principle of colour reaction between calcium ions and Arsenazo III at moderate pH. This reaction produces a blue-purple complex and the color intensity is directly proportional to the calcium concentration in the sample

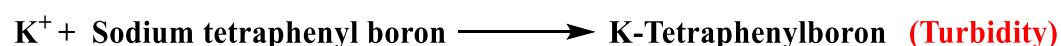


The absorbance was read using UV-Vis spectrophotometer at a wavelength of 650nm and calculate the calcium concentration in the samples according to the following equation:

$$\text{Concentration of calcium } \text{mg/dl} = \frac{\text{Abs. T}}{\text{Abs. S}} \times 10$$

2.4.7.5.6 Potassium

Potassium concentration in serum samples was measured manually using the final colorimetric method. This method uses the Monotest potassium reagent from Biosam, Dubai UAE. The test is based on the following reaction:



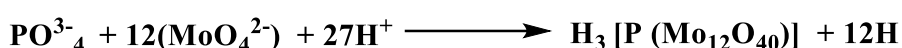
Potassium concentration was calculated by measuring absorbance at a wavelength of 630 nm using a UV-Vis spectrophotometer according to the equation:

$$\text{Concentration of Potassium } \left(\frac{\text{mEq}}{\text{L}}\right) = \frac{\text{Abs. T}}{\text{Abs. S}} \times 5$$

2.4.7.5.7 Phosphorus

The concentration of inorganic phosphorus in serum was determined manually using the colorimetric phosphomolybdate method, with reagents supplied by Spinreact, Spain.

This method is based on the reaction of inorganic phosphate ions with molybdic acid to form a phosphomolybdic complex, according to the following reaction:



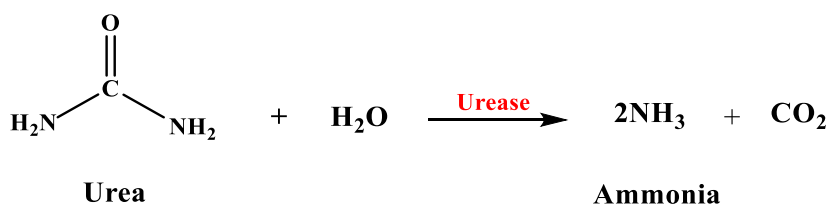
The resulting complex is subsequently reduced in an alkaline medium, yielding a blue molybdenum complex (molybdenum blue).

The absorbance of the colored complex was measured at a wavelength of 710 nm using a UV–Vis spectrophotometer, and the phosphorus concentration in serum (mg/dL) was calculated using the following equation:

$$\text{Phosphorus conc (mg/dl)} = \frac{(\text{A})_{\text{sample}} - (\text{A})_{\text{blank}}}{(\text{A})_{\text{standard}} - (\text{A})_{\text{blank}}} \times 5 (\text{Standard conc})$$

2.4.7.5.8 Urea

Urea concentration in serum samples was determined manually using the Urease–Berthelot method, with reagents obtained from Randox, UK. In this method, urea is enzymatically hydrolyzed by urease to produce ammonia and carbon dioxide, as represented by the following reaction:



The ammonia formed then reacts with salicylate and sodium hypochlorite (NaOCl) in the presence of sodium and phenolic ions to form a

green-colored complex known as 2,2-dicarboxyindophenol, according to the following simplified reaction:

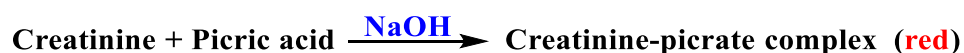


The intensity of the green color was measured at a wavelength of 600 nm using a UV–Vis spectrophotometer, and the urea concentration (mg/dL) was calculated using the equation :

$$\text{Urea concentraion (mg/dl)} = \frac{A_{\text{sample}}}{A_{\text{standard}}} \times \text{Standard conc}$$

2.4.7.5.9 Creatinine

Creatinine concentration in blood serum samples was determined manually using Jaffé colorimetric-kinetic method, which relies on the reaction of creatinine with picric acid in an alkaline medium, forming a red complex.



The rate of change in absorbance was measured at a wavelength of 492 nm using a UV-Vis spectrophotometer . Reagents from Spinreact, Spain, were used to measure creatinine concentration. Creatinine concentration in the samples was calculated using the equation.

$$\text{Concentration of Creatinine mg/dl} = \frac{\Delta A_{\text{sample}} - \Delta A_{\text{blank}}}{\Delta A_{\text{standard}} - \Delta A_{\text{blank}}} \times 2 (\text{Standard Conc})$$

All analyses were performed according to the instructions supplied with the reagents

2.4.7.6 Statistical Analysis

Statistical Package for the Social Sciences (SPSS) program was used to analyze the data statistically, and data were expressed as mean \pm standard deviation. One-way analysis of variance (ANOVA) was used to compare the mean of the four groups to find statistically significant differences. Followed by the least significant difference test (LSD) to find the difference between the means of each two groups at a significance level ($P < 0.05$).

Chapter Three

Results and Discussions

3. Results and Discussions

3.1 Characterization of Baclofen

3.1.1. Baclofen melting point

The results of measuring the melting point of baclofen (208-210°C) showed values close to the reference values (206-208°C). This slight difference is attributed to the possibility of the presence of a different crystalline form of the baclofen used [86].

3.1.2 Wavelength maximum (λ_{\max}) of Baclofen

Using a UV-Vis spectrophotometer, a spectral scan was performed in the range (200-400 nm) for a solution containing 25 $\mu\text{g/mL}$ of baclofen in PBS. As shown in Figure (3-1) the maximum absorption peak was observed (λ_{\max}) at 218 nm, which is close to the maximum absorption value (λ_{\max}) determined in previous studies [133].

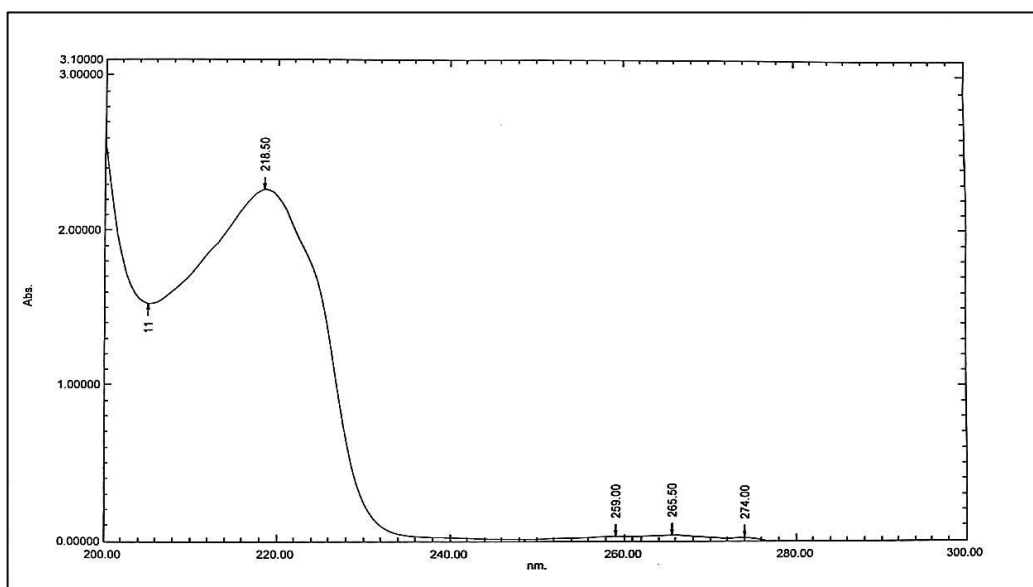


Figure (3-1): Absorption Spectrum of Baclofen in PBS

3.1.3 Baclofen Calibration Curve

Using a series of standard solutions diluted of baclofen in PBS at 218 nm, a calibration curve for BFN was determined as shown in figure (3-2). A straight line value ($R = 0.9993$) was observed when plotting absorbance versus concentration, indicating a strong linear relationship consistent with the Beer-Lambert law and confirming the reliability of the calibration curve.

Table (3-1): Graph data of Baclofen in (PBS) pH 6.8

S.no	Conc.($\mu\text{g/mL}$)	Abs.
1	0	0
2	5	0.235 ± 0.001
3	10	0.459 ± 0.037
4	15	0.653 ± 0.002
5	20	0.869 ± 0.0014
6	25	1.101 ± 0.068

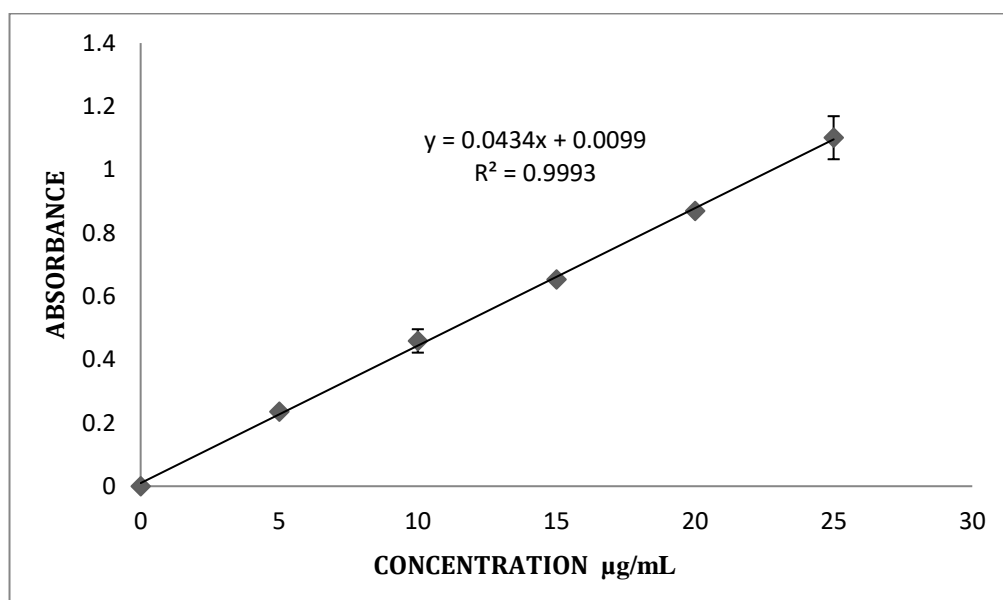


Figure (3-2): Calibration Curve of Baclofen in PBS

3.2 Characterization of Liposomes

3.2.1 Fourier Transform Infrared Spectroscopy (FTIR)

In this study, Fourier transform infrared spectroscopy was used to identify the chemical and physical interactions between baclofen and baclofen liposomes vesicles. The FTIR spectrum of baclofen showed distinct absorption peaks at 3522 cm^{-1} , attributed to the N–H stretching vibrations of the amino group, and at 3381 cm^{-1} , attributed to the O–H stretching vibrations of the hydroxyl group. The aliphatic C–H group exhibited a medium absorption band extending between (2926 and 2895 cm^{-1}). A peak at 1647 cm^{-1} was also identified, attributed to the vibrational stretching of the carboxylic C=O bond, and a peak at 1508 cm^{-1} was attributed to the vibrational stretching of the aromatic C=C bond. A peak at 785 cm^{-1} was observed, attributed to the bending stretching of the C–Cl bond, figure (3-3). The spectrum of baclofen nano liposome vesicles showed a slight shift in the main baclofen peaks. This shift may be due to physical interactions, such as hydrogen bonding, dipole-dipole interaction, or van der Waals forces, between the functional groups in the drug and the nano liposome components. This shift did not result in a chemical change in the drug structure, indicating successful loading of baclofen into the nano liposomes. This confirms the good compatibility between baclofen and the additives. The results of this study are consistent with previous studies [134] [135].

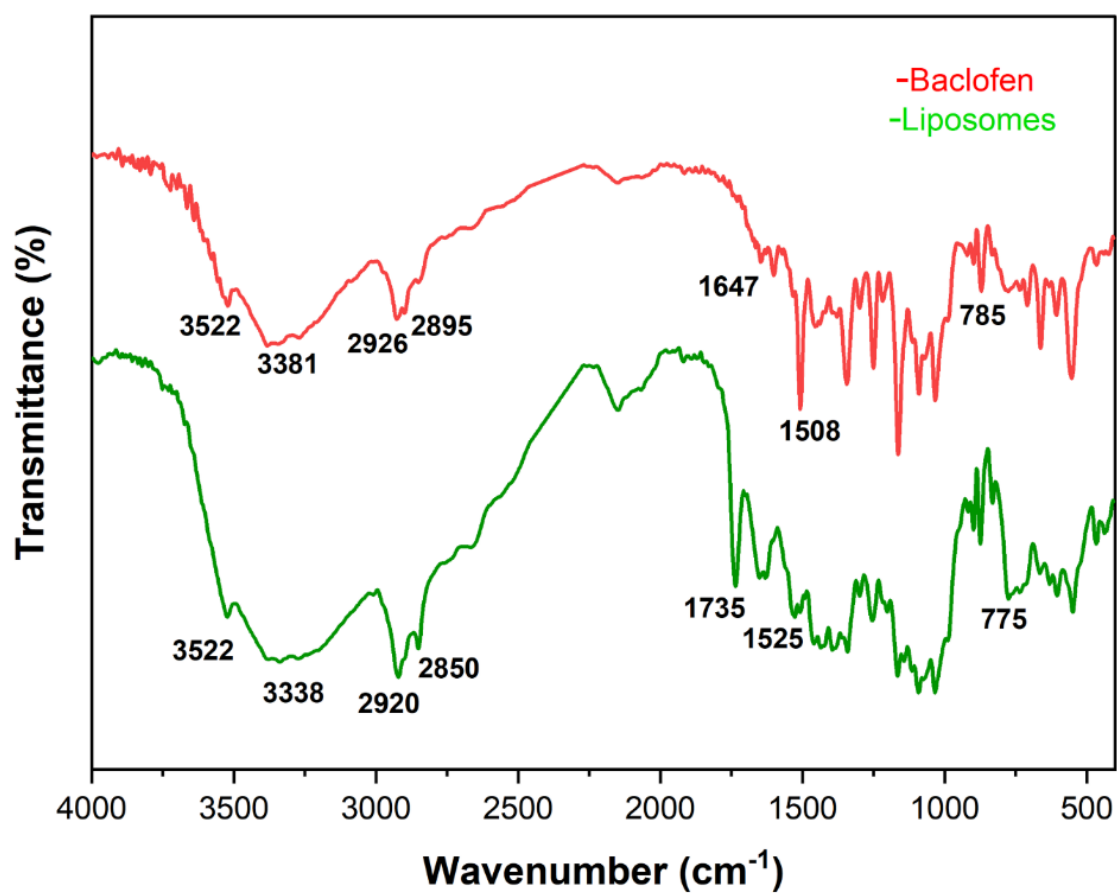


Figure (3-3) : FT-IR Spectrum of the Baclofen and nano Liposome

3.2.2 Field Emission Scanning Electronic Microscope (FESEM) of Baclofen Liposome Vesicles

FESEM images in figure (3-4) show that the baclofen-loaded liposomes exhibit non-spherical morphology and irregular shapes. Although liposomes are generally defined as vesicles with a spherical shape, their appearance under the scanning electron microscope can be influenced by the preparation steps required prior to imaging. These include fixation to preserve the surface structure, followed by freezing/lyophilization, and coating with a conductive layer to enhance electron conductivity. Collectively, these procedures may induce mechanical stress and relative shrinkage, leading to deviation from the ideal spherical shape [136].

In addition, loading liposomes with a hydrophilic drug such as baclofen can increase the osmotic pressure inside the vesicles, resulting in partial water loss, which may also contribute to morphological deformations [137].

It is important to note that the non-spherical shape does not necessarily indicate reduced drug efficiency, as recent studies have suggested that intentionally designing non-spherical nanocarriers may offer improved pharmacological properties, such as reducing cellular uptake rate, prolonging residence time, enhancing permeability, and consequently increasing particle accumulation at the target therapeutic site [138].

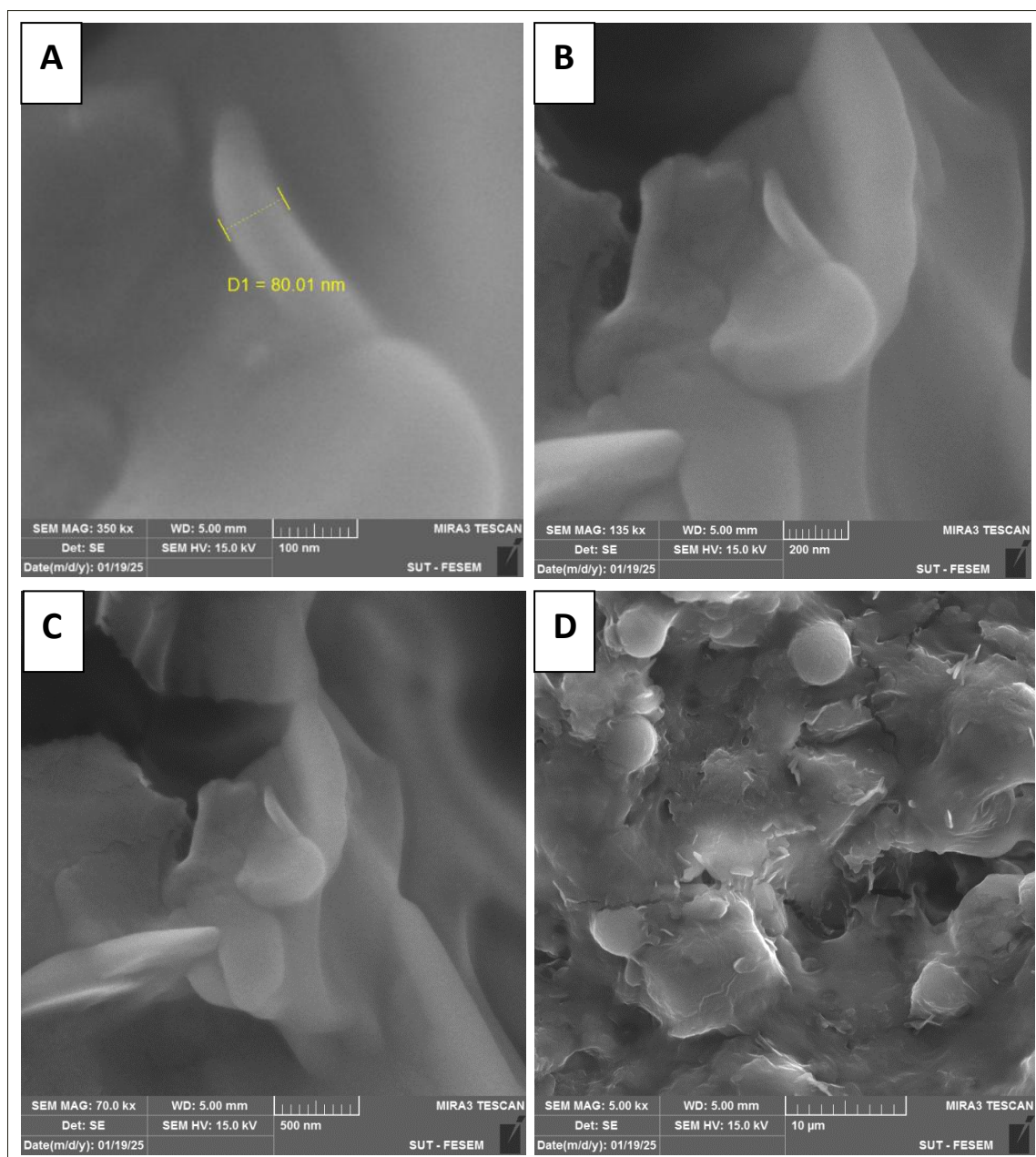


Figure (3-4): Field Emission Scanning Electron Micrographs (FESEM) of Baclofen Liposome Vesicles at Different Magnifications: (A) 100 nm scale; (B) 200 nm scale, (C) 500 nm scale, (D) 10 μm scale.

3.2.3 Dynamic Light Scattering (DLS) Analysis of Baclofen Liposome Vesicles

The average hydrodynamic diameters and polydispersity indices of liposomes were determined by Dynamic light scattering (DLS) analysis. DLS measures the hydrodynamic diameter of particles in aqueous solution based on Brownian motion and also measures the particle size including the hydration layer of surrounding water molecules [127]. The results showed a significant difference in the average hydrodynamic diameter of the liposome samples. The average diameter of the sample containing a mixture of Tween 80 and Span 80 was 172.6 nm figure (3-5), while the average diameter of the sample containing Tween 80 was 36.67 nm figure (3-6). The sample containing Span 80 showed an average diameter of 167.2 nm figure (3-7), while the sample containing sodium deoxycholate recorded an average diameter of 169.8 nm figure (3-8). This variation in liposome sizes can be explained by the different types and ratios of surfactants used in the liposome composition, as these directly affect the nature of the phospholipid membrane and its chemical and physical properties, which is reflected in the size of the resulting liposome. The introduction of Tween 80 into the liposome preparation resulted in a decrease in their size. This is logical because Tween 80 increases the spontaneous curvature of the phospholipid membrane, and to accommodate this curvature, liposomes are smaller. Furthermore, Tween 80 reduces the high surface tension of the liposomes due to its hydrophilic nature, resulting in the production of small, homogeneous liposomes [139]. While samples containing Span 80 showed larger liposomes compared to those containing Tween 80, this is attributed to the lipophilic nature of Span80, which can interact with the lipophilic chains of the phospholipids and lipid substances such as cholesterol, leading to competition and clustering within the membrane, thus increasing the relative size of the particles [65].

Sodium deoxycholate is amphipathic, containing a hydrophilic part and lipophilic part. Therefore, it does not completely cover the liposome surface like Tween 80. Therefore, the surface layer is less stable, and the surface pressure decreases, allowing liposomes to be larger [140]. However, mixing Tween 80 with Span 80 results in larger liposomes. This may be attributed to the imbalance in the internal arrangement of the particles and the interaction of the different properties of Sp80 and Tw80.

The polydispersity index (PDI) values for all samples were within the acceptable range of 0.369–0.663, as shown in Table (3-2). It is well established that PDI values below 0.7 indicate a uniform nanoparticle size distribution and the absence of significant agglomeration [141].

Table (3-2): All Formulation hydrodynamic diameters and PDI

Formulation	Hydrodynamic diameters	PDI
BLV ₁	173.6 nm	0.486
BLV ₂	36.67 nm	0.359
BLV ₃	167.2 nm	0.514
BLV ₄	169.8 nm	0.663

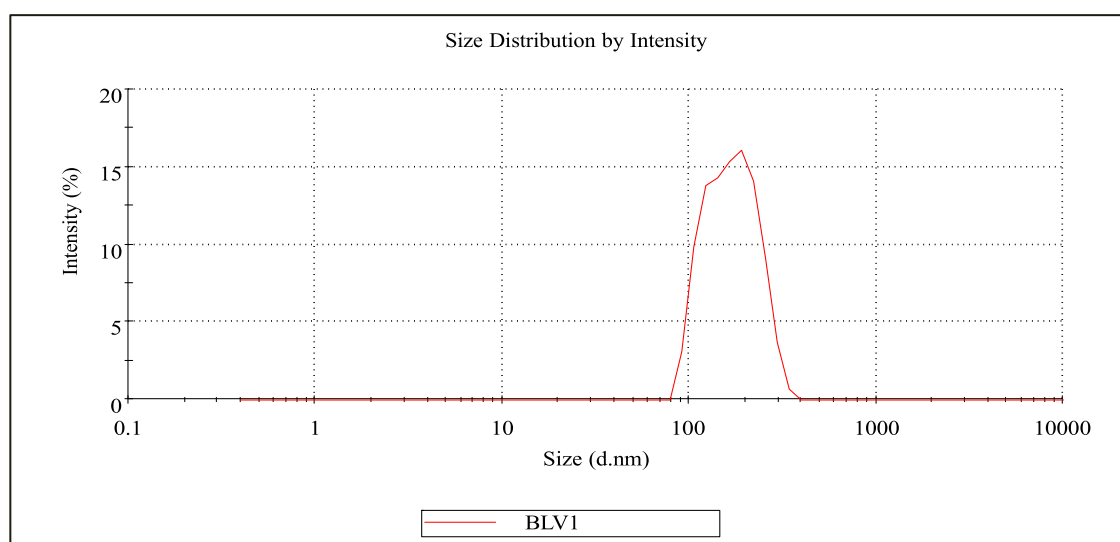


Figure (3-5): Size Distribution by Intensity of the BLV₁

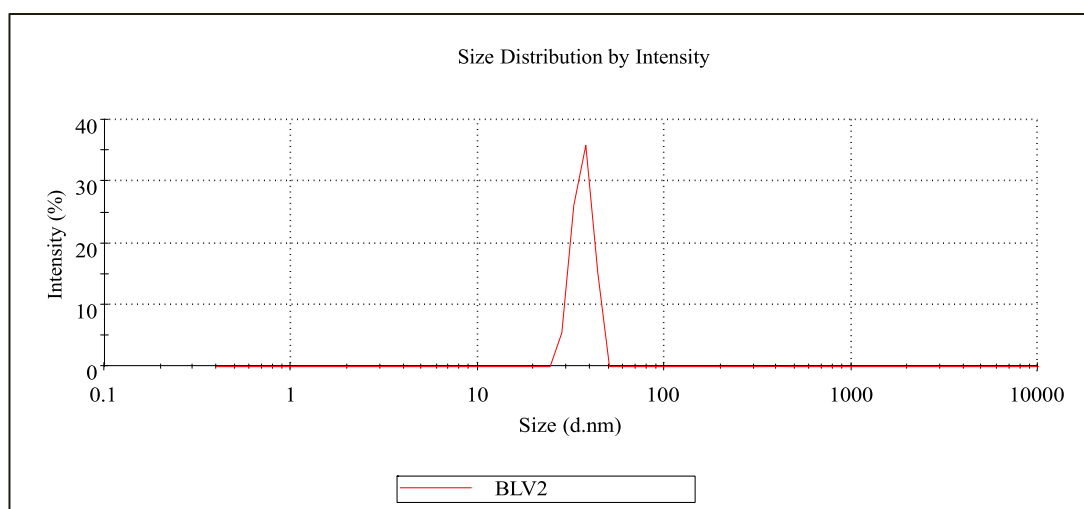
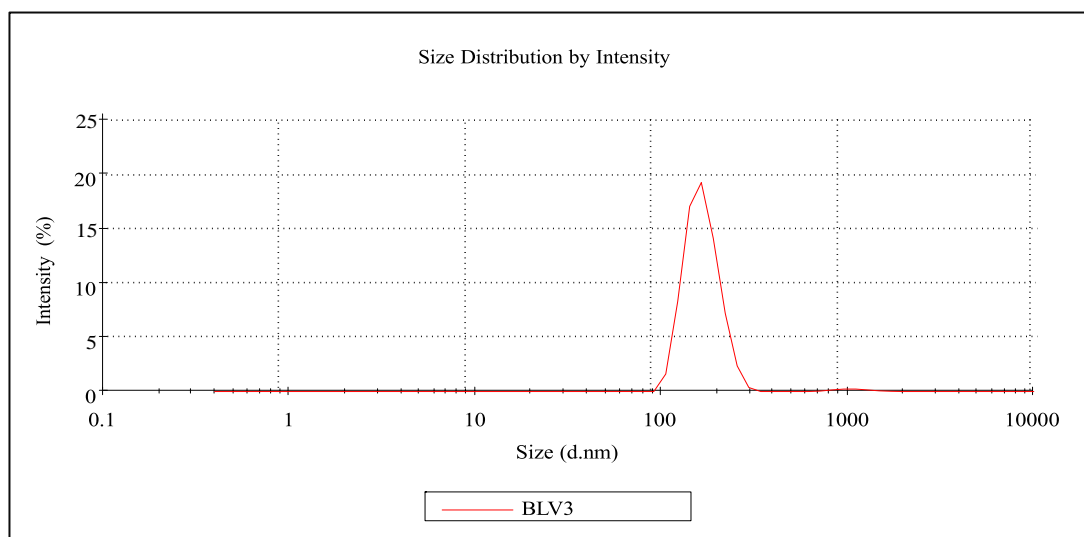
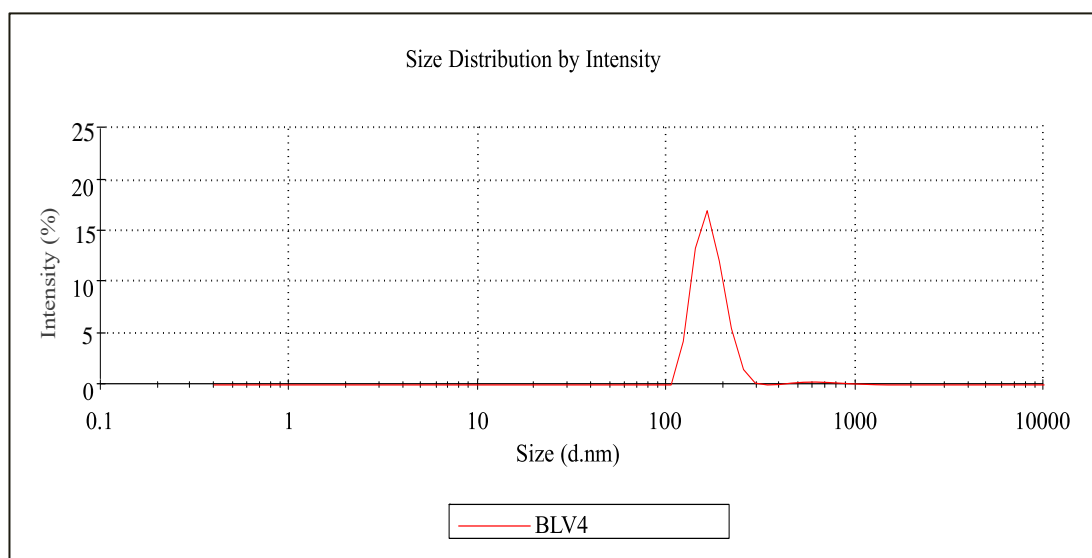
Figure (3-6): Size Distribution by Intensity of the BLV₂

Figure (3-7): Size Distribution by Intensity of the BLV

Figure (3-8): Size Distribution by Intensity of the BLV₄

3.2.4 Field Emission Scanning Electronic Microscope (FESEM) of BLV₂ Gel

FESEM images in figure (3-9 A) of the carbopol gel containing baclofen-loaded liposomes show a homogeneous surface structure with a branched network pattern. This pattern indicates a clear physical interaction between the carbopol network and the liposomes within the gel matrix, suggesting the formation of a stable three-dimensional structure. This structural behavior results from the incorporation of liposomes into the gel framework, which modifies the internal structure of carbopol and improves the physical and rheological properties of the gel, such as viscosity, shrinkage, and swelling capacity.

The accompanying histogram in figure (3-9 B) illustrates the particle size distribution of the liposome vesicles within the gel. The curve indicates that most of the particles fall within a size range of 40–80 nm, with an average diameter of approximately 60 nm. This relatively narrow distribution reflects particle size uniformity and the successful encapsulation of liposomes within the gel matrix in an orderly manner.

These findings confirm the high efficiency of liposome loading within the carbopol gel and are consistent with previous research indicating the role of liposomes in enhancing the structural and mechanical properties of hydrogel materials [142][92].

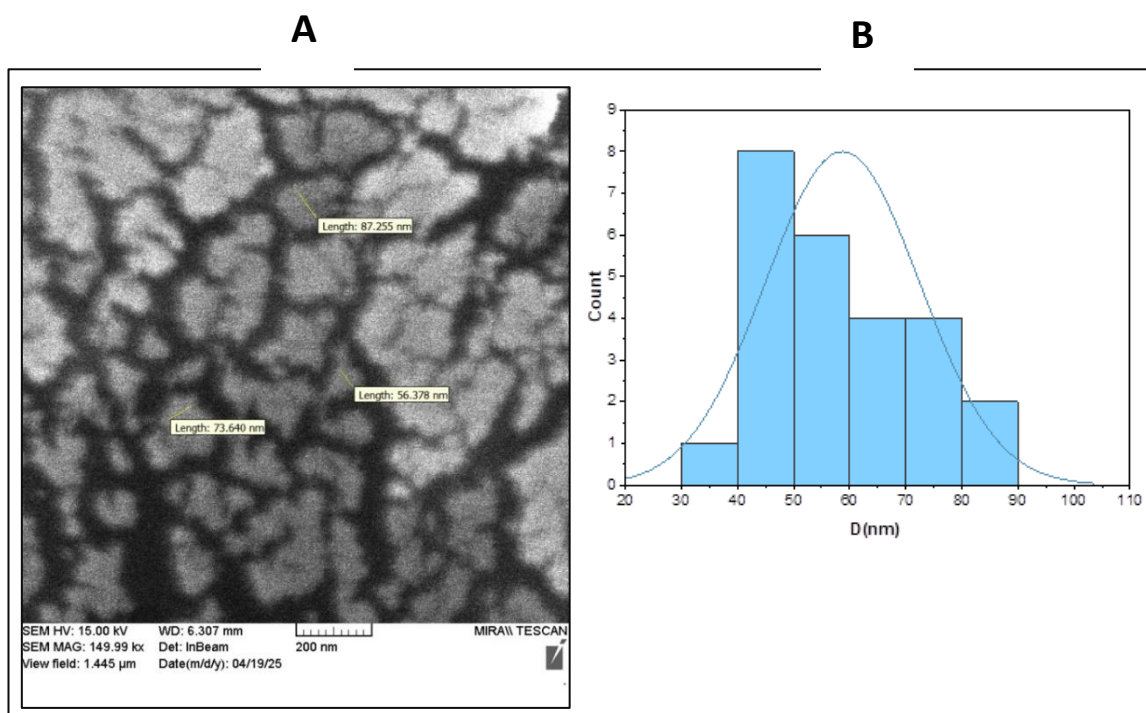


Figure (3-9): (A) Field Emission Scanning Electron Micrographs of BLV₂ Gel, (B) Particles Diameters Distribution

3.2.5 Zeta Potential Analysis

The zeta potential measures the surface charge of particles and is an important indicator of their physical stability. With an increase in the magnitude of the zeta potential, whether positive or negative, the electrostatic repulsion between particles increases, which prevents aggregation or sedimentation and makes the particles more stable.

As shown in figure (3-10), the zeta potential of liposomes (BLV2) was -65.6 mV, with an electrophoretic mobility of -0.000508 cm²/V·s. This high negative charge reflects the ability of the liposomes to resist aggregation or sedimentation, confirming their good physical stability. These results are consistent with the findings of Naemeh et al [143], which showed that a high negative charge increases particle stability and reduces aggregation.

After encapsulating the liposomes in Carbopol gel, the zeta potential slightly decreased to -63.3 mV, which is close to the original value of BLV2. This indicates that the encapsulation process did not adversely affect the surface charge or stability, demonstrating good compatibility between Carbopol gel and BLV2.

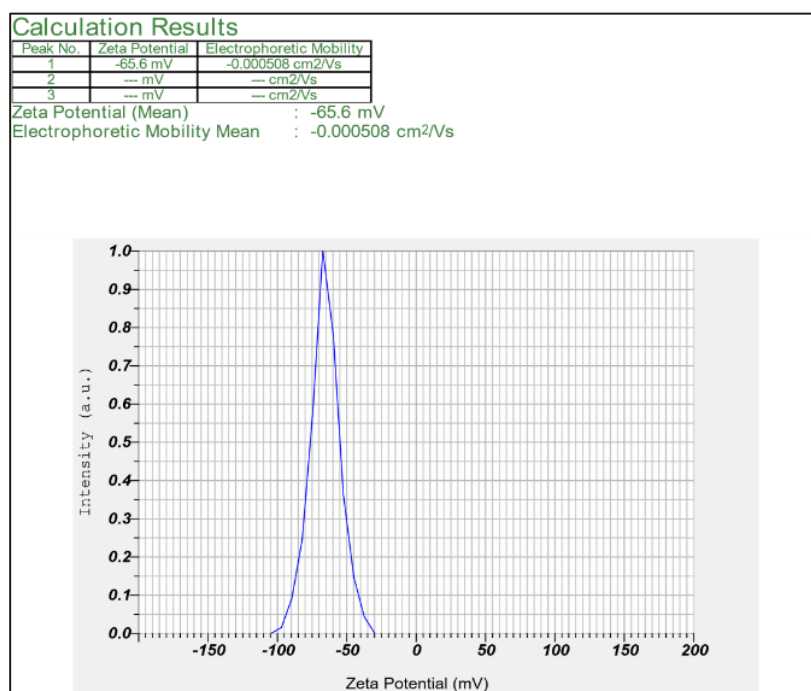


Figure (3-10) : Zeta Potential of BLV₂

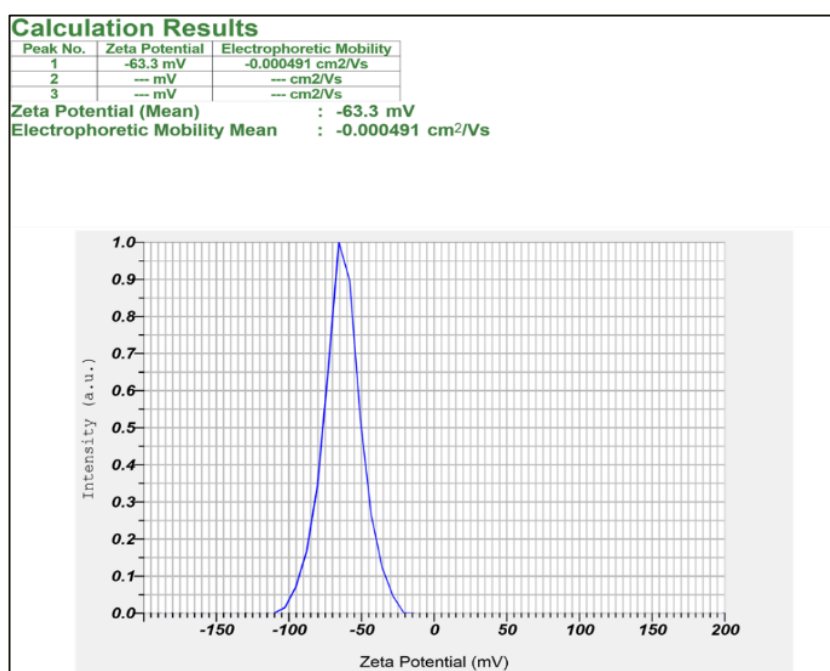


Figure (3-11) : Zeta Potential of BLV₂ gel

3.3 Field Emission Scanning Electronic Microscope (FESEM) of Nylon 6,6 Nanofibers

The field emission scanning electron microscopy (FESEM) images show figure (3-12 A,B,C) the morphological characteristics of the Electrospun nanofibers made from nylon 6,6 polymer. The images reveal that the fibers exhibit a uniform and interconnected network structure forming a dense web of interlaced fibers, and they are free from beads, which typically appear as a result of low polymer solution viscosity or poor homogeneity.

The absence of beads in this system is attributed to the optimal balance in polymer solution viscosity and its compatibility with the electrospinning process parameters, which allowed the formation of homogeneous and stable nanofibers. The images also show that the fibers display a high degree of interconnection and visible porosity, indicating the successful production of nanofibers with a porous structure suitable for applications requiring high permeability, such as filtration [144].

Figure (3-13 B) illustrates the distribution of nanofiber diameters, showing an average diameter of approximately 57.29 nm. The distribution curve indicates that most of the fibers fall within the range of 40–80 nm, reflecting uniformity in nanofiber size and the absence of agglomeration or significant diameter variations.

These results confirm that the preparation conditions were optimal for obtaining fine and uniform nanofibers and are consistent with previous studies, which have demonstrated that increasing the viscosity of the polymer solution and precisely controlling the electrospinning parameters result in bead-free nanofibers with homogeneous size distribution [145][146].

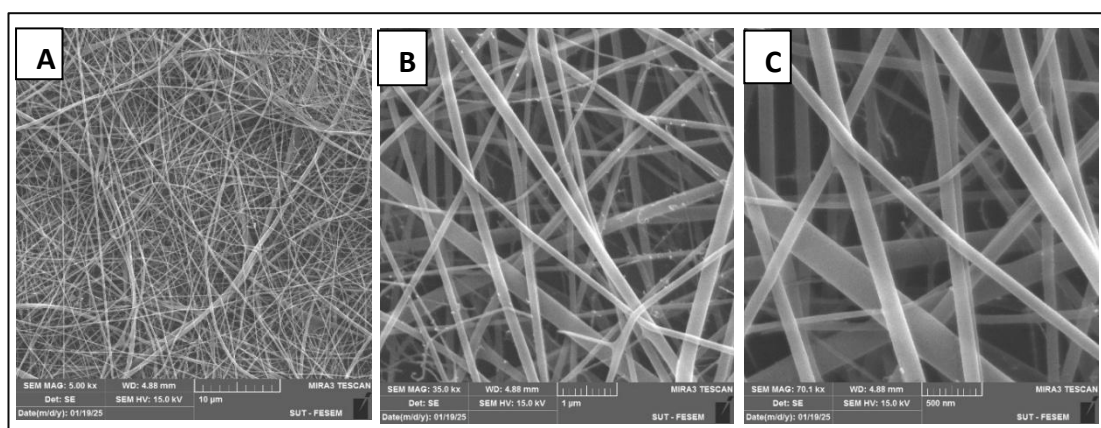


Figure (3-12): FESEM Images of Nylon 6,6 Nanofibers at Different Magnifications (a) 10 μm scale, (b) 1 μm scale, (c) 500 nm scale

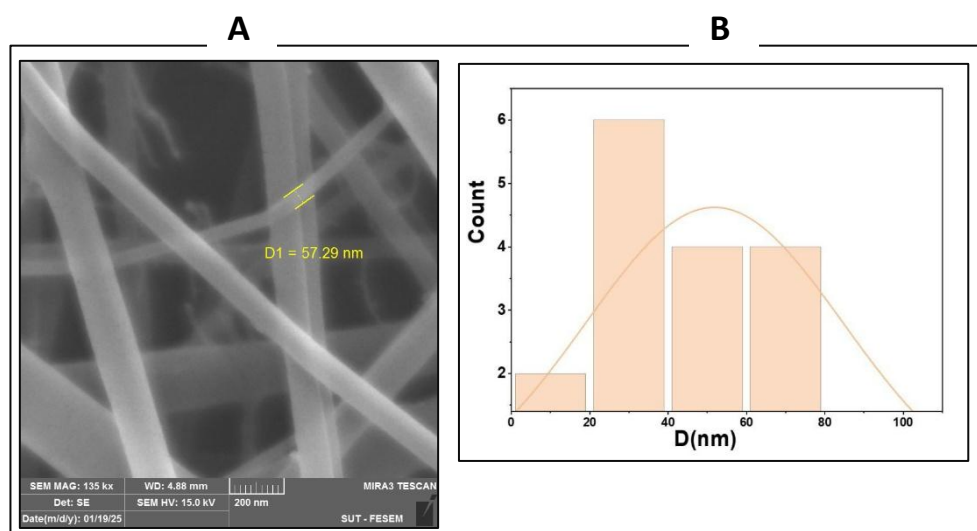


Figure (3-13): (A) Field Emission Scanning Electron Micrographs of Nylon 6,6 Nanofibers Showing Diameter Measurement, (B) Nanofibers Diameters Distribution

3.4 Applications for Baclofen nano-Liposome Vesicles (BLV₂) *in vitro*

3.4.1 Determination of the effect of BLV₂ on inhibition of Lactate Dehydrogenase enzyme (LDH)

Table (3-3) presents the relationship between substrate concentration and the rate of enzymatic reaction for LDH in the absence of an inhibitor while table (3-5) illustrates the effect of adding BLV₂ on the same enzymatic reaction. Figure (3-14) illustrates the Michaelis-Menten curve, showing that at high substrate concentrations, the enzymatic reaction rate reaches V_{\max} due to the saturation of all active enzyme binding sites. This observation confirms that further increases in substrate concentration do not lead to a higher reaction rate due to full occupancy of the active sites [147]. The values of V_{\max} and K_m in the absence of an inhibitor were 2500 and 1, respectively. Upon addition of BLV₂, both V_{\max} and K_m decreased to 769 and 0.3, respectively, as shown in table (3-6). Theoretically, this behavior could be described as competitive inhibition, as the inhibitor is capable of binding to the ES complex. However, practically, the simultaneous decrease in both V_{\max} and K_m is characteristic of uncompetitive inhibition, where the inhibitor binds only to the ES complex, resulting in a reduction of both the maximum velocity and the affinity constant figure (3-15) [148].

Table (3-4) shows the percentage inhibition of LDH enzyme activity estimated at 356IU/L using six dilute concentrations of baclofen nanoliposomes vesicles. The inhibition reached its highest value of 52% at the highest dilute concentration. This supports the inhibitor's ability to affect the enzyme's activity by binding to ES through hydrogen bonds that are believed to form between the functional groups in baclofen and the active binding sites in enzyme [149].

Table (3-3): Substrate concentrations values and enzymatic reaction rate of LDH Before adding baclofen nanoliposome vesicles as an inhibitor .

V IU/L	130	170	259	332	348	356
[S]mmol/L	0.05	0.07	0.11	0.15	0.018	0.2

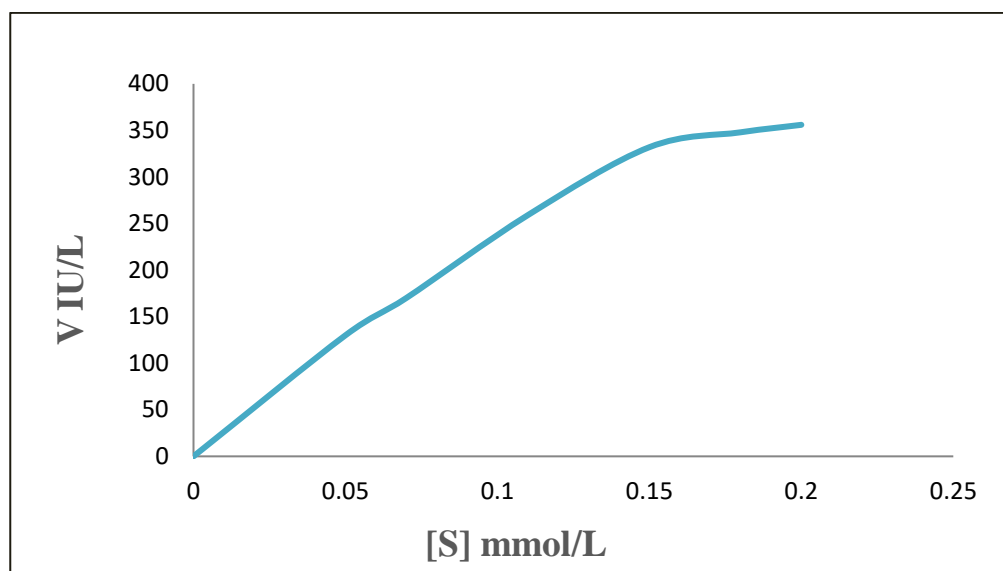


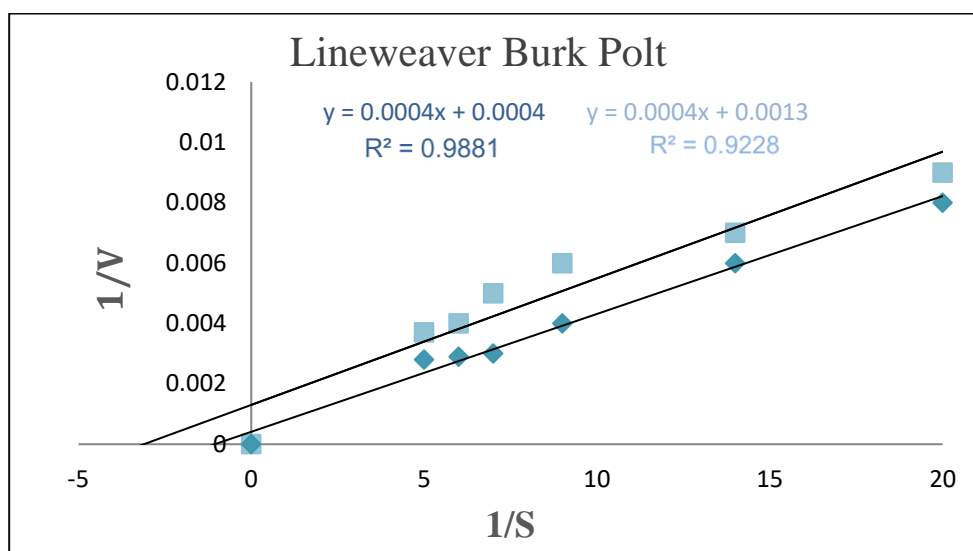
Figure (3-14): Michaelis-Menten Equation's curve between the rate of enzymatic reaction V and Substrate concentration [S].

Table (3-4): The estimated effectiveness of baclofen nanoliposome vesicles in inhibiting the LDH enzyme was 356 IU/L.

Inhibitor conc. Ppm	Enzyme Activity IU/L	% Inhibitor
15	300	16
30	275	23
45	227	36
60	219	38
75	194	46
100	170	52

Table (3-5): Substrate concentrations values and enzymatic reaction rate of LDH after adding baclofen nanoliposome vesicles as an inhibitor.

V IU/L	117	137	162	202	227	267
[S] mmol/L	0.05	0.07	0.11	0.15	0.18	0.2



V^{-1} with inhibitor

V^{-2} without inhibitor

Figure (3-15): (Line Weaver Burk Plot) Equation of LDH enzyme without and with inhibitor

Table (3-6):The kind of inhibition for Baclofen nanoliposome vesicles affecting the LDH enzyme.

Name of compound	Kind of Inhibition	K_m	V_{max}
baclofen nano liposome vesicles	Uncompetitive Inhibition	Without inhibitor	Without inhibitor
		1	2500
		With inhibitor	With inhibitor
		0.3	769

3.4.2 Determination of the effect of BLV₂ on inhibition of Creatine Kinase enzyme (CK)

The data presented in table (3-7) show the relationship between substrate concentration and the rate of enzymatic reaction in the absence of any inhibitor while table (3-9) illustrates the effect of adding BLV₂ on the same reaction. Figure (3-16) illustrates a typical Michaelis-Menten curve for CK, representing the behavior of enzymes that follow the Michaelis-Menten equation in the absence of an inhibitor. It is observed that the enzymatic reaction rate increases with increasing substrate concentration due to the availability of active binding sites in the enzyme. However, as the substrate concentration continues to increase, the rate of increase in reaction velocity gradually decreases until the velocity reaches its maximum (V_{\max}), when all active sites of the enzyme are saturated [147]. According to table (3-10), the values of V_{\max} and K_m in the absence of an inhibitor are 588 and 45, respectively. Upon addition of BLV₂, V_{\max} decreased to 500 while K_m remained constant. Theoretically, this behavior could be interpreted as competitive inhibition because the inhibitor can interact with the enzyme. However, practically, the reduction V_{\max} in without any change in K_m indicates a non-competitive inhibition, where the inhibitor can bind to the enzyme whether it is free or substrate-bound, leading to a decrease in enzymatic activity without altering the affinity constant figure (3-17) [148].

Table (3-8) shows percentage inhibition CK enzyme active estimated 440 IU/L Using six diluted concentrations of baclofen nanoliposomes vesicles, the highest inhibition rate reached 66% at the highest diluted concentration. This supports the inhibitor's ability to affect the activity of the CK enzyme by binding to ES and E via hydrogen bonds believed to form between the functional groups in baclofen and the active binding sites in enzyme [149].

Table (3-7) : Substrate concentrations values and enzymatic reaction rate of CK Before baclofen nanoliposome vesicles as an inhibitor.

V IU/L	234	325	385	410	440
[S] mmol/L	30	60	90	120	150

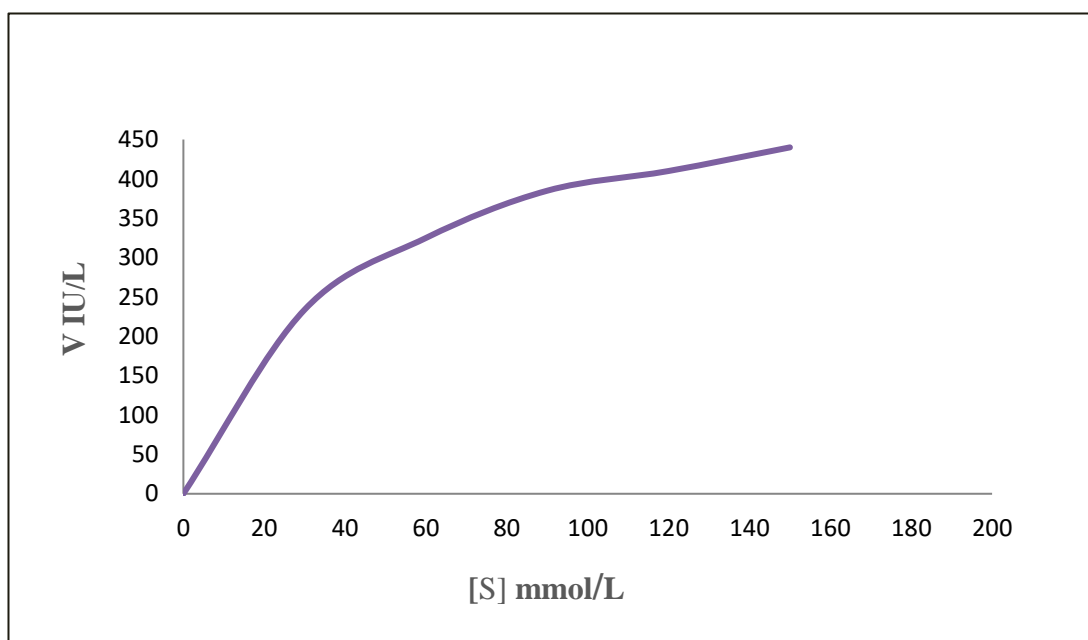


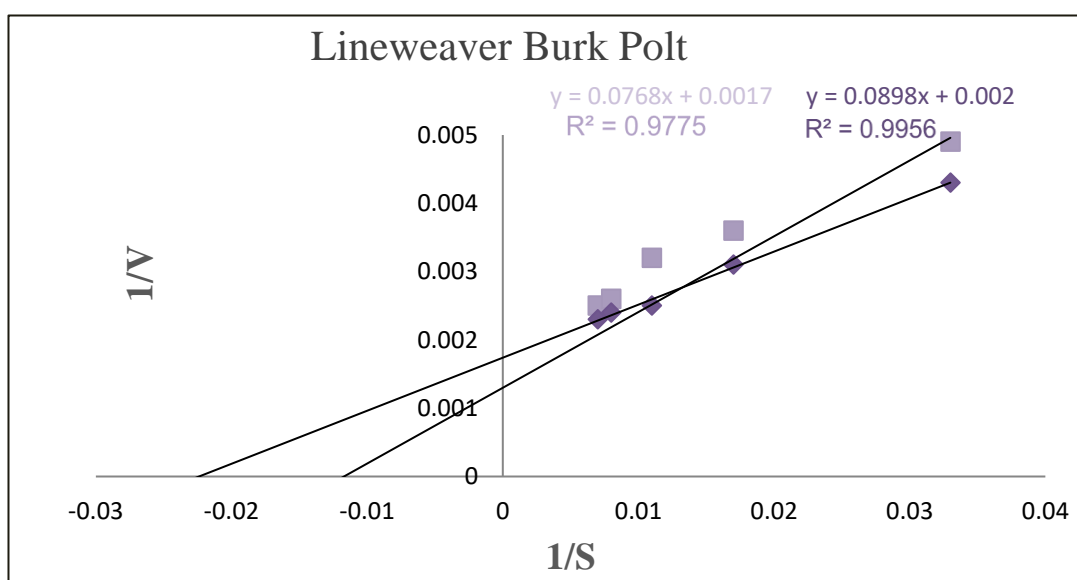
Figure (3-16): Michaelis-Menten Equation's curve between the rate of enzymatic reaction V and Substrate concentration [S].

Table (3-8): The estimated effectiveness of baclofen nanoliposome vesicles in inhibiting the CK enzyme was 440 IU/L.

Inhibitor conc. Ppm	Enzyme Activity U/L	% Inhibitor
15	400	10
30	345	21
45	305	31
60	243	45
75	213	52
100	152	66

Table (3-9): Substrate concentrations values and enzymatic reaction rate of CK after adding baclofen nanoliposome vesicles as an inhibitor.

V IU/L	202	265	310	382	401
[S] mmol/L	30	60	90	120	150



V^{-1} with inhibitor

V^{-2} without inhibitor

Figure (3-17): (LineWeaver Burk Plot) Equation of CK enzyme without and with inhibitor

Table (3-10):The kind of inhibition for baclofen nanoliposome vesicles affecting the CK enzyme.

Name of compound	Kind of Inhibition	K_m	V_{max}
baclofen nano liposome vesicles	Non-Competitive Inhibition	Without inhibitor	Without inhibitor
		45	588
		With inhibitor	With inhibitor
		45	500

3.4.3 Half-maximal inhibitory concentration IC₅₀ Calculations

The IC₅₀ value represents the concentration of the inhibitor (BLV₂) required to inhibit the enzymatic reaction rate by 50% [150]. In this study, the results showed that the IC₅₀ value for BLV₂ was 72.48µg/ml for inhibiting the CK enzyme, and 86.354µg/ml for inhibiting the LDH enzyme, as shown in two Figures (3-18) (3-19).

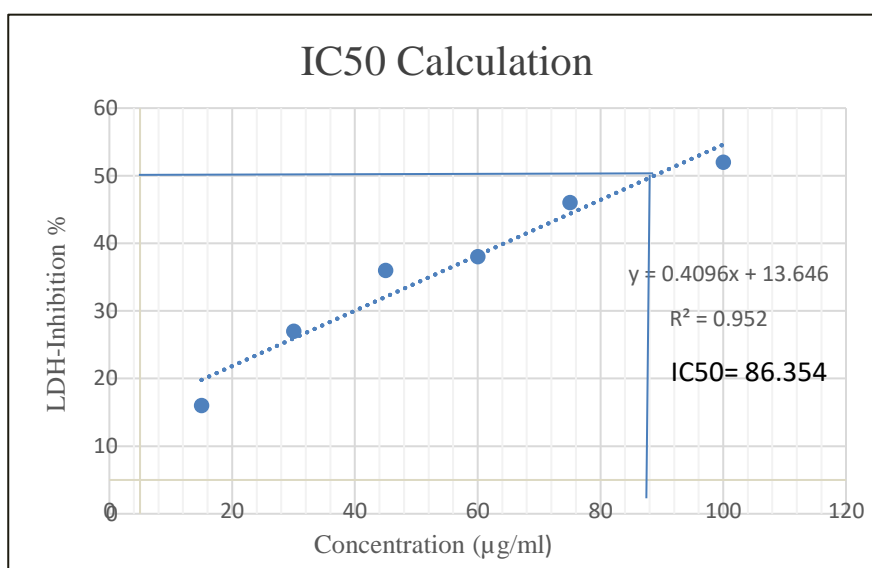


Figure (3-18): IC₅₀ of BLV₂ as inhibitor to LDH- enzyme

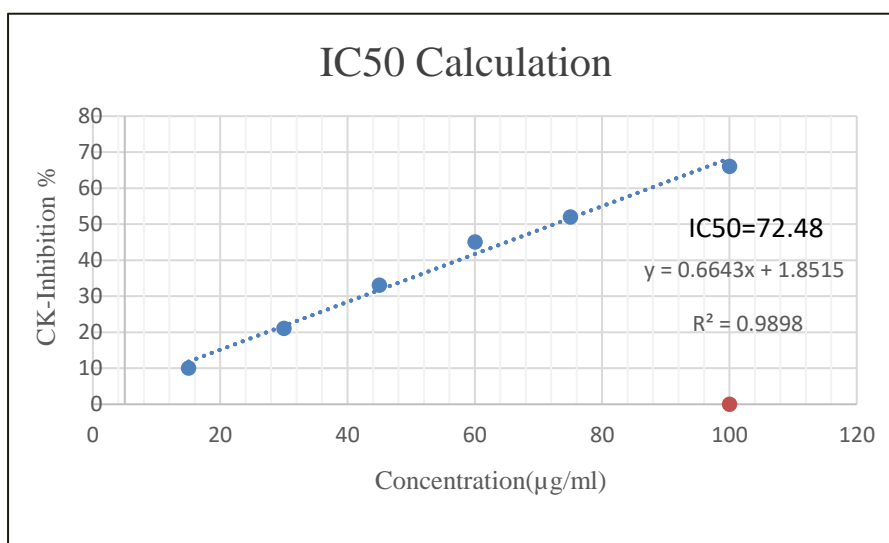


Figure (3-19): IC₅₀ of BLV₂ as inhibitor to CK-enzyme

3.4.4 *In vitro* release of Baclofen from BLV₂ Gel in PBS for 1-10 hour

The *in vitro* release results of baclofen from BLV₂ gel formulations containing different concentrations of Carbopol 934 (0.5%, 1%, and 1.5%) show distinct differences in cumulative release percentages among the formulations over the experimental period. The formulation containing 0.5% Carbopol exhibited the highest cumulative baclofen release within 10 hours, followed by the 1% and then the 1.5% formulations, as shown in Figure (3-20) and Table (3-11). This behavior is related to the properties of the gel itself, as decreasing the Carbopol concentration reduces the gel viscosity, allowing easier drug diffusion and consequently increasing the cumulative release percentage. Conversely, increasing the Carbopol concentration leads to higher gel viscosity, which hinders drug molecule mobility and reduces the rate and extent of drug release over time. These results are in agreement with previous studies that have reported a correlation between gel viscosity and the smoothness of drug release [151].

Table (3-11): Percentage release of BLV₂ Gel

Time(hr.)	BLV ₂ with 0.5% Carbopol	BLV ₂ with 1% Carbopol	BLV ₂ with 1.5% Carbopol
0	0	0	0
1	13.3 ± 0.02	9.46±0.015	6.75±0.02
2	19 ± 0.0264	16.81±0.15	15.06±0.1
3	29.58 ± 0.102	25.76±0.019	23.55±0.09
4	43.87 ± 0.210	39.83±0.054	38.25±0.05
5	49.78 ± 0.07	45.71±0.801	43.27±0.016
6	58.423±0.489	52.56±0.3	48.50±0.02
7	65.52±0.453	57.58±0.2	54.77±0.61
8	71.65±0.300	64.29±0.005	60.43±0.5
9	75.45±0.736	71.94±0.2	66.25±0.12
10	80.75±0.11	74.38±0.1	70.25±0.89

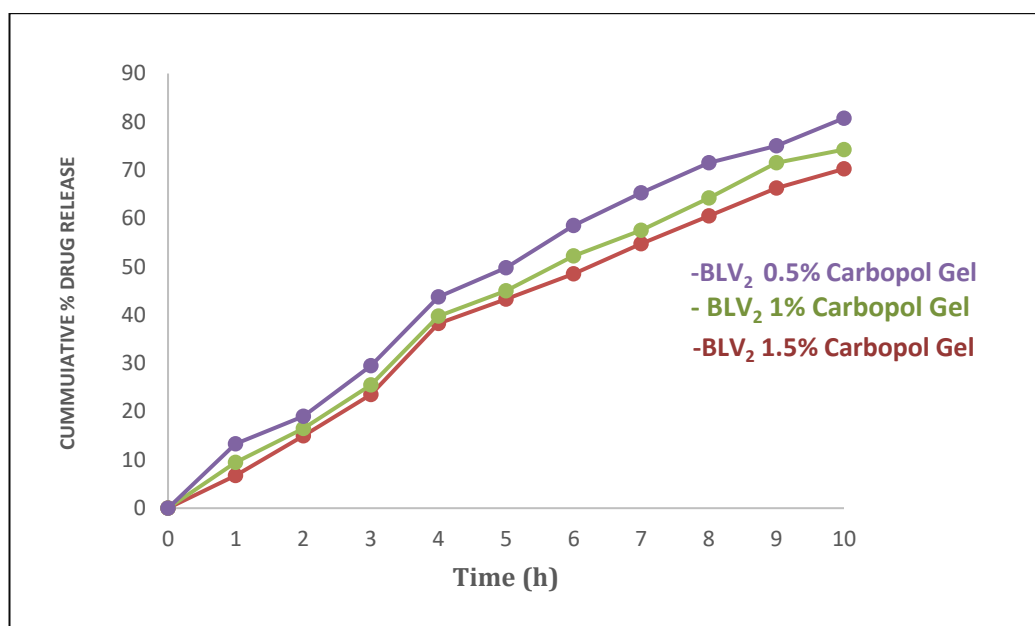


Figure (3-20) : *In vitro* release of BLV₂ gel With Different concentrations of carbopol 934 in PBS.

3.5 Applications for BLV₂ Gel *In vivo*

The results of this study indicate that inducing muscle spasms by lactic acid injections with strenuous exercise led to disturbances in ionic and enzymatic balance and kidney function. Mean values \pm Standard Deviation were analyzed using one-way analysis of variance (ANOVA), followed by Least Significant Difference test (LSD) for post hoc comparisons with a significance level of $\alpha = 0.05$.

As shown in table (3-12), the Spasm-Induced group (B) and the untreated group (C) showed a significant decrease in calcium (Ca^{2+}) levels compared to the control group (A) ($P < 0.05$). This reduction can be attributed to the accumulation of inorganic phosphate within the muscle fibers, which impairs the release of Ca^{2+} from the sarcoplasmic reticulum through the formation of CaPi complexes. Consequently, the availability of releasable calcium stores is diminished, thereby contributing to increased muscle fatigue and spasm.

In contrast, the Treated group (D), which received baclofen liposome vesicle gel, showed calcium levels that returned to near-normal values, with no significant differences from the Control group (A). This finding indicates that the treatment effectively stabilized calcium release mechanisms.

With respect to potassium (K^+), the Spasm-Induced group (B) showed a significant increase compared with the Control group (A) ($P < 0.05$), due to the efflux of potassium ions from muscle cells into the extracellular space as a result of hyperexcitability and acidosis. Although potassium levels decreased relatively in the Untreated group (C) after 3-5 days, they remained significantly higher than those of the Control group (A), reflecting a persistent ionic imbalance.

Similarly, inorganic phosphorus (P_i) concentrations were significantly elevated in both the Spasm-Induced group (B) and the Untreated group (C) compared with the Control group (A) ($P < 0.05$). However, no significant differences in K^+ or P_i levels were detected between the Treated group (D) and the Control group (A), confirming the efficacy of baclofen liposome vesicles in restoring ionic balance.

These findings are further supported by Figure (3-21), which illustrates decreased Ca^{2+} and elevated K^+ and P_i levels in the Spasm-Induced and Untreated groups, whereas values in the Treated group returned to near-normal levels, highlighting the effectiveness of the treatment system in correcting ionic disturbances associated with muscle spasms.

Table (3-12): Comparison of bio-ions parameters among study groups and control

Parameters	Mean \pm SD			
	Group A Control	Group B Spasm-Induced	Group C Untreated Spasm	Group D Treated
Ca mg/dl	10.24 \pm 0.61887 ^a	7.54 \pm 0.594138 ^b	8.14 \pm 0.230217 ^c	9.54 \pm 0.673053 ^a
K mEq/dl	4.36 \pm 0.403733 ^a	6.58 \pm 0.389872 ^b	5.62 \pm 0.258844 ^c	4.82 \pm 0.443847 ^a
Phosphorus mg/dl	4.5 \pm 0.355353 ^a	6.5 \pm 0.228035 ^b	5.24 \pm 0.288097 ^c	4.68 \pm 0.402492 ^a

Data are given as mean \pm SD; Different small letters indicate statistically significant differences ($P < 0.05$) between groups; Similar small letters indicate no statistically significant differences between groups

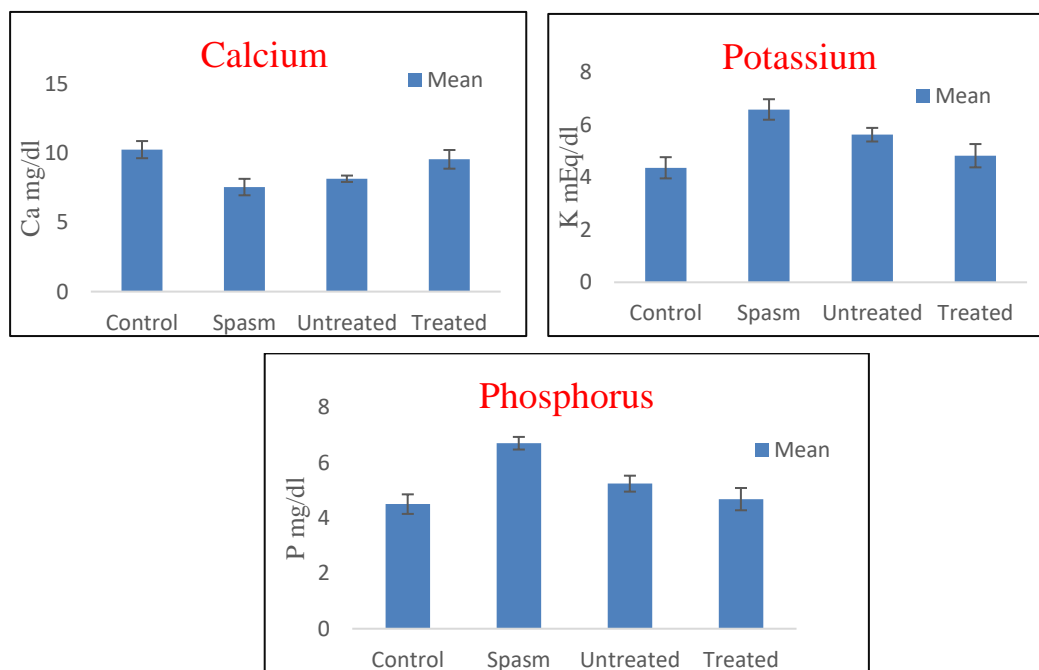


Figure (3-21): Calcium , Potassium and Phosphorus concentrations in rabbit groups (Control , Spasm-Induce, Untreated Spasm, Treated)

As shown in table (3-13), creatine kinase (CK) and lactate dehydrogenase (LDH) exhibited a significant elevation in the Spasm-Induced group (B) and the Untreated Spasm group (C) compared with the Control group (A) ($P < 0.05$), reflecting muscle fiber damage resulting from spasms. Although the Treated group (D), which received baclofen liposome

vesicle gel, showed a significant reduction in CK and LDH levels compared with the Spasm-Induced group (B), statistically significant differences remained when compared with the Control group (A). This can be attributed to residual muscle damage following spasms or to the insufficient duration of treatment to allow complete muscle recovery. CK and LDH are highly sensitive markers of muscle injury, and even minor physiological changes whether due to partial structural damage or localized drug effects can produce measurable variations in their levels, even in the absence of overt clinical symptoms.

Regarding liver enzymes (AST and ALT), both showed significant increases in the Spasm-Induced group (B) and the Untreated Spasm group (C) compared with the Control group (A) ($P < 0.05$). However, no significant differences were observed between the Treated group (D) and the Control group (A), indicating that treatment with baclofen liposome vesicle gel effectively reduced the enzyme disturbances associated with muscle spasms.

Figure (3-22) further supports these findings, demonstrating elevated CK, LDH, AST, and ALT levels in the Spasm-Induced and Untreated groups, whereas the Treated group exhibited substantial improvement, confirming the therapeutic effectiveness of the system.

Table (3-13): Comparison of bio-enzymes parameters among study groups and control

Parameters	Mean \pm SD			
	Group A Control	Group B Spasm-Induced	Group C Untreated Spasm	Group D Treated
CK U/L	267.4 \pm 20.04495 ^a	974.6 \pm 21.44295 ^b	515.8 \pm 17.3839 ^c	361.4 \pm 21.5244 ^d
LDH U/L	269.8 \pm 28.83921 ^a	807.6 \pm 26.67021 ^b	575.2 \pm 30.40888 ^c	376.4 \pm 27.42809 ^d
AST U/L	67.6 \pm 7.127412 ^a	122.6 \pm 6.348228 ^b	88 \pm 7.615773 ^c	74 \pm 8.514693 ^a
ALT U/L	51.2 \pm 4.658326 ^a	68.8 \pm 5.167204 ^b	61.4 \pm 7.127412 ^c	54.2 \pm 3.898718 ^a

Data are given as mean \pm SD; Different small letters indicate statistically significant differences ($P < 0.05$) between groups; Similar small letters indicate no statistically significant differences between groups.

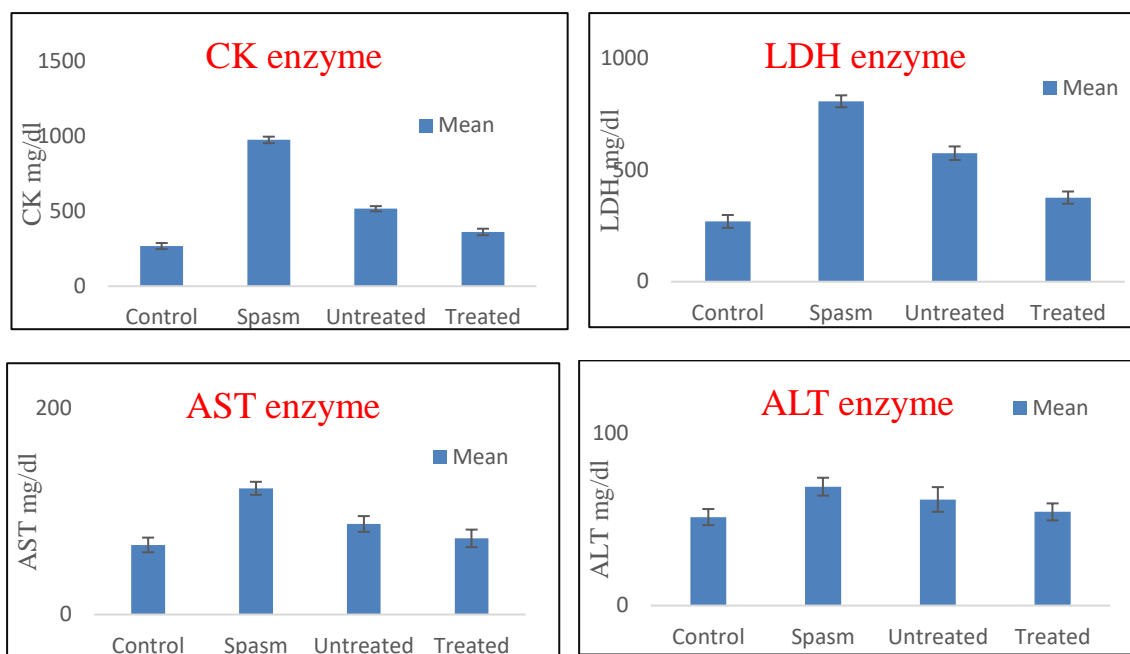


Figure (3-22):CK, LDH, ALS and ALT enzyme activities in rabbit groups (Control , Spasm-Induce, Untreated Spasm, Treated)

As for the kidney function indicators urea and creatinine, a significant increase was observed in the Spasm-Induced group (B) and the Untreated Spasm group (C) compared with the Control group (A) ($P < 0.05$). However, these elevations remained within the normal physiological range, suggesting that the increase is most likely related to enhanced muscle protein breakdown associated with muscle spasms and muscle damage, rather than reflecting true renal dysfunction. No significant differences were detected between the Treated group (D) and the Control group (A), which reinforces the protective role of the applied gel in mitigating muscle damage, as shown in table (3-14).

Figure (3-23) further illustrates that urea and creatinine concentrations were elevated in the Spasm-Induced and Untreated groups, whereas their levels in the Treated group were comparable to those of the Control, indicating the effectiveness of the treatment system in restoring values to the normal range.

Table (3-14): Comparison of Kidney Function Tests among study groups and control

Parameters	Mean \pm SD			
	Group A Control	Group B Spasm-Induced	Group C Untreated Spasm	Group D Treated
Urea mg/dl	27.6 \pm 3.209361 ^a	37 \pm 2.54951 ^b	31.8 \pm 2.588436 ^c	28 \pm 2.588436 ^a
Creatinine mg/dl	0.78 \pm 0.238747 ^a	1.52 \pm 0.496991 ^b	1.26 \pm 0.279285 ^c	0.86 \pm 0.260768 ^a

Data are given as mean \pm SD; Different small letters indicate statistically significant differences ($P < 0.05$) between groups; Similar small letters indicate no statistically significant differences between groups

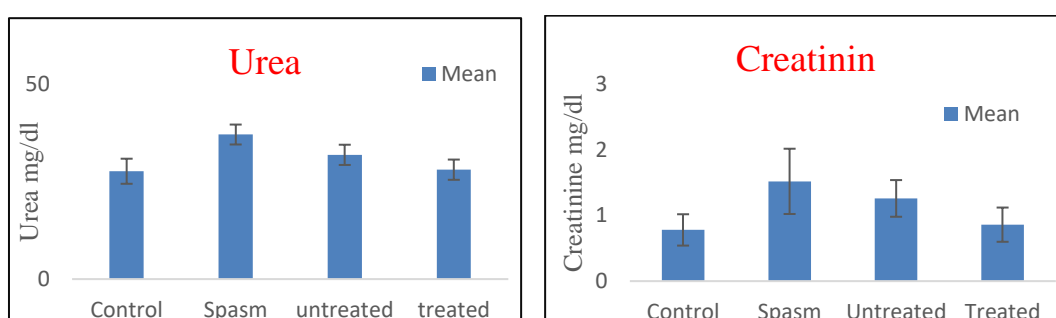


Figure (3-23): Urea and Creatinine concentrations in rabbits groups (Control , Spasm-Induce, Untreated Spasm, Treated)

These results indicate that the use of Baclofen Liposome Vesicles gel led to a significant improvement in certain ionic and enzymatic parameters ,as well as kidney function, compared to the Spasm-Induce and untreated groups. However, the treatment period (5 days) was not sufficient to achieve complete muscle recovery from damage. This may be explained by the fact that muscle damage resulting from spasms may require a longer recovery period, or that the formulation and dosing frequency of the baclofen liposomal vesicle gel need to be optimized to achieve maximum therapeutic efficacy.

Chapter Four

Conclusion and Recommendations

Conclusion

This study successfully achieved its intended objectives through the design, formulation, characterization, and evaluation of a novel nanoliposome-based baclofen gel system for the treatment of induced muscle spasms.

1. In alignment with the initial objective, a gel-based nanoliposome baclofen vesicular formulation was successfully designed and developed. Among the prepared formulations, the optimized sample BLV₂ was selected based on its superior physicochemical properties and encapsulation efficiency. This optimized formulation was then incorporated into a Carbopol 934 gel base at a concentration of 0.5% (w/w) for topical application. The prepared gel exhibited desirable consistency and homogeneity, suitable for transdermal drug delivery.
2. Consistent with the second aim, polyamide (Nylon 6,6) nanofibers were fabricated using the electrospinning technique and utilized for filtering and refining the liposomal suspension. The resulting fibers displayed a uniform, bead-free morphology with an average diameter of approximately 57 nm, confirming their efficiency in producing homogeneous nanoliposomes suitable for pharmaceutical use.
3. To simulate acute muscle spasticity, a direct muscle spasm model was established by injecting specific concentrations of lactic acid into the muscles of laboratory animals. This approach effectively reproduced the physiological and biochemical characteristics of acute muscle spasm conditions.
4. Several clinical, physiological, and biochemical parameters related to muscle spasm severity were monitored, including LDH, CK, AST, and ALT enzyme activities, as well as Ca²⁺, K⁺, P, blood urea, and serum creatinine levels. These parameters provided comprehensive insight into the therapeutic effects of the developed formulation.

5. In accordance with the fifth objective, the therapeutic efficacy of the optimized nanoliposome baclofen gel (BLV₂, 0.5%) was evaluated both in vitro and in vivo. The formulation exhibited a controlled and sustained drug release profile, which significantly reduced muscle spasm intensity and improved biochemical parameters compared to the untreated and conventionally treated groups ($P < 0.05$). The treated animals showed notable recovery in muscle function and biochemical balance, indicating the effectiveness of the topical nanoliposome baclofen gel in alleviating muscle spasm symptoms.

In conclusion, this research provides the first comprehensive evidence supporting the use of BLV₂ nanoliposome-based baclofen gel (0.5%) as a safe, stable, and efficient transdermal therapeutic system. The findings highlight its promising role in Nano formulation-based targeted therapy for muscle spasms, paving the way for future advancements in nanomedicine and controlled drug delivery technologies.

Recommendations

1. Study the new systems for transdermal delivery of baclofen such as niosomes or ethosomes .
2. Study the physicochemical properties of the gel, such as viscosity and stability, to determine their suitability for pharmaceutical applications.
3. Conduct pharmacokinetic studies to evaluate absorption, distribution, metabolism, and excretion.
4. Evaluate the effect of BLV₂ gel on inflammatory enzymes.

References

Reference

- [1] B. Salehi *et al.*, “Multivesicular liposome (Depofoam) in human diseases,” *Iran. J. Pharm. Res.*, vol. 19, no. 2, pp. 9–21, 2020.
- [2] N. J. Koehl, L. J. Henze, M. Kuentz, R. Holm, and B. T. Griffin, “Supersaturated lipid-based formulations to enhance the oral bioavailability of venetoclax,” *Pharmaceutics*, vol. 12, no. 6, pp. 1–20, 2020.
- [3] K. Juskiewicz, A. F. Sikorski, and A. Czogalla, “Building blocks to design liposomal delivery systems,” *Int. J. Mol. Sci.*, vol. 21, no. 24, pp. 1–22, 2020.
- [4] A. Crasta *et al.*, “Transdermal drug delivery system: A comprehensive review of innovative strategies, applications, and regulatory perspectives,” *OpenNano*, vol. 24, no. April, p. 100245, 2022.
- [5] P. Karande and S. Mitragotri, “Enhancement of transdermal drug delivery via synergistic action of chemicals,” *Biochim. Biophys. Acta - Biomembr.*, vol. 1788, no. 11, pp. 2362–2373, 2009.
- [6] V. Phatale, K. K. Vaiphei, S. Jha, D. Patil, M. Agrawal, and A. Alexander, “Overcoming skin barriers through advanced transdermal drug delivery approaches,” *J. Control. release*, vol. 351, pp. 361–380, 2022.
- [7] F. Abdallah, L. Mijouin, and C. Pichon, “Skin Immune Landscape: Inside and Outside the Organism,” *Mediators Inflamm.*, vol. 2017, 2017.
- [8] E. Musielak and V. Krajka-Kuźniak, “Liposomes and Ethosomes: Comparative Potential in Enhancing Skin Permeability for Therapeutic and Cosmetic Applications,” *Cosmetics*, vol. 11, no. 6, 2024.
- [9] K. Fukuda *et al.*, “Three stepwise pH progressions in stratum corneum for homeostatic maintenance of the skin,” *Nat. Commun.*, vol. 15, no. 1, 2024.

- [10] S. Malik and Y. Waheed, “Emerging Applications of Nanotechnology in Dentistry,” *Dent. J.*, vol. 11, no. 11, pp. 1–30, 2023.
- [11] D. Tanmesh and S. S. Siddheshwar, “A Review on Liposomes in Cosmetics,” *Res. J. Top. Cosmet. Sci.*, vol. 15, no. 4, pp. 43–46, 2024.
- [12] W. Rangsimawong, P. Opanasopit, T. Rojanarata, and T. Ngawhirunpat, “Effect of Various Nonionic Surfactants Incorporated in Liposomes on Dermal Delivery of Hydrophilic Compound,” *Adv. Mater. Res.*, vol. 1060, pp. 12–16, 2014.
- [13] W. Y. Jeong, M. Kwon, H. E. Choi, and K. S. Kim, “Recent advances in transdermal drug delivery systems: a review,” *Biomater. Res.*, vol. 25, no. 1, 2021.
- [14] A. Wagner and K. Vorauer-Uhl, “Liposome Technology for Industrial Purposes,” *J. Drug Deliv.*, vol. 2011, pp. 1–9, 2010.
- [15] S. S. Chrai, R. Murari, and I. Ahmad, "Liposomes (a Review) Part One: Manufacturing Issues," *L. Production*, Nov. vol. 24, no. 4, 2001.
- [16] U. Bulbake, S. Doppalapudi, N. Kommineni, and W. Khan, “Liposomal formulations in clinical use: An updated review,” *Pharmaceutics*, vol. 9, no. 2, pp. 1–33, 2017.
- [17] P. Liu, G. Chen, and J. Zhang, “A Review of Liposomes as a Drug Delivery System : Current,” *Molecules*, vol. 27, no. 4, p. 1372, 2022.
- [18] A. Hussain, S. Singh, D. Sharma, T. J. Webster, K. Shafaat, and A. Faruk, “Elastic liposomes as novel carriers: Recent advances in drug delivery,” *Int. J. Nanomedicine*, vol. 12, pp. 5087–5108, 2017.
- [19] J. Chen, W. L. Lu, W. Gu, S. S. Lu, Z. P. Chen, and B. C. Cai, “Skin permeation behavior of elastic liposomes: Role of formulation ingredients,” *Expert Opin. Drug Deliv.*, vol. 10, no. 6, pp. 845–856, 2013.

- [20] G. Cevc, S. Mazgareanu, M. Rother, and U. Vierl, "Occlusion effect on transcutaneous NSAID delivery from conventional and carrier-based formulations," *Int. J. Pharm.*, vol. 359, no. 1–2, pp. 190–197, 2008.
- [21] A. Schätzlein and G. Cevc, "Non-uniform cellular packing of the stratum corneum and permeability barrier function of intact skin: A high-resolution confocal laser scanning microscopy study using highly deNBformable vesicles (Transfersomes)," *Br. J. Dermatol.*, vol. 138, no. 4, pp. 583–592, 1998.
- [22] M. M. A. Elsayed, O. Y. Abdallah, V. F. Naggar, and N. M. Khalafallah, "Lipid vesicles for skin delivery of drugs: Reviewing three decades of research," *Int. J. Pharm.*, vol. 332, no. 1–2, pp. 1–16, 2007.
- [23] B. H.A.E., "Transfersomes for transdermal drug delivery," *Expert Opin. Drug Deliv.*, vol. 3, no. 6, pp. 727–737, 2006.
- [24] R. Chen *et al.*, "Ultradeformable Liposomes: a Novel Vesicular Carrier For Enhanced Transdermal Delivery of Procyanidins: Effect of Surfactants on the Formation, Stability, and Transdermal Delivery," *AAPS PharmSciTech*, vol. 18, no. 5, pp. 1823–1832, 2017.
- [25] B. Pradhan, N. Kumar, S. Saha, and A. Roy, "Liposome: method of preparation, advantages, evaluation and its application," *Journal of Applied Pharmaceutical Research*, vol. 3, no. 3, pp. 01–08, 2015.
- [26] S. Pandey, A. Verma, A. Singh, and A. K. Singh, "Liposomes : As An Important Drug Delivery System," *Int. J. Pharm.*, vol. 2, no. 5, pp. 1127–1136, 2024, doi: 10.5281/zenodo.11236835.
- [27] A. Akbarzadeh, R. Rezaei-sadabady, S. Davaran, S. W. Joo, and N. Zarghami, "Liposome : classification , preparation , and applications," *Nanoscale Res. Lett.*, vol. 8, no. 1, pp. 1–9, 2013.

- [28] B. S. Pattni, V. V. Chupin, and V. P. Torchilin, "New developments in liposomal drug delivery," *Chemical Reviews*, vol. 115, no. 19, pp. 10938–10966, 2015.
- [29] D. Guimarães, A. Cavaco-Paulo, and E. Nogueira, "Design of liposomes as drug delivery system for therapeutic applications," *Int. J. Pharm.*, vol. 601, 2021.
- [30] M. Alavi, N. Karimi, and M. Safaei, "Application of various types of liposomes in drug delivery systems," *Adv. Pharm. Bull.*, vol. 7, no. 1, pp. 3–9, 2017.
- [31] B. Pradhan, N. Kumar, S. Saha, and A. Roy, "Liposome: method of preparation, advantages, evaluation and its application," *J. Appl. Pharm. Res.*, vol. 3, no. 3, pp. 01–08, 2015.
- [32] S. K. Sahoo and V. Labhasetwar, "Nanotech approaches to drug delivery and imaging," *Drug Discov. Today*, vol. 8, no. 24, pp. 1112–1120, 2003.
- [33] Y. Fan, M. Marioli, and K. Zhang, "Analytical characterization of liposomes and other lipid nanoparticles for drug delivery," *J. Pharm. Biomed. Anal.*, vol. 192, p. 113642, 2021.
- [34] A. Sharma and U. S. Sharma, "Liposomes in drug delivery: Progress and limitations," *Int. J. Pharm.*, vol. 154, no. 2, pp. 123–140, 1997.
- [35] B. Krushna, W. Jayshri, V. Pankaj, and S. Madhu, "Navigating The Landscape Of Liposome-Based Drug Delivery Systems: A Comprehensive Review," *Int. J. Pharm.*, vol. 2, no. 5, pp. 1091–1103, 2024.
- [36] L. Van De Cauter *et al.*, "Optimized cDICE for Efficient Reconstitution of Biological Systems in Giant Unilamellar Vesicles," *ACS Synth. Biol.*, vol. 10, no. 7, pp. 1690–1702, 2021.

- [37] D. Guimarães, A. Cavaco-Paulo, and E. Nogueira, “Design of liposomes as drug delivery system for therapeutic applications,” *Int. J. Pharm.*, vol. 601, no. February, 2021.
- [38] S. Vemuri and C. T. Rhodes, “Preparation and characterization of liposomes as therapeutic delivery systems: a review,” *Pharm. Acta Helv.*, vol. 70, no. 2, pp. 95–111, 1995.
- [39] L. Maja, K. Željko, and P. Mateja, “Sustainable technologies for liposome preparation,” *J. Supercrit. Fluids*, vol. 165, 2020.
- [40] M. Alavi, M. Rai, R. S. Varma, M. Hamidi, and M. R. Mozafari, “Micro Nano Bio Aspects Conventional and novel methods for the preparation of micro and nanoliposomes,” *Micro Nano Bio Asp.*, vol. 2022, no. 1, pp. 18–29, 2022.
- [41] K. Sahil, S. Premjeet, B. Ajay, A. Middha, and K. Bhawna, “Issn 2229-3566 Stealth Liposomes : a Review,” *International Journal of Research in Ayurveda and Pharmacy*, vol. 2, no. 5, pp. 1534–1538, 2011.
- [42] T. M. Allen, “Ligand-targeted therapeutics in anticancer therapy,” *Nat. Rev. Cancer*, vol. 2, no. 10, pp. 750–763, 2002.
- [43] Y. Lee and D. H. Thompson, “Stimuli-responsive liposomes for drug delivery,” *Wiley Interdiscip. Rev. Nanomedicine Nanobiotechnology*, vol. 9, no. 5, 2017.
- [44] Y. Negishi *et al.*, “Local Gene Delivery System by Bubble Liposomes and Ultrasound Exposure into Joint Synovium,” *J. Drug Deliv.*, vol. 2011, pp. 1–7, 2011.
- [45] H. Wu *et al.*, “Cholesterol-tuned liposomal membrane rigidity directs tumor penetration and anti-tumor effect,” *Acta Pharm. Sin. B*, vol. 9, no. 4, pp. 858–870, 2019.

- [46] S. Kaddah, N. Khreich, F. Kaddah, C. Charcosset, and H. Greige-Gerges, “Cholesterol modulates the liposome membrane fluidity and permeability for a hydrophilic molecule,” *Food Chem. Toxicol.*, vol. 113, pp. 40–48, 2018.
- [47] M. L. Immordino and L. Cattel, “Stealth Liposomes : Review of the Basic Science , Rationale , and Clinical Applications , Existing and Potential Stealth liposomes : review of the basic science , rationale , and clinical applications , existing and potential,” *nternational J. Nanomedicine*, vol. 1, no. 3, pp. 297–315, 2016.
- [48] H. Hatakeyama, H. Akita, and H. Harashima, “The polyethyleneglycol dilemma: Advantage and disadvantage of PEGylation of liposomes for systemic genes and nucleic acids delivery to tumors,” *Biol. Pharm. Bull.*, vol. 36, no. 6, pp. 892–899, 2013.
- [49] V. P. Torchilin, “Recent advances with liposomes as pharmaceutical carriers,” *Nat. Rev. Drug Discov.*, vol. 4, no. 2, pp. 145–160, 2005.
- [50] K. He and M. Tang, “Safety of novel liposomal drugs for cancer treatment: Advances and prospects,” *Chem. Biol. Interact.*, vol. 295, pp. 13–19, 2018.
- [51] H. Nsairat, D. Khater, U. Sayed, F. Odeh, A. Al Bawab, and W. Alshaer, “Liposomes: structure, composition, types, and clinical applications,” *Heliyon*, vol. 8, no. 5, p. e09394, 2022.
- [52] T. O. B. Olusanya, R. R. H. Ahmad, D. M. Ibegbu, J. R. Smith, and A. A. Elkordy, “Liposomal drug delivery systems and anticancer drugs,” *Molecules*, vol. 23, no. 4, pp. 1–17, 2018.
- [53] R. M. Senjab, N. AlSawaftah, W. H. Abuwatfa, and G. A. Hussein, “Advances in liposomal nanotechnology: from concept to clinics,” *RSC Pharm.*, vol. 1, no. 5, pp. 928–948, 2024.

- [54] K. Maruyama, O. Ishida, T. Takizawa, and K. Moribe, “Possibility of active targeting to tumor tissues with liposomes,” *Adv. Drug Deliv. Rev.*, vol. 40, no. 1–2, pp. 89–102, 1999.
- [55] S. Mura, J. Nicolas, and P. Couvreur, “Stimuli-responsive nanocarriers for drug delivery,” *Nat. Mater.*, vol. 12, no. 11, pp. 991–1003, 2013.
- [56] M. Ashrafizadeh *et al.*, “Stimuli-responsive liposomal nanoformulations in cancer therapy: Pre-clinical & clinical approaches,” *J. Control. Release*, vol. 351, no. September, pp. 50–80, 2022.
- [57] C. Sun, “Bubble Liposome: a Modern Theranostic Approach of New Drug Delivery,” *World J. Pharm. Pharm. Sci.*, no. May, pp. 1290–1314, 2017.
- [58] K. Sakaguchi, N. Kudo, K. Yamamoto, R. Suzuki, and K. Maruyama, “Characterization of bubble liposomes by of ultrasound attenuation effects of shell materials,” *Proc. - IEEE Ultrason. Symp.*, pp. 1675–1678, 2008.
- [59] M. Grazia Calvagno *et al.*, “Effects of Lipid Composition and Preparation Conditions on Physical-Chemical Properties, Technological Parameters and In Vitro Biological Activity of Gemcitabine-Loaded Liposomes,” *Curr. Drug Deliv.*, vol. 4, no. 1, pp. 89–101, 2006.
- [60] N. Monteiro, A. Martins, R. L. Reis, and N. M. Neves, “Liposomes in tissue engineering and regenerative medicine,” *J. R. Soc. Interface*, vol. 11, no. 101, 2014.
- [61] A. A. Jovanović *et al.*, “Comparative Effects of Cholesterol and β -Sitosterol on the Liposome Membrane Characteristics,” *Eur. J. Lipid Sci. Technol.*, vol. 120, no. 9, 2018.

- [62] D. Uhrí, *The effects of cholesterol and β -sitosterol on the structure of saturated diacylphosphatidylcholine bilayers*, M.S. thesis, 2010.
- [63] G. Bozzuto and A. Molinari, “Liposomes as nanomedical devices,” *Int. J. Nanomedicine*, vol. 10, pp. 975–999, 2015.
- [64] D. Cipolla, H. Wu, I. Gonda, S. Eastman, T. Redelmeier, and H. K. Chan, “Modifying the release properties of liposomes toward personalized medicine,” *J. Pharm. Sci.*, vol. 103, no. 6, pp. 1851–1862, 2014.
- [65] I. Khan *et al.*, “Impact of phospholipids, surfactants and cholesterol selection on the performance of transfersomes vesicles using medical nebulizers for pulmonary drug delivery,” *J. Drug Deliv. Sci. Technol.*, vol. 66, p. 102822, 2021.
- [66] G. M. M. El Maghraby, A. C. Williams, and B. W. Barry, “Interactions of surfactants (edge activators) and skin penetration enhancers with liposomes,” *Int. J. Pharm.*, vol. 276, no. 1–2, pp. 143–161, 2004.
- [67] T. A. Khan, H. Mahler, and R. S. K. Kishore, “Key interactions of surfactants in therapeutic protein formulations : A review European Journal of Pharmaceutics and Biopharmaceutics Key interactions of surfactants in therapeutic protein formulations : A review,” *Eur. J. Pharm. Biopharm.*, vol. 97, no. July, pp. 60–67, 2016.
- [68] D. E. Large, R. G. Abdelmessih, E. A. Fink, and D. T. Augustine, “Liposome composition in drug delivery design, synthesis, characterization, and clinical application,” *Adv. Drug Deliv. Rev.*, vol. 176, p. 113851, 2021.
- [69] B. K. Brandley and R. L. Schnaar, “Cell-surface carbohydrates in cell recognition and response,” *J. Leukoc. Biol.*, vol. 40, no. 1, pp. 97–111, 1986.

- [70] T. M. Allen, C. Hansen, and J. Rutledge, “Liposomes with prolonged circulation times: factors affecting uptake by reticuloendothelial and other tissues,” *BBA - Biomembr.*, vol. 981, no. 1, pp. 27–35, 1989.
- [71] A. Plucinski, Z. Lyu, and B. V. K. J. Schmidt, “Polysaccharide nanoparticles: From fabrication to applications,” *J. Mater. Chem. B*, vol. 9, no. 35, pp. 7030–7062, 2021.
- [72] D. Peer and R. Margalit, “Tumor-targeted hyaluronan nanoliposomes increase the antitumor activity of liposomal doxorubicin in syngeneic and human xenograft mouse tumor models,” *Neoplasia*, vol. 6, no. 4, pp. 343–353, 2004.
- [73] M. M. Mady, M. M. Darwish, S. Khalil, and W. M. Khalil, “Biophysical studies on chitosan-coated liposomes,” *Eur. Biophys. J.*, vol. 38, no. 8, pp. 1127–1133, 2009.
- [74] H. Luiz, J. O. Pinho, and M. M. Gaspar, “Advancing Medicine with Lipid-Based Nanosystems — The Successful Case of Liposomes,” *Pharmaceutics*, 2023.
- [75] F. Bray, J. Ferlay, I. Soerjomataram, R. L. Siegel, L. A. Torre, and A. Jemal, “Global cancer statistics 2018: GLOBOCAN estimates of incidence and mortality worldwide for 36 cancers in 185 countries,” *CA. Cancer J. Clin.*, vol. 68, no. 6, pp. 394–424, 2018.
- [76] A. G. Niculescu and A. M. Grumezescu, “Novel Tumor-Targeting Nanoparticles for Cancer Treatment— A Review,” *Int. J. Mol. Sci.*, vol. 23, no. 9, 2022.
- [77] S. P. Vemuri, P. Karnati, K. P. Vadayar, and P. Singh, “Harnessing Liposomes for Advanced Gene Therapy : A Comprehensive Review” *Journal of Bio-X Research*, vol. 8, Article 0050, Apr. 2025.

- [78] Y. Wang and W. Shao, “Innate Immune Response to Viral Vectors in Gene Therapy,” *Viruses*, vol. 15, no. 9, 2023.
- [79] S. A. Ayatollahi Mousavi *et al.*, “Advances of liposomal mediated nanocarriers for the treatment of dermatophyte infections,” *Heliyon*, vol. 9, no. 8, p. e18960, 2023.
- [80] N. Tasharrofi, M. Nourozi, and A. Marzban, “How liposomes pave the way for ocular drug delivery after topical administration,” *J. Drug Deliv. Sci. Technol.*, vol. 67, no. December, p. 103045, 2022.
- [81] H. U. Ryu, H. J. Kim, B. S. Shin, and H. G. Kang, “Serial electroencephalography changes in low-dose baclofen intoxication,” *Quant. Imaging Med. Surg.*, vol. 13, no. 10, pp. 7404–7409, 2023.
- [82] R. Chou, K. Peterson, O. Health, and M. Helfand, “Drug Class Review on Skeletal Muscle Relaxants for Spasticity and Musculoskeletal Conditions,” no. January, 2004.
- [83] J. W. Romito *et al.*, “Baclofen therapeutics , toxicity , and withdrawal : A narrative review,” *SAGE Open Med.*, vol. 9, 2021.
- [84] M. J. McLaughlin and M. T. Fisher, “A critical evaluation of oral baclofen in pediatric patients with cerebral palsy,” *J. Pediatr. Rehabil. Med.*, vol. 16, no. 1, pp. 3–9, 2023.
- [85] S. Malignancies, D. Glioblastoma, and R. A. Astrocytoma, “This label may not be the latest approved by FDA . pp. 1–21, 2019.
- [86] T. Based, D. Gel, O. F. Baclofen, F. O. R. Management, and O. F. Chronic, “Transfersomes based dermal gel of baclofen for management of chronic pain,” *European Chemical Bulletin*, vol. 12, no. 10, pp. 8417–8440, 2023.
- [87] A. M. Yussef, S. M. Fayez, and W. Sakran, “Formulation and

- Evaluation of Baclofen Polymeric Nanoparticles for Transdermal Delivery In-vitro and Ex-vivo Optimization,” vol. 0547, no. 2, pp. 248–259, 2021.
- [88] A. Dario and G. Tomei, “A benefit-risk assessment of baclofen in severe spinal spasticity,” *Drug Saf.*, vol. 27, no. 11, pp. 799–818, 2004.
- [89] N. Y. Leung, I. M. Whyte, and G. K. Isbister, “Baclofen overdose: Defining the spectrum of toxicity,” *EMA - Emerg. Med. Australas.*, vol. 18, no. 1, pp. 77–82, 2006.
- [90] G.P. Mohanta, S. B. P. P. K, and S. S. Panda, "Carbopol Polymers: A Versatile Polymer for Pharmaceutical Applications," *International Journal of Applied Engineering Research*, vol. 3, no. 3, pp. 672–675, 2010.
- [91] S.Sahoo, S. C. Mishra, and S. K. Singh, "Qualitative analysis of controlled release ciprofloxacin/carbopol 934 mucoadhesive suspension," in AIP Conference Proceedings, 2023, vol. 2521, no. 1, p. 020005. doi: 10.1063/5.0112864.
- [92] R. Binaymotlagh, F. Hajareh Haghighi, L. Chronopoulou, and C. Palocci, “Liposome–Hydrogel Composites for Controlled Drug Delivery Applications,” *Gels*, vol. 10, no. 4, 2024.
- [93] M. M. Nounou, L. K. El-Khordagui, N. A. Khalafallah, and S. A. Khalil, “In vitro release of hydrophilic and hydrophobic drugs from liposomal dispersions and gels,” *Acta Pharm.*, vol. 56, no. 3, pp. 311–324, 2006.
- [94] R. Patel, H. Patel, and A. Baria, “Formulation and Evaluation of Carbopol Gel Containing Liposomes of Ketoconazole. (Part-II),” *Int. J. Drug Deliv. Technol.*, vol. 1, no. 2, pp. 42–45, 2009.

- [95] A. Ortan, C. D. Parvu, M. V. Ghica, L. M. Popescu, and L. Ionita, “Rheological study of a liposomal hydrogel based on carbopol,” *Rom. Biotechnol. Lett.*, vol. 16, no. 1 SUPPL., pp. 47–54, 2011.
- [96] M. J Lespasio, “Muscle Spasm: A Primer,” *Int. J. Clin. Stud. Med. Case Reports*, vol. 44, no. 4, pp. 1–8, 2024.
- [97] A. M. Grapperon and S. Attarian, “Disorders of motor neurons manifested by hyperactivity,” *Rev. Neurol. (Paris)*, vol. 173, no. 5, pp. 345–351, 2017.
- [98] N. L. Nelson and J. R. Churilla, “A narrative review of exercise-associated muscle cramps: Factors that contribute to neuromuscular fatigue and management implications,” *Muscle and Nerve*, vol. 54, no. 2, pp. 177–185, 2016.
- [99] K. Sahlin, L. Edstrom, H. Sjoholm, and E. Hultman, “Effects of lactic acid accumulation and ATP decrease on muscle tension and relaxation,” *Am. J. Physiol. - Cell Physiol.*, vol. 9, no. 2, 1981.
- [100] R. J. Maughan and S. M. Shirreffs, “Muscle Cramping During Exercise: Causes, Solutions, and Questions Remaining,” *Sport. Med.*, vol. 49, no. s2, pp. 115–124, 2019.
- [101] I. Y. Kuo and B. E. Ehrlich, “Signaling in muscle contraction,” *Cold Spring Harb. Perspect. Biol.*, vol. 7, no. 2, pp. 1–14, 2015.
- [102] H. Xu and H. Van Remmen, “The SarcoEndoplasmic Reticulum Calcium ATPase (SERCA) pump: a potential target for intervention in aging and skeletal muscle pathologies,” *Skelet. Muscle*, vol. 11, no. 1, pp. 1–9, 2021.
- [103] M. I. Lindinger and G. Sjøgaard, “Potassium Regulation during Exercise and Recovery,” *Sport. Med.*, vol. 11, no. 6, pp. 382–401, 1991.

- [104] M. J. McKenna, J. Bangsbo, and J.-M. Renaud, “Muscle K⁺, Na⁺, and Cl disturbances and Na⁺-K⁺ pump inactivation: implications for fatigue.,” *J. Appl. Physiol.*, vol. 104, no. 1, pp. 288–295, Jan. 2008.
- [105] J. A. Leppik, R. J. Aughey, I. Medved, I. Fairweather, M. F. Carey, and M. J. McKenna, “Prolonged exercise to fatigue in humans impairs skeletal muscle Na⁺-K⁺-ATPase activity, sarcoplasmic reticulum Ca²⁺ release, and Ca²⁺ uptake.,” *J. Appl. Physiol.*, vol. 97, no. 4, pp. 1414–1423, Oct. 2004.
- [106] D. G. Allen and H. Westerblad, “Role of phosphate and calcium stores in muscle fatigue,” *J. Physiol.*, vol. 536, no. 3, pp. 657–665, 2001.
- [107] M. Tojima, K. Noma, and S. Torii, “Changes in serum creatine kinase, leg muscle tightness, and delayed onset muscle soreness after a full marathon race.,” *J. Sports Med. Phys. Fitness*, vol. 56, no. 6, pp. 782–788, Jun. 2016.
- [108] A. J. Koch, R. Pereira, and M. Machado, “The creatine kinase response to resistance exercise,” *J. Musculoskelet. Neuronal Interact.*, vol. 14, no. 1, pp. 68–77, 2014.
- [109] R. Klein, O. Nagy, C. Tóthová, and F. Chovanová, “Clinical and Diagnostic Significance of Lactate Dehydrogenase and Its Isoenzymes in Animals,” *Vet. Med. Int.*, vol. 2020, 2020.
- [110] K. Weibrecht, M. Dayno, C. Darling, and S. B. Bird, “Liver Aminotransferases Are Elevated with Rhabdomyolysis in the Absence of Significant Liver Injury,” *J. Med. Toxicol.*, vol. 6, no. 3, pp. 294–300, 2010.
- [111] T. Mahbub, F. Jahan, H. Dm, and C. Mnu, “Case Report Acute Kidney Injury due to Rhabdomyolysis,” *Journal of Armed Forces Medical College, Bangladesh* .vol. 11, no. 1, pp. 93–95, 2015.

- [112] A. K. Lim, “Abnormal liver function tests associated with severe rhabdomyolysis,” *World J. Gastroenterol.*, vol. 26, no. 10, pp. 1020–1028, Mar. 2020.
- [113] K. Raveendhra, S. Kothamasu, S. Swain, and M. S. Babu, “Formulation and Evaluation of Controlled Release Topical Gel of Baclofen,” *Pharma Innov. J.*, vol. 7, no. 7, pp. 638–648, 2018.
- [114] R. K. Keservani and S. P. Gautam, “Formulation and evaluation of baclofen liposome vesicles using lecithin,” *Ars Pharm.*, vol. 61, no. 3, pp. 175–180, 2020.
- [115] M. Umbarkar, S. Thakare, T. Surushe, A. Giri, and V. Chopade, “Formulation and Evaluation of Liposome by Thin Film Hydration Method,” vol. 11, no. 1, pp. 72–76, 2021.
- [116] S. Tayal, A. Siddiqui, M. M. Ansari, and B. Phurailatpam, “Preparation and Evaluation of Diclofenac Sodium Loaded Liposomal Hydrogel in the Treatment of Rheumatoid Arthritis,” *Middle East J. Appl. Sci. Technol.*, vol. 07, no. 02, pp. 04–15, 2024.
- [117] R. Jia *et al.*, “Liposomes-in-Gel as the Docetaxel Delivery for the Effective Treatment of Psoriasis by Inhibiting the Proliferation of Blood Vessels,” *Gels*, vol. 11, no. 4, 2025.
- [118] N. Fatima, N. Ilyas, and S. Babu, “Formulation and in-vitro Evaluation of Baclofen loaded Transfersosomal Gel,” *J. Drug Deliv. Ther.*, vol. 13, no. 12, pp. 4–14, 2023.
- [119] N. M. AbdulKhaleq, Formulation and Evaluation of Baclofen as a Model Gastroretentive Solid Drug Delivery System Using FDM 3D Printing Technique, Ph.D. dissertation, Dept. of Pharmaceutics, Coll. of Pharmacy, Univ. of Baghdad, Baghdad, Iraq, 2023.

- [120] A. D. Bangham, M. M. Standish, and J. C. Watkins, "Diffusion of univalent ions across the lamellae of swollen phospholipids," *J. Mol. Biol.*, vol. 13, no. 1, pp. 238–252, 1965.
- [121] M. Mishra, N. Ravichandran, and M. Pichandy, "Drug excipient interaction studies in dopamine loaded lipid-surfactant based drug carrier," *Asian J. Chem.*, vol. 23, no. 6, pp. 2732–2734, 2011.
- [122] P. Mura *et al.*, "Improvement of butamben anesthetic efficacy by the development of deformable liposomes bearing the drug as cyclodextrin complex," *Pharmaceutics*, vol. 13, no. 6, 2021.
- [123] S. Sagar, D. Singh, and G. Das Gupta, "In vitro and ex vivo evaluation of triamcinolone acetonide-loaded transfersome gel-based novel carrier for the treatment of osteoarthritis," *Pharmaspire*, vol. 14, no. 01, pp. 10–17, 2022.
- [124] N. Jee Kanu, S. S Chavan, G. V. Jadhav, N. S. Hude, R. P. Ganesh, and J. T. Patil, "Manufacturing of Nylon 6, 6 Nanofibers using Electrospinning," *Int. J. Anal. Exp. Finite Elem. Anal.*, vol. 6, no. 2, pp. 67–69, 2019.
- [125] S. Bairagi *et al.*, "High-Performance Triboelectric Nanogenerators Based on Commercial Textiles: Electrospun Nylon 66 Nanofibers on Silk and PVDF on Polyester," *ACS Appl. Mater. Interfaces*, vol. 14, no. 39, pp. 44591–44603, 2022,.
- [126] X. Shi *et al.*, "Electrospinning of Nanofibers and Their Applications for Energy Devices," *J. Nanomater.*, vol. 2015, 2015.
- [127] M. K. Taher, I. Q. Falih, and Y. J. Abdullah, "Design of Delivery Systems (Nanoemulsions and Biopolymer)," *Journal of Pharmaceutical Development and Therapeutics*, 2024.

- [128] P. Chavan, K. Bavaskar, R. Sawant, and A. Jain, "Preparation and Optimization of Clotrimazole Transdermal Gel of Nanosize Transfersome with Different Non-Ionic Surfactant," *International Journal of Research in Pharmacy and Allied Science (IJRPAS)*, vol. 3, no. 1, pp. 123–140, 2024.
- [129] S. Aziz, "Biosynthesis of Zinc oxide Nanoparticles using Capparis Spinosa Plant extract and study of Biological activity," M.Sc. thesis, College of Science, University of Misan, Maysan, Iraq, 2023.
- [130] J. M. Hernández-Meza and J. G. Sampedro, "Trehalose Mediated Inhibition of Lactate Dehydrogenase from Rabbit Muscle. The Application of Kramers' Theory in Enzyme Catalysis.," *J. Phys. Chem. B*, vol. 122, no. 15, pp. 4309–4317, Apr. 2018.
- [131] S. P. Cairns and M. I. Lindinger, *Lactic acidosis: implications for human exercise performance*, vol. 125, no. 7. Springer Berlin Heidelberg, 2025.
- [132] J. Bangsbo and M. Hostrup, "[Lactate production contributes to development of fatigue during intense exercise in humans].," *Ugeskr. Laeger*, vol. 181, no. 8, Feb. 2019.
- [133] K. B. Gabhane, A. M. Jaiswal, and K. K. Tapar, "Research Journal of Pharmaceutical , Biological and Chemical Sciences Simple and Validated Ultraviolet Spectrophotometric Method for the Estimation of Baclofen in Bulk Form " *Research Journal of Pharmaceutical, Biological and Chemical Sciences*, vol. 5, no. 104, pp. 104–109.
- [134] N. M. Abdulkhaleq and M. M. Ghareeb, "Development of Gastro-floating drug delivery system by 3D Printing: Impact of formulation and design on the release profile of Baclofen," *J. Contemp. Med. Sci.*, vol. 8, no. 6, pp. 413–419, 2022.

- [135] B. Layek and B. Mukherjee, "Tamoxifen citrate encapsulated sustained release liposomes: Preparation and evaluation of physicochemical properties," *Sci. Pharm.*, vol. 78, no. 3, pp. 507–515, 2010.
- [136] Y. Perrie, H. Ali, D. J. Kirby, A. U. Mohammed, S. E. McNeil, and A. Vangala, "Environmental scanning electron microscope imaging of vesicle systems.," *Methods Mol. Biol.*, vol. 606, no. 2, pp. 319–331, 2010.
- [137] M. L. Immordino, F. Dosio, and L. Cattel, "Stealth liposomes: Review of the basic science, rationale, and clinical applications, existing and potential," *Int. J. Nanomedicine*, vol. 1, no. 3, pp. 297–315, 2006.
- [138] R. W. Mathäs, "Non-spherical micro- and nanoparticles: fabrication, characterization, and in-vitro investigations," *Expert Opinion on Drug Delivery*, vol. 12, no. 3, pp. 481–492, Mar. 2015.
- [139] I. K. Mkam Tsengam *et al.*, "Transformation of Lipid Vesicles into Micelles by Adding Nonionic Surfactants: Elucidating the Structural Pathway and the Intermediate Structures," *J. Phys. Chem. B*, vol. 126, no. 11, pp. 2208–2216, 2022.
- [140] Y. Sun *et al.*, "Development of Liposome containing sodium deoxycholate to enhance oral bioavailability of itraconazole," *Asian J. Pharm. Sci.*, vol. 12, no. 2, pp. 157–164, 2017.
- [141] M. Danaei *et al.*, "Impact of particle size and polydispersity index on the clinical applications of lipidic nanocarrier systems," *Pharmaceutics*, vol. 10, no. 2, pp. 1–17, 2018.
- [142] H. Kim *et al.*, "Combined skin moisturization of liposomal serine incorporated in hydrogels prepared with carbopol ETD 2020, rhesperse RM 100 and hyaluronic acid," *Korean J. Physiol. Pharmacol.*, vol. 19, no. 6, pp. 543–547, 2015.

- [143] S. A. Neamah, S. Albukhaty, I. Q. Falih, Y. H. Dewir, and H. B. Mahood, "Biosynthesis of Zinc Oxide Nanoparticles Using Capparis spinosa L. Fruit Extract: Characterization, Biocompatibility, and Antioxidant Activity," *Appl. Sci.*, vol. 13, no. 11, pp. 1–14, 2023.
- [144] I. Sriyanti, M. P. Agustini, J. Jauhari, S. Sukemi, and Z. Nawawi, "Electrospun Nylon-6 Nanofibers and Their Characteristics," *J. Ilm. Pendidik. Fis. Al-Biruni*, vol. 9, no. 1, pp. 9–19, 2020.
- [145] I. Sriyanti, D. Edikresnha, A. Rahma, M. M. Munir, H. Rachmawati, and K. Khairurrijal, "Correlation between Structures and Antioxidant Activities of Polyvinylpyrrolidone/ Garcinia mangostana L. Extract Composite Nanofiber Mats Prepared Using Electrospinning," *J. Nanomater.*, vol. 2017.
- [146] J. Jauhari, S. Wiranata, A. Rahma, Z. Nawawi, and I. Sriyanti, "Polyvinylpyrrolidone/cellulose acetate nanofibers synthesized using electrospinning method and their characteristics," *Mater. Res. Express*, vol. 6, no. 6, pp. 0–6, 2019.
- [147] R. Roskoski, "Michaelis-Menten Kinetics☆," *Reference Module in Biomedical Sciences*, no. December 2015, 2015.
- [148] G. L. Waldrop, "Protein function: Kinetics of enzyme inhibition," *Encycl. Biol. Chem. Third Ed.*, vol. 3, pp. 14–20, 2021.
- [149] S. Neamah, I. Falih, S. Albukhaty, and S. P., "Phytochemical Characteristic Analysis and Biological Activity for Capparis spinosa L. Fruit extract," *Rafidain J. Sci.*, vol. 33, no. 1, pp. 68–77, 2024.
- [150] S. Aykul and E. Martinez-Hackert, "Determination of half-maximal inhibitory concentration using biosensor-based protein interaction analysis," *Analytical Biochemistry*, vol. 508, pp. 97–103, Sep. 2016.

Reference

- [151] A. Begum Nooreen, S. A. Azeez Basha, and A. Mannan, “Formulation and Evaluation of Gentamicin-Loaded Transfersomal Gel,” *Int. J. Heal. Sci. Res.*, vol. 13, no. 12, pp. 307–321, 2023.

الخلاصة

تهدف هذه الدراسة إلى تطوير نظام لإيصال دواء الباكلوفين عبر الجلد، وهو دواء مرخ للعضلات يُستخدم لعلاج التشنجات العضلية. وعلى الرغم من أن الباكلوفين يقدم فوائد علاجية كبيرة، إلا أن فعاليته السريرية محدودة بسبب قصر عمره النصفي وانخفاض توافره الحيوي عند إعطائه بالطرق التقليدية. وهذا ما يبرز الحاجة إلى استراتيجيات متقدمة لتعزيز امتصاصه وفعاليته العلاجية. وتُعد الأنظمة المعتمدة على تقنية النانو، وخاصة الحويصلات الدهنية (Liposomes)، من أكثر الأساليب الواعدة لتحسين إيصال الدواء بفضل قدرتها على زيادة استقراره، واختراق الحواجز البيولوجية، وتوفير إطلاق دوائي مستمر. علاوة على ذلك، فإن دمج الحويصلات الشحمية في مصفوفات هلامية (hydrogel) يعزز من استقرارها وأدائها.

في هذا البحث، تم تحضير أربع تركيبات من الحويصلات الشحمية المحملة بالباكوفين والمعدلة بالمواد الخافضة للتوتر السطحي باستخدام طريقة الترطيب الغشاء الدهني الرقيق، تليها عملية الترشيح عبر ألياف النايلون 6,6 النانوية للحصول على حويصلات أحادية الطبقة صغيرة الحجم. وأكدت عمليات التحليل باستخدام FT-IR و DLS وفرق الجهد الكهربائي (zeta potential) والمجهر الإلكتروني الماسح الميداني (FESEM) تكوين الحويصلات الشحمية النانوية بنجاح، حيث تراوحت أحجام الجسيمات بين 36.67 و 172.6 نانومتر، ومؤشرات تباين الحجم بين 0.369 و 0.663، وجهد زيتا مقداره -65.6 ملي فولت، مع طول موجي أقصى (λ_{max}) للباكوفين عند 218 نانومتر.

من بين التركيبات المحضرة، تم اختيار التركيبة BLV₂ كنظام مُحسن بناءً على نتائج التوصيف. ثم أُجريت دراسة إطلاق دوائي في المختبر بعد دمج التركيبة المختارة في هلام مائي (الكاربوبول 934) بتركيزات مختلفة (0.5%، 1%، 1.5%) لتقييم إطلاق الدواء. وأظهرت النتائج أن أعلى معدل لإطلاق الباكلوفين تحقق عند تركيز كاربوبول 0.5%، ولذلك تم اختياره للتطبيقات الحيوية اللاحقة في الجسم الحي.

في الدراسة الحيوانية، تم تقسيم عشرين أرنباً ذكراً إلى أربع مجموعات: مجموعة ضابطة، ومجموعة محفزة بالتشنج باستخدام الحقن العضلي لحمض اللاكتيك (30 Mm) في عضلة الفخذ، ومجموعة محفزة بالتشنج غير معالجة، ومجموعة غُلجت بهلام الحويصلات الشحمية النانوية للباكوفين (0.5%). مرتين يومياً لمدة خمسة أيام.

تم جمع عينات الدم من الوريد الأذني كما يلي: من المجموعة الضابطة بعد فترة التهيئة، ومن المجموعة المحفزة بالتشنج بعد 12 ساعة من حقن حمض اللاكتيك، ومن المجموعة غير المعالجة بعد خمسة أيام، ومن المجموعة المعالجة بعد خمسة أيام من التطبيق اليومي لهلام الحويصلات الباكلوفين الشحمية النانوية (0.5%). وقد استُخدمت العينات لتحليل أيونات الدم (Pi ، K^+ ، Ca^{2+})، وإنزيمات تلف العضلات (LDH، CK)، وإنزيمات الكبد (ALT، AST)، ومؤشرات وظائف الكلى (اليوريا، الكرياتينين). أظهرت التركيبة المحسنة نشاطاً مثبطاً للإنزيمات بشكل ملحوظ، بقيم IC_{50} تقارب 72.480 $\mu g/mL$ لإنزيم CK، 86.359 $\mu g/mL$ لإنزيم LDH.

ولوحظت تحسنات ذات دلالة إحصائية ($P < 0.05$) في المجموعة المعالجة مقارنةً بالمجموعات المحفزة بالتشنج، مما يشير إلى انخفاض واضح في مؤشرات تلف العضلات وتحسن في المعايير الفسيولوجية. تُظهر هذه النتائج أن هلام الحويصلات الشحمية النانوية للباكوفين يوفر منصة فعالة للإيصال عبر الجلد، تضمن إطلاقاً دوائياً مستمراً، وتحسين الفعالية العلاجية، وتقليل المؤشرات الحيوية المرتبطة بالتشنج العضلي. وتشكل هذه الدراسة أول دليل علمي يدعم أمان وفعالية الباكلوفين

الموضعي النانوي البنية في علاج التشنجات، مما يمهد الطريق لتطبيقات مستقبلية أوسع في مجال إيصال الأدوية عبر الجلد بطريقة مستهدفة .



جمهورية العراق
وزارة التعليم العالي والبحث العلمي
جامعة ميسان
كلية العلوم
قسم الكيمياء

دراسة تصميم وإيصال الدواء الأمثل داخل الجسم وخارجه لحويصلات الباكلوفين الشحمية النانوية

رسالة مقدمة الى
مجلس كلية العلوم / جامعة ميسان
وهي جزء من متطلبات نيل
شهادة الماجستير في علوم الكيمياء

من الطالبة
حسناء كاظم طالب
بكالوريوس علوم كيمياء / جامعة ميسان (2022)

بإشراف
أ.م.د. اسراء قصي فالح

